THE HYDROGEOLOGICAL IMPACT OF HEAVY METAL-LADEN ASH LANDFILLING AT THE WLSSD LANDFILL, RICE LAKE, MINNESOTA

A THESIS

SUBMITTED TO THE FACULTY OF THE GRADUATE SCHOOL

OF THE UNIVERSITY OF MINNESOTA

BY

MARTIN WALTER WANGENSTEEN

IN PARTIAL FULFILLMENT OF THE REQUIREMENTS

FOR THE DEGREE OF

MASTER OF SCIENCE

MAY, 1988

Abstract

Starting in August of 1985 the Western Lake Superior Sanitary District (WLSSD) began processing garbage to produce a combustible fuel for use in incinerating heavy metal-laden sewage sludge. The end product of the incineration process is a fine ash which is ultimately deposited at the WLSSD landfill, Rice Lake Township, Minnesota. To assess the environmental implications of the ash landfilling, a hydrogeologic study of the landfill area and a heavy metal adsorption/transport study were conducted.

The WLSSD landfill is situated in a complicated ice stagnation complex known as the Highland Moraine. Sediment analyses indicate that the site is located in the silt-rich (sand/silt/clay ratio: 45/46/9) Upper Cromwell Formation. Subsurface exploration data reflect the heterogeneity of the glacial deposits at the study site. Resistivity survey results and well log data suggest that the silty sand unit underlying the study area is overlain by a silt and clay-rich layer in the western and southwestern portions of the site. Previous studies indicate that this fine-textured layer places a slight confining pressure on the water-bearing silty sand unit.

Water-level measurements made from observation wells reveal that groundwater flows from a groundwater divide

toward the Wild Rice Lake Basin to the northwest at about 0.28 m/year, and the Miller Creek Basin to the southeast at about 1.05 to 1.46 m/year. Flow lines suggest that much of the groundwater flowing through the refuse is intercepted by the leachate collection system located in the southeastern edge of the landfill.

Laboratory batch adsorption studies of heavy metals indicate that the local sediment has the highest affinity for Pb, followed by Cu, Cd, Zn, and Ni. The heavy metal adsorption data conformed to the Langmuir adsorption isotherm, suggesting that the heavy metal adsorption follows a kinetic rather than thermodynamic adsorption path.

Elution curves produced from the step input of a heavy-metal spiked solution into silt loam and sandy loam sediment columns imply that Cu, Cd, Ni, and Zn migrate through the respective sediments at about the same rate, while Pb migrates through the sediments at a significantly slower rate. These experiments suggest that the silt loam is more effective in retarding the heavy metals than the sandy loam. Sediment texture appears to be the main controlling factor in heavy metal attenuation: the finer grained a sediment, the more effective it is in attenuating heavy metals.

An error-function model fit to the elution curves predicts that Cu, Zn, Cd, and Ni solute profiles migrate

about 14 percent as fast as the groundwater in the silt loam and about 28 percent as fast as the groundwater in the sandy loam. Pb, which is strongly attenuated by the soil, was calculated to migrate about 95 percent slower than the groundwater in the silt loam and about 86 percent slower in the sandy loam.

Due to the small amounts of heavy metals leached from the ash in water and acid extraction tests performed by WLSSD personnel, the sediments' relatively high affinity for Pb, Cu, Cd, Ni, and Zn, and the low groundwater flow rates observed at the study site, it is unlikely that the groundwater environment will be adversely affected by ash landfilling. To insure groundwater protection, three main steps should be taken: (1) the ash should be landfilled within areas where the groundwater flow direction is towards the leachate collection system; (2) the ash should be landfilled in areas where the underlying sediment has a high percentage of silt and clay; and (3) the ash should be kept separate from the other waste to minimize heavy metal chelation.

Acknowledgments

The author wishes to express his sincere appreciation to Dr. George Rapp Jr., thesis advisor, and committee members Drs. C.L. Matsch, J.C. Green, and R. M. Carlson. The author is grateful for their guidance and assistance throughout the study.

Sincere appreciation is also extended to Steve Knight and Joe Steppun of the Western Lake Superior Sanitary District, Duane Long, Dr. D. P. Christian, and Dr. Michael Sydor of the University of Minnesota, Duluth, and Glenn Evavold of RREM, Inc., for their assistance in this study.

Table of Contents

LIST OF FIGURES

LIST OF TABLES

GENERAL INTRODUCTION

Landfills have been used for many years as a means of waste disposal. Due to the tremendous volume of waste generated each year, many landfills are nearing full capacity. In an effort to extend the operating life of a landfill, as well as to protect the environment, many solid waste facilities are experimenting with waste reduction methods. Although waste reduction methods offer a unique alternative to the landfilling of many wastes, these methods do not offer the ultimate solution to the waste disposal problem due to the resulting residue that must be treated or landfilled. Albeit these residues are generally less reactive than the parent material, hazardous metal constituents can still be leached, and migrate into the groundwater regime. As a result of this concern, environmental hazards associated with the land disposal of waste treatment residues must be examined.

Beginning August 1985, the Western Lake Superior Sanitary District (WLSSD) in Duluth, Minnesota began processing garbage (municipal waste) to produce a refuse derived fuel (RDF) for use in incinerating sewage sludge. The end product of the incineration process is a fine ash, which, along with the noncombustible waste is finally transported to the landfill for ultimate disposal.

Since the ash is a product of the incineration of RDF

and heavy metal-bearing sewage sludge, its disposal poses the possible threat of environmental contamination with heavy metals. Heavy metals such as copper, nickel, and zinc can be harmful to vegetation if applied in excessive concentrations (Sidle, 1976). Heavy metals such as cadmium and lead can be harmful to humans, causing skeletal deformation and renal dysfunction (Moore and Ramamoorthy, 1984). Even though the data indicate that the extractable amounts of Pb, Zn, Cd, Ni, and Cu from the WLSSD ash are not alarmingly high, the pollution potential of the ash landfilling must still be examined.

This thesis is divided into two separate but related studies. The first chapter discusses the results of a hydrogeologic investigation of the Rice Lake Sanitary Landfill. The objective of this study is to characterize the hydrologic setting of the landfill by: examining borehole logs and resistivity survey results; performing grain-size analyses on selected soil samples; and interpreting water level measurements taken from monitoring wells located within the study site.

The second chapter contains the results of a heavy metal adsorption study which describes the kinetics of the heavy metal adsorption process, and examines the migration rates of Cd, Cu, Ni, Zn, and Pb in unconsolidated sediment. Research in this chapter includes a batch adsorption study where the adsorption kinetics of the heavy metals with the

sediment are examined, and a soil-column study, where input data are generated for use in a user-oriented predictive equation for pollutant transport.

HYDROGEOLOGIC STUDY

Location

The study site is the WLSSD landfill located within Rice Lake Township, just north of the Duluth, Minnesota city boundary (Figure 1). The study area includes Section 1, Township 51N, Range 14W, and a portion of Section 36, Township 51N, Range 15W and is in the United States Geological Survey's Duluth Heights 7 1/2' topographic quadrangle.

Physiography

Elevations within the study area range from just under 1400 feet (426 m) to just over 1460 feet (445 m). The topographic expression is continually changing in the center and eastern parts of the study area due to the landfilling of waste, and the collection of cover material (Figure 2). The dominant topographical features are numerous kettles (depressions in the glacial sediment commonly filled with water) and kames (conical mounds). The average relief of the kames is about 20 feet (6.1 m). Swamps dominate the western and northwestern parts of the study area. The elevation of these swamps is usually just below 1420 feet. The swamps are indicative of a poorly drained area which is characteristic of ice disintegration complexes.

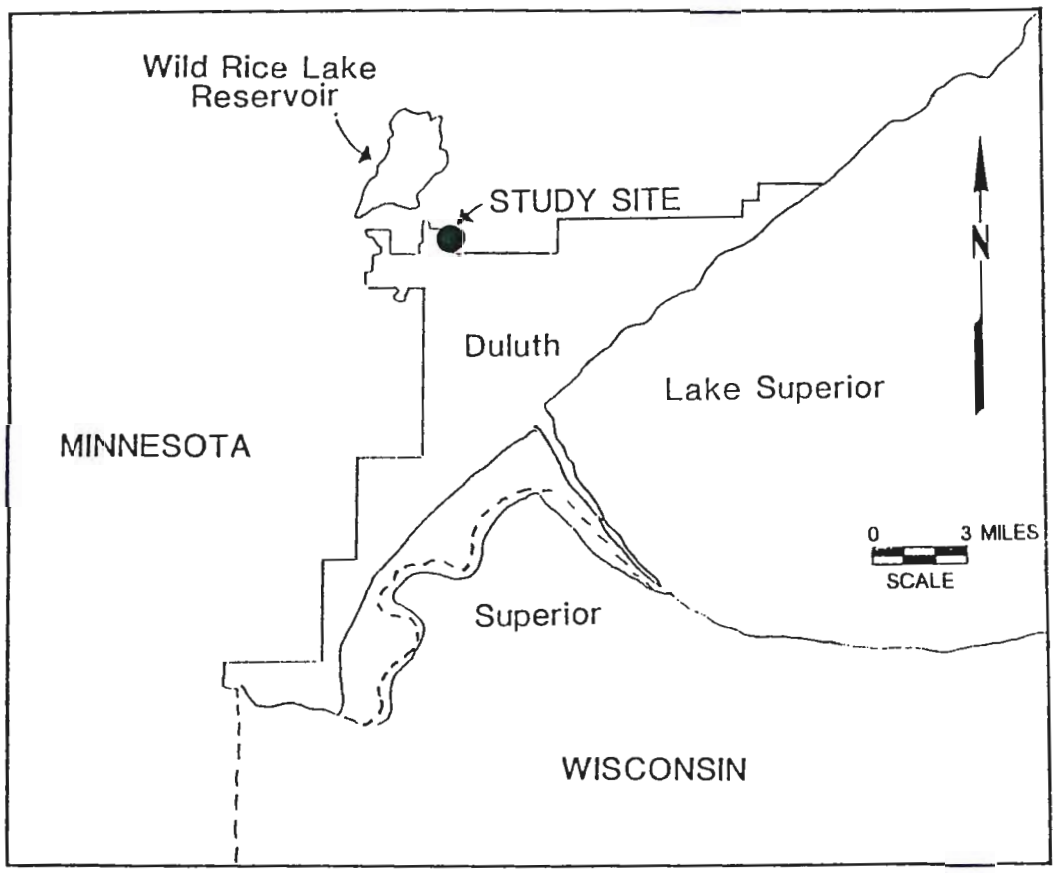

Figure 1: Study area location (After Knight and others, 1983).

Figure 2: Map of study area showing topographic expression, areas of the landfill used for refuse disposal, and location of cover material reserves.

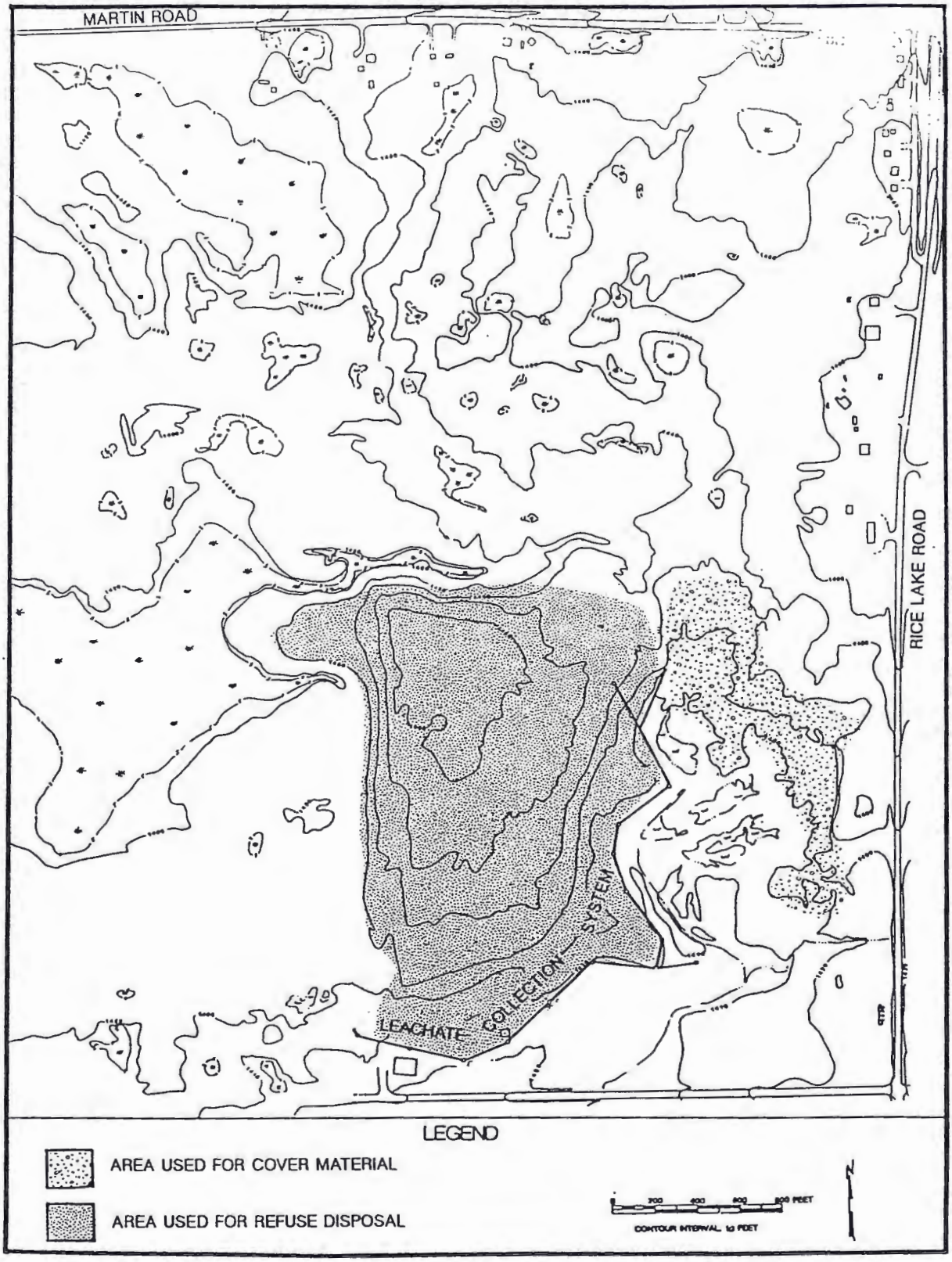
MARTIN ROAD
RICE LAKE ROAD
LEACHATE COLLECTION SYSTEM
LEGEND
AREA USED FOR COVER MATERIAL
AREA USED FOR REFUSE DISPOSAL
CONTOUR INTERVAL 10 FEET

Climate

The Duluth region has a continental-type climate modified locally by Lake Superior (Harrison and others, 1983). The mean annual air temperature for the Duluth area is about 39 ^{o}F (RREM, Inc., 1983). The Duluth region experiences about 30 inches of annual rainfall, 20 to 24 inches of open water evaporation, 13 inches of annual land evaporation, and 6 to 9 inches of transpiration resulting in 8 to 11 inches of total annual yield from upland vegetated areas in the form of surface and groundwater flows (Knight and others, 1983).

Regional Geology

Bedrock Geology

The bedrock in the Duluth area consists of a sequence of rocks that are Middle to Late Precambrian (Early to Middle Proterozoic) in age (Figure 3). The oldest unit present is the Middle to Late Precambrian Thomson Formation. The Thomson Formation consists of interbedded greywacke and slate (Bonnichsen, 1972) that was deposited in a large basin approximately 2100 m.y. ago and then deformed during the Penokean Orogeny at about 1800 m.y. ago (Van Schmus, 1976).

Due to continental rifting during Keweenawan (Middle

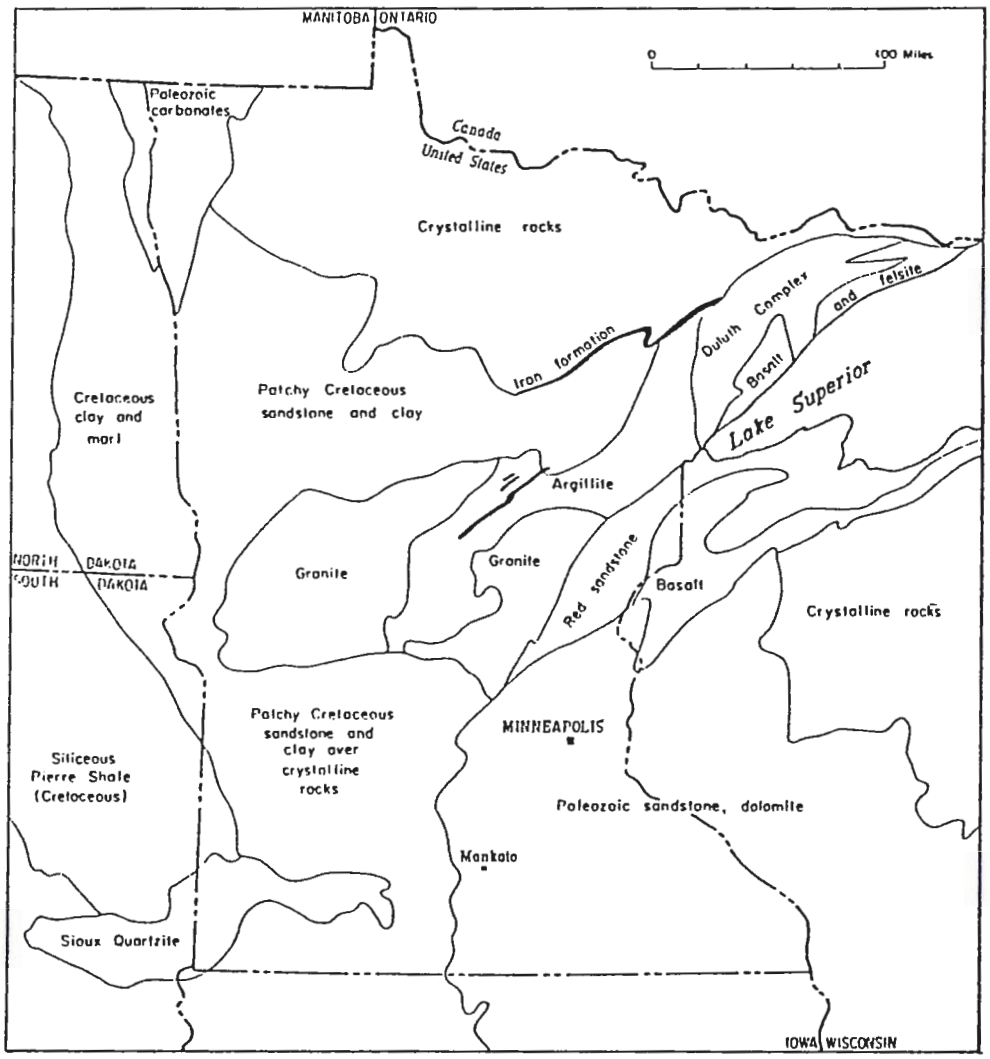

Figure 3: Generalized bedrock map of Minnesota and parts of adjacent states (From Wright, 1972).

Proterozoic) times, a series of lava flows were erupted through fissures between 1225 and 1100 m.y. ago (Van Schmus and others, 1982). The rock types present in this sequence, which is called the North Shore Volcanic Group, consist mainly of olivine tholeites and olivine basalts with some quartz tholeites, andesites, icelandites, and rhyolites (Green, 1972, 1982). Green (1983) proposes that the lava flows were accumulated in a subsiding basin. Within this sequence are interflow sedimentary rocks, composed of red sandstone and conglomerates, some exceeding 100 feet (31 m) in thickness (Craddock, 1972).

Approximately 1100 m.y. ago (Van Schmus and others, 1982) the North Shore Volcanic Group was intruded by anorthositic, troctolitic, gabbroic, and granodioritic magmas collectively known as the Duluth Complex. The Duluth Complex cropsout in an arcuate belt from Duluth nearly to the northeastern tip of Minnesota. This is the rock body that directly underlies the WLSSD landfill. Subsidence and tilting, which were associated with the intrusion of the magma, probably created a new basin in which Upper Keweenawan sediments (predominantly quartz sandstone and lithic sandstone) were able to accumulate (Ojakangas and Morey, 1982).

Quaternary Geology

Northern Minnesota has experienced a complicated history of glacial advances and retreats, resulting in both deposition and erosion of material.

All of the glacial drift in the Duluth area is attributed to deposition by the various phases of the Superior lobe, which originated from the Laurentide Ice Sheet during Late Wisconsin glaciation approximately 25,000 to 10,000 years before present (Wright and others, 1969). According to Wright (1972) (Figure 4), there were four main advances during the Late Wisconsin. The oldest, the St. Croix phase, involved the simultaneous advance of the Rainy and Superior lobes in a southwesterly direction. The drift associated with this phase is a gray to brown coarse-textured boulder-rich till, dominated by fragments of gabbro. The next advance, the Automba phase, is associated with the movement of the Superior lobe in a westerly direction. The Highland Moraine was constructed along the northwestern margin of the Superior lobe as it moved out of the Lake Superior basin, during this phase. In the third phase, or Split Rock phase, the Superior lobe re-advanced in a southwesterly direction incorporating the lake sediments which contributed the clay and silt that produced the distinctive red clayey till. The final phase, which was the Nickerson phase, advanced a relatively short distance and produced the Nickerson Moraine. A red clayey

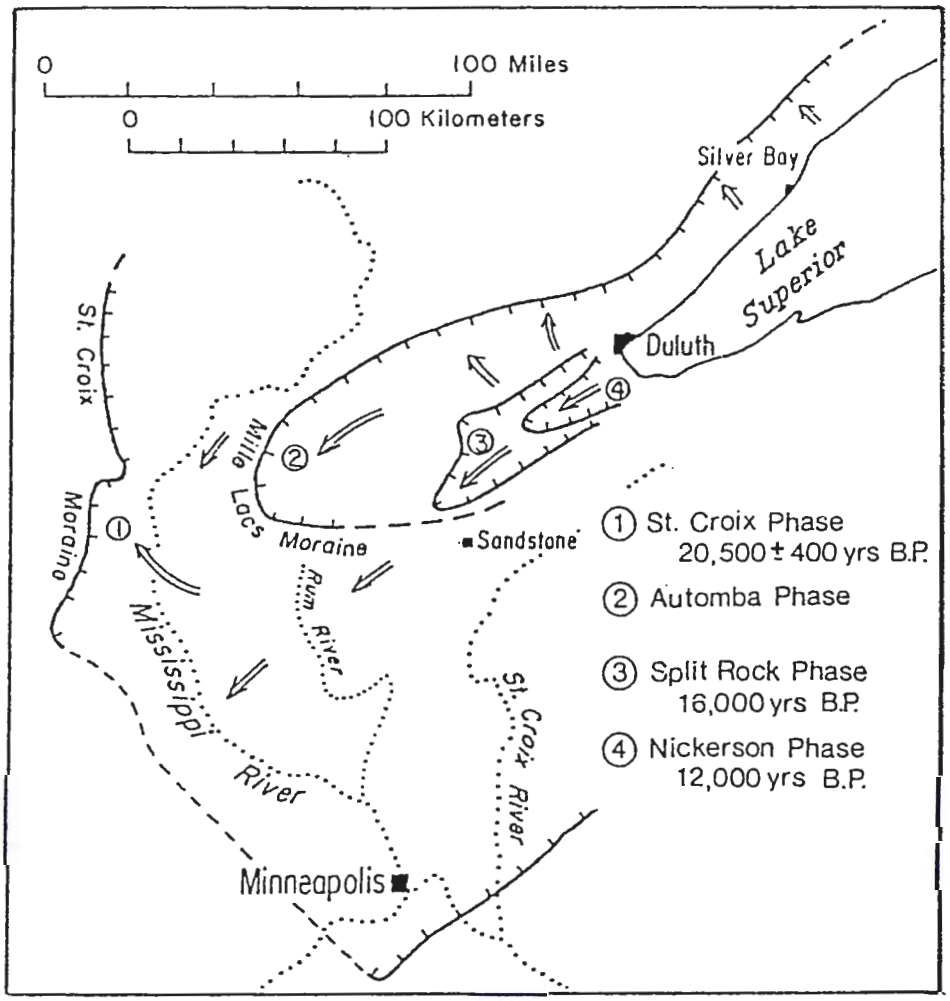

Figure 4: Advances of the Superior lobe during Late Wisconsin glaciation, northeastern Minnesota (From Wright, 1973).

till is also associated with this phase.

The present topography is a result of glacial and post-glacial erosional and depositional processes. The topography formed during the glacial period was the result of the deposition and erosion of material from glacial meltwater along with deposition of sediments by stagnant glacier ice. Post-glacial erosion and deposition have been mainly due to streams and rivers flowing towards Lake Superior.

Regional Hydrogeology

Groundwater movement in the Duluth area is mainly through shallow unconfined and semi-confined flow systems within the unconsolidated sediment and underlying bedrock. This shallow groundwater system discharges water to local streams and lakes, and through springs at the base of the slope near the Lake Superior shore (Olcott and others, 1978).

Bedrock Hydrogeology

The bedrock geology can play a major role in a hydrogeologic system. The lithology of the bedrock can have an effect on the hydrogeologic setting in two ways: (1) its mineral composition can affect the primary and secondary porosity of the aquifer; and, (2) where glacial

deposits are present, highlands and lowlands produced from the differential erosion of the bedrock can influence the type of glacial deposits by the channelization of ice lobes. Structural features, such as fractures, faults, and folds can also have a pronounced effect on the water-bearing capacity of the bedrock by increasing the secondary porosity.

Kanivetsky (1978), classified the bedrock hydrogeology around Duluth into three main units: the Keweenawan Volcanic Rocks Aquifer; the Proterozoic Aquifer; and a Precambrian igneous and metamorphic rock unit (not an aquifer except locally in faults and fractures). The Keweenawan Volcanic Rocks Aquifer is composed mainly of basaltic lava flows with interbedded sediments (see Regional Geology section). Only the fractured and weathered zones which occur irregularly within the upper 300 to 400 feet (91-122 m), and breciated and vesicular zones within the lava flows constitute the aquifer (Kanivetsky, 1978). Water primarily enters this aquifer in the uplands surrounding Lake Superior. Typical yields of wells located in this aquifer range from 1 gallon per minute (gpm) to 25 gpm (Olcott and others, 1978).

The Proterozoic Aquifer, composed of argillite, slate and metagraywacke, yields limited quantities of water near the Duluth area mostly from joints and fractures. In other

areas of the state, such as the Mesabi Range, yields of individual wells have been as high as 500 gpm from this aquifer.

Precambrian igneous and metamorphic rocks such as the Duluth Gabbro are not considered a bedrock regional aquifer because of the lack of primary porosity. In some areas where local secondary porosity has been developed, sufficient water for domestic supplies can be obtained. Table 1 is a summary of the hydrogeologic characteristics of the bedrock in the Duluth area.

Quaternary Hydrogeology

Northern Minnesota has a variety of glacial deposits as a consequence of its complex glacial history. The Quaternary hydrogeology can be very complex as a result of the diverse glacial sediments present. Kanivetsky (1979), describes two main Quaternary hydrogeologic units around the Duluth area: outwash sand and gravel, and glacial till associated with end moraines. The deposits are generally less than 50 to 75 feet (15-23 m) thick. The thin draping of sediments and hummocky topography have helped produce an area with a high water table and numerous wetlands. Most wells completed in the unconsolidated deposits in the North Shore area are less than 10 feet (3 m) in depth and produce yields of up to 10 gpm (Olcott and others, 1978). Shallow

Table 1: Summary of regional bedrock hydrogeologic characteristics (After Olcott and others, 1978).

SOURCE OF WATER	GEOLOGIC UNIT	REPORTED YIELD RANGE MEDIUM (gpm)	PRESENT DEVELOPMENT
KEWEENAWAN VOLCANIC ROCKS AQUIFER	NORTH SHORE VOLCANIC GROUP (Basalt and inter-flow sediments)	0.5 TO 60 10 (38 WELLS)	Slightly developed for domestic use throughout area where sufficiently thick and saturated. Water obtained from springs, shallow dug and driven wells, and drilled wells as much as 150 ft (45.7 m) deep. Yields less than 10 gpm in 68 percent of reported wells. Aquifer under water table conditions.
PROTEROZOIC AQUIFER	THOMSON FORMATION (Slate and graywacke)	1.5 TO 25 12 (5 WELLS)	Virtually undeveloped. Occurs only in extreme northern part of area. Water obtained from shallow to deep wells as much as 325 ft (99.1 m) deep. All wells completed open hole.
PRECAMBRIAN IGNEOUS AND METAMORPHIC ROCKS UNIT	DULUTH GABBRO AND OTHER INTRUSIVES	0.25 TO 45 4.5 (33 WELLS)	Slightly developed for domestic and stock use. Water obtained from shallow to deep wells as much as 400 ft (121.9 m) deep. All wells completed open hole.

flow systems most likely dominate with local recharge and discharge areas.

Site Geology

Introduction

The study site is located on rolling hummocky terrain characteristic of the Highland Moraine. The Highland Moraine is an ice-stagnation complex associated with the advance, stagnation and retreat of the Superior lobe during the Automba phase of glaciation (Wright, 1972; Gross, 1982). The till associated with the Automba phase is called the Upper Cromwell Formation (Wright and others, 1969; Wright, 1972).

The Upper Cromwell Formation consists of supraglacial sediments (mainly contained within the Highland Moraine) and subglacial sediments (Gross, 1982). Associated with the Highland Moraine is a hummocky kame and kettle topography and numerous outwash bodies. These features were formed as detached ice blocks melted followed by the collapse, transport, and deposition of the sediment.

The Upper Cromwell Formation is rich in silt (Moss, 1977; Gross, 1982; and Lannon, 1986). The siltier texture may be from: (1) the incorporation of proglacial lake sediments into the ice during the Automba readvance; and (2) progressive pulverization of incorporated sediment by

crushing and abrasion processes (Dreimanis, 1979).

Surface Soils

It is important to investigate the type of soil and its properties in any project involving the change of land use or construction. United States Department of Agriculture (USDA) Soil Conservation Survey (SCS) soil survey maps and soil scientists interpretations are useful for this purpose. A basic soil map for St. Louis County compiled by the SCS indicates that there are three main types of soils present at the study area (Figure 5).

The most abundant soil type at the site are soils grouped into the Ahmeek Series. The Ahmeek Series consists of moderately well drained soils found in a loamy mantle overlying firm glacial till on uplands (Soil Conservation Service, 1986). A dark brown to grayish-brown silt loam and reddish-brown sandy loam are typical of this series.

The next most abundant soil type at the site is the Seelyeville Series. Seelyeville Series soils are deep, very poorly drained soils formed in organic material under marsh vegetation in low areas (Soil Conservation Service, 1986). These soils consist mainly of black and very dark brown muck.

The third soil type present, in an appreciable amount, is known as the Hermantown Series. This series consists of deep, somewhat poorly drained soils that formed

Figure 5: Soil map prepared from Soil Conservation Service data (Soil Conservation Service, 1986).

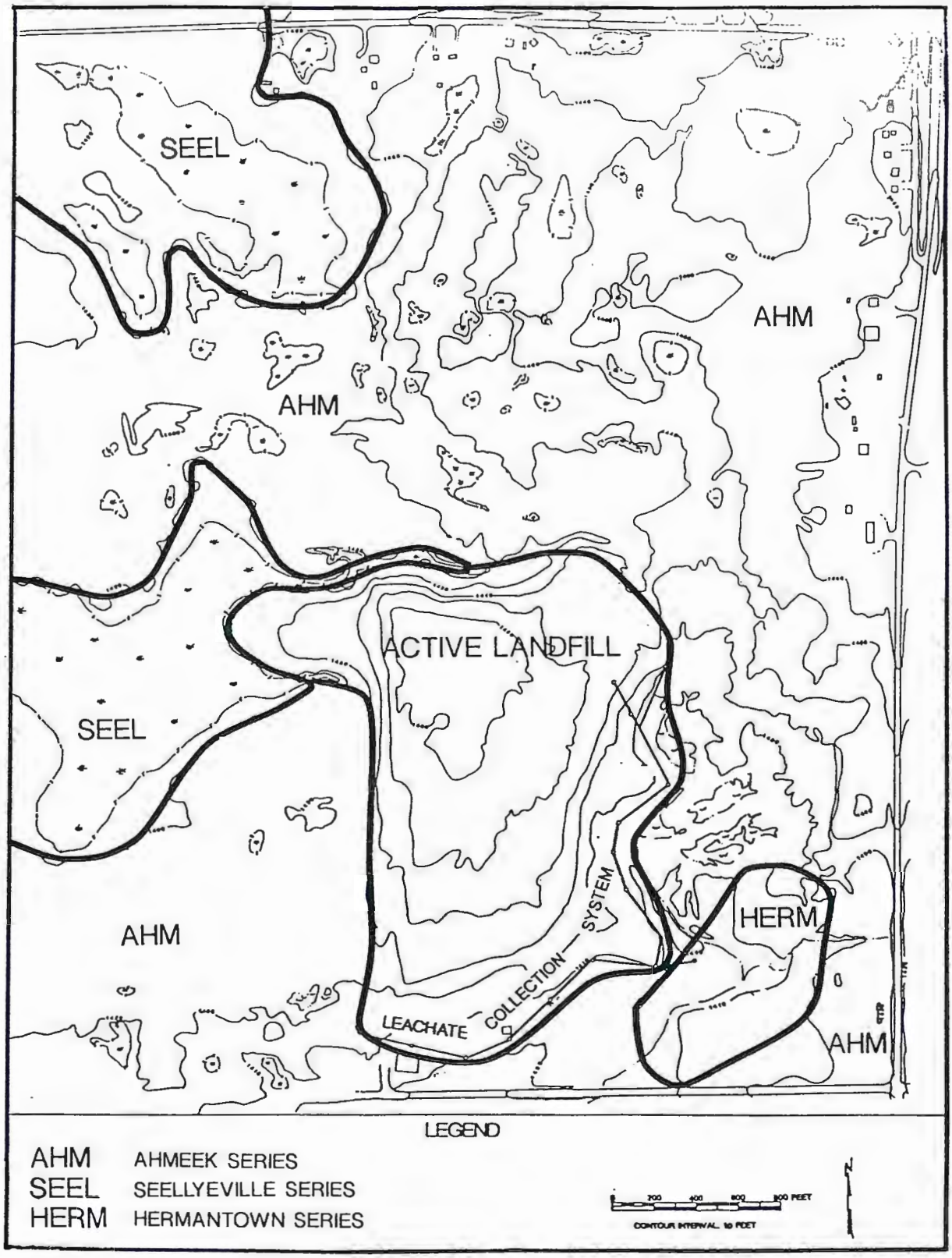
SEEL
AHM
AHM
ACTIVE LANDFILL
SEEL
AHM
HERM
AHM
LEACHATE COLLECTION SYSTEM
LEGEND
AHM AHMEEK SERIES
SEEL SEELLYEVILLE SERIES
HERM HERMANTOWN SERIES
CONTOUR INTERVAL 10 FEET

in loamy mantle and dense glacial till on uplands (Soil Conservation Service, 1986). Typical soils in this series consist of grayish-brown to brown silt loam and a reddish-brown to dark reddish-brown sandy loam. Properties of these soils are listed in Table 2.

Subsurface Exploration Methods

In every groundwater investigation it is essential that the subsurface geology of the site be examined. The best way to become acquainted with the lithology of the geologic materials at a site is to study borehole logs, interpret results of geophysical tests, and analyze sediment samples (Driscoll, 1986).

The subsurface geology of the study site was investigated by examining all available well logs and electrical resistivity survey results. Sediment samples were also collected for grain size analyses.

The soil borings were drilled by Lakehead Testing Laboratory, Inc. in 1976, 1979, 1982, 1983, and 1984. The locations of the borings are shown in Figure 6. As the samples were obtained in the field, they were classified by the crew chief in accordance with ASTM:D2488-69 (Lakehead Testing Laboratory Inc., 1976). Representative portions of all samples were then returned to the laboratory for further examination and for verification of the field classification.

Table 2: Summary of soil properties (From Soil Conservation Service, 1986).

SOIL SERIES	DEPTH (IN)	USDA TEXTURE	LIQUID LIMIT	PLASTICITY INDEX	CLAY (PCT)	MOIST BULK DENSITY (G/CM^3)	PERMEABILITY (IN/HR)	SOIL REACTION (pH)
AHMEEK SERIES	0 - 2	L, SIL	<25	2 - 7	5 - 15	1.30 - 1.50	0.6 - 2.0	4.5 - 6.0
	0 - 2	FSL, FFSL	<25	NP - 5	5 - 12	1.30 - 1.50	0.6 - 2.0	4.5 - 6.0
	2 - 14	FSL, L, SL	<25	NP - 7	5 - 15	1.30 - 1.50	0.6 - 2.0	4.5 - 6.0
	14 - 33	FSL, SL	<30	NP - 10	6 - 18	1.70 - 1.85	0.2 - 0.6	5.1 - 6.5
	33 - 60	FSL,SL	<30	NP - 10	6 - 18	1.80 - 2.00	0.06 - 0.2	6.1 - 7.3
SEELYEVILLE SERIES	0 - 4	SP, MUCK	---	--------	-----	0.10 - 0.25	0.2 - 6.0	4.5 - 8.4
	0 - 4	HM, MPT	---	--------	-----	0.10 - 0.25	0.2 - 6.0	4.5 - 8.4
	0 - 60	SP	---	--------	-----	0.10 - 0.25	0.2 - 6.0	4.5 - 8.4
HERMANTOWN SERIES	0 - 10	SIL	<30	NP - 7	5 - 15	1.30 - 1.50	0.6 - 2.0	4.5 - 6.0
	0 - 10	VFSL FSL	<25	NP - 5	5 - 12	1.30 - 1.50	0.6 - 2.0	4.5 - 6.0
	10 - 15	FSL, VFSL	<30	NP - 7	5 - 15	1.30 - 1.50	0.6 - 2.0	4.5 - 6.0
	15 - 28	SL, FSL	20 -30	4 - 9	8 - 18	1.55 - 1.75	0.6 - 2.0	5.1 - 6.0
	28 - 45	SL, GR-SL	<25	NP - 7	5 - 15	1.80 - 2.00	0.2 - 0.6	5.1 - 6.0
	45 - 60	SL, GR-SL	<25	NP - 7	5 - 10	1.80 - 2.00	0.2 - 0.6	6.1 - 7.3

Figure 6: Soil boring locations.

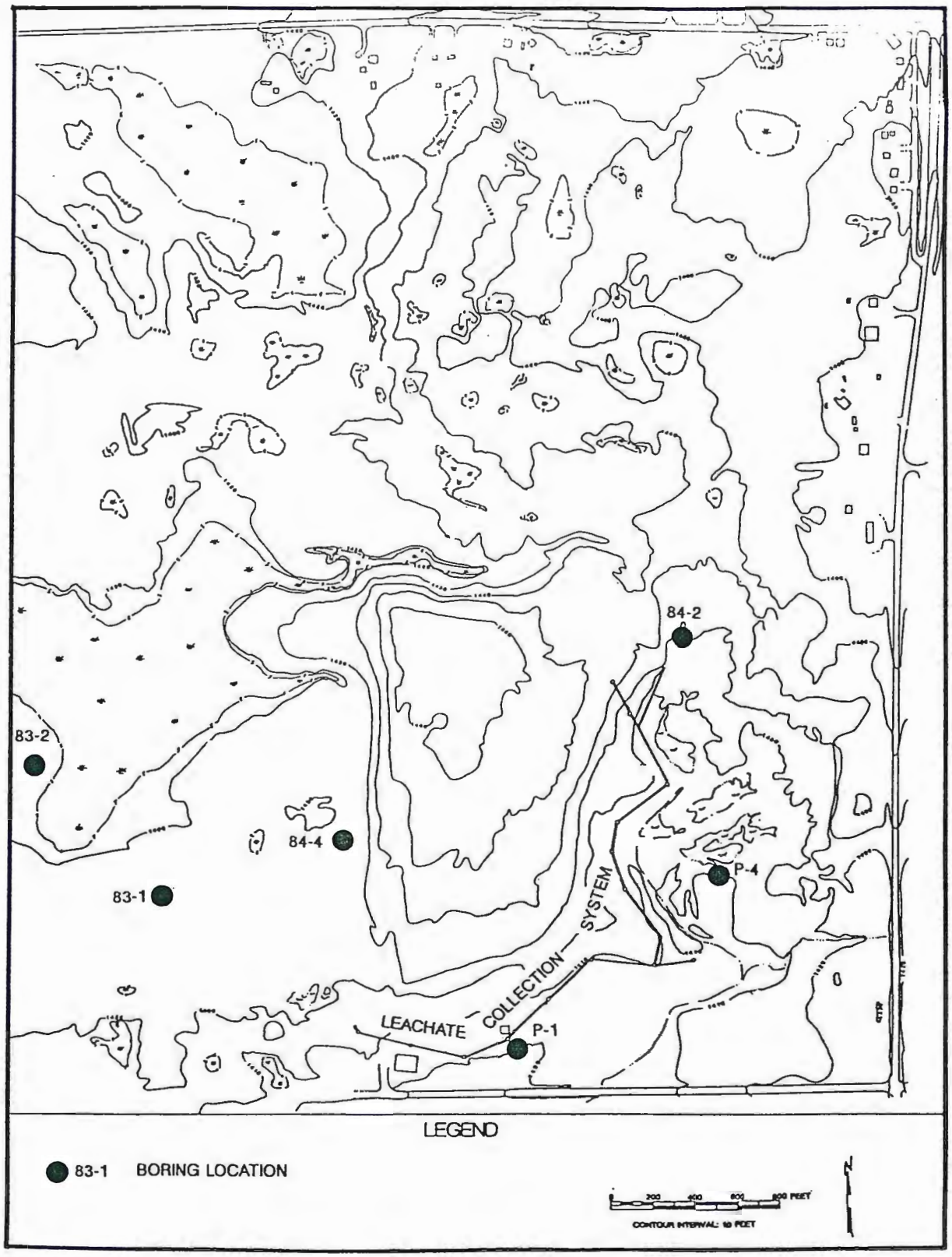
84-2
83-2
84-4
83-1
P-4
LEACHATE COLLECTION SYSTEM
P-1
LEGEND
83-1 BORING LOCATION
CONTOUR INTERVAL: 10 FEET

The electrical resistivity survey was performed by Soil Exploration Company in September 1983 using a Bison Instruments Model 2350 A earth resistivity meter (Soil Exploration Company, 1983). The soundings were spaced 400 feet (122 m) apart along survey lines staked in the field by RREM, Inc.

A resistivity survey characterizes soils according to their electrical characteristics. Three main factors that determine the ability of a lithologic unit to conduct an electrical current are the amount of open space between particles (porosity), the degree of interconnections between those open spaces, and the volume and conductivity of the water in the pores (Minning, 1973). The presence of water and its chemical character are the principal controls on the flow of electrical current since most rock particles offer high resistance to electrical flow (Driscoll, 1986). Accordingly, the electrical resistivity decreases as the porosity, water content, hydraulic conductivity, salinity and amount of dissolved metals and conductive minerals increase. Dry sand and gravel have the highest resistivities of unconsolidated materials, followed by saturated sand and gravel and then by clay, which exhibits low resistivities. Crystalline bedrock generally exhibits high resistivity values. The bedrock underlying the study area exhibits very high resistivity values.

The resistivity values obtained in the field were

interpreted by Soil Exploration Company. Correlations between sediment types and resistivity values were made by using known ranges of values for various sediment and rock types, past experience, and representative samples by drilling or other means (Soil Exploration Company, 1983).

Sediment samples were collected at various locations within the western and northwestern sections of the study site. The samples were taken from cuts in the land surface produced from the acquisition of cover material. Grain size distributions were determined by standard sieve and pipette analyses (Folk, 1980). The sediment's textural class was then determined by its respective percentages of sand, silt, and clay using the United States Department of Agriculture (USDA) classification scheme. The results and interpretation of the well logs, resistivity survey data, and grain size distribution data are discussed in the following section.

Surficial Geology

Well Logs

Borings of the surficial material reflect the heterogeneity of the glacial deposits at the study site. Generally, the sediments encountered were mixtures of sand, silt, and clay with varying amounts of gravel. Figure 7 shows the location of two geologic cross-sections compiled from the well log data. The cross sections (Figures 8 and

Figure 7: Location of cross-sections A - A′, and B - B′

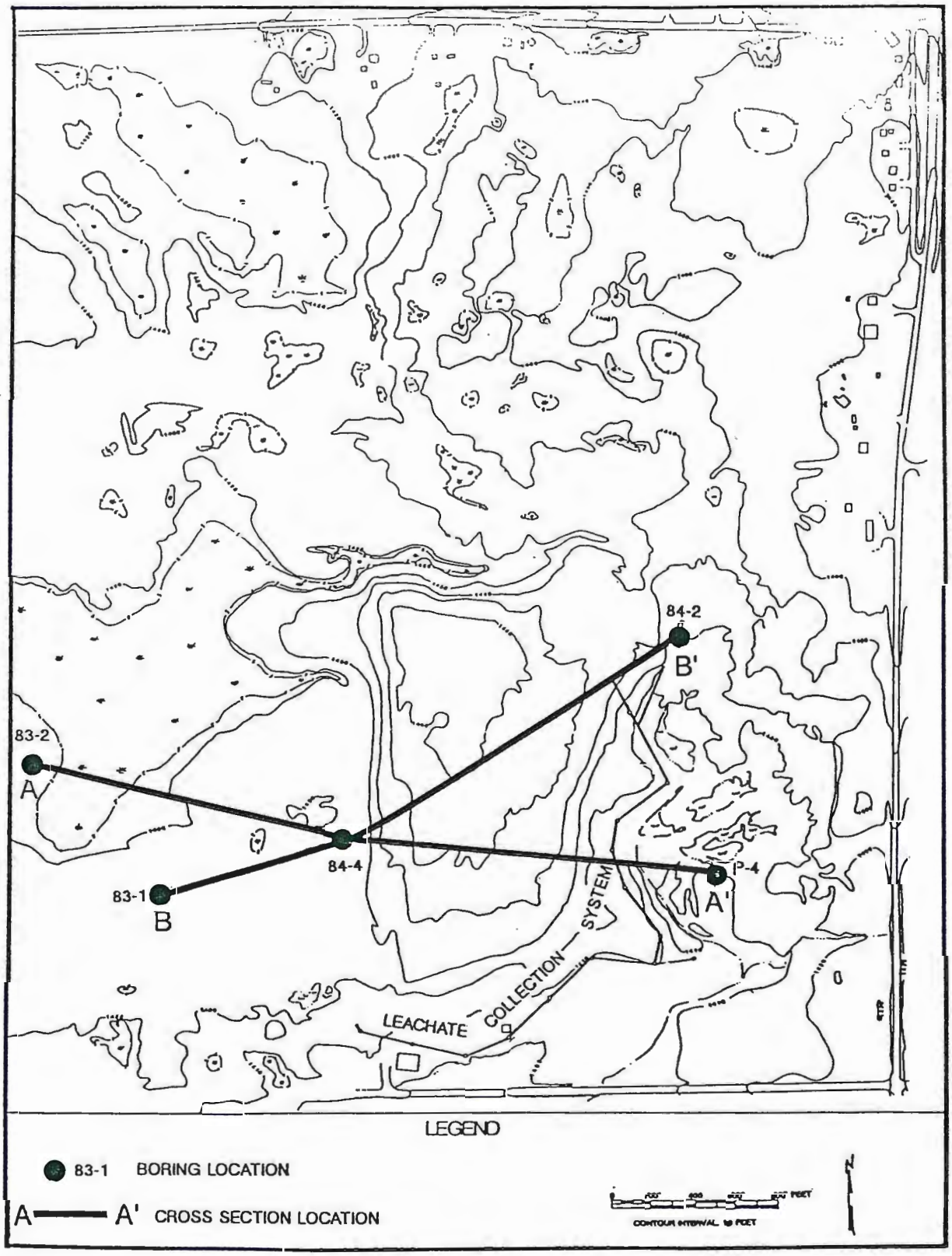
84-2
B'
83-2
A
84-4
P-4
83-1
B
A'
LEACHATE COLLECTION SYSTEM
LEGEND
83-1 BORING LOCATION
A A' CROSS SECTION LOCATION
CONTOUR INTERVAL 10 FEET

9) give a pictorial view of the surface topography and the lithologic relationships found at the site. Due to the classification scheme used in the well log interpretations (Unified Soil Classification), only general trends and approximate lithologic boundaries are described. Logs for the borings are contained in Appendix A.

The well logs indicate that a large part of the study area is underlain by a brown silty sand. The silty sand shows varying degrees of consolidation. Data are too sparse to show a definite trend, but logs of wells 83-2 and 84-4 suggest that the density of the silty sand increases with depth. Minor grain size variations within the silty sand were observed in all borings: varying amounts of gravel were encountered along with occasional lenses of sand and gravel.

Borings 83-1, 83-2, and 84-2 indicate the presence of a silty clay layer overlying the silty sand layer. The true lateral extent of this layer is unknown. Inspection of logs of wells destroyed during landfill expansion indicate that the silty clay layer did extend at least to a midpoint between wells 84-4 and 84-2. Unfortunately, the lateral extent of the silty clay layer can only be estimated due to the limited documentation as to the exact location of the abandoned wells.

To better define the stratigraphy of the surficial sediments, further drilling is needed. Grain size analysis

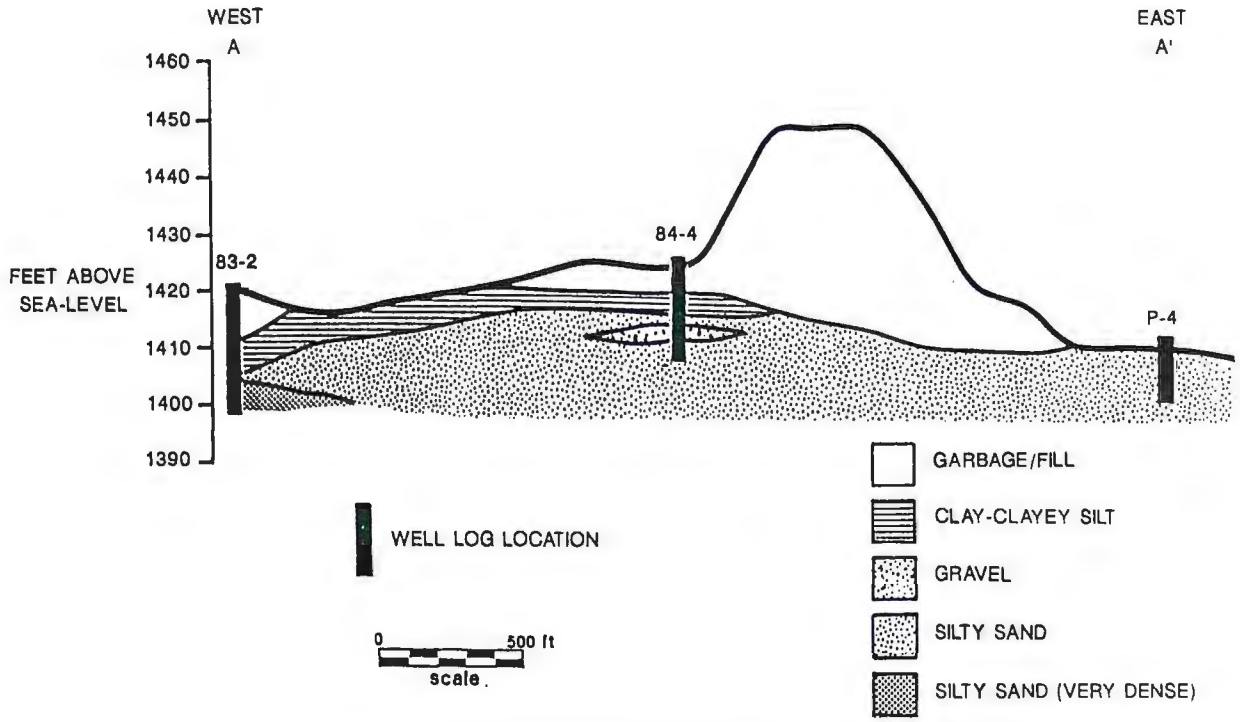

Figure 8: cross-section A-A' showing geology and topographic expression.

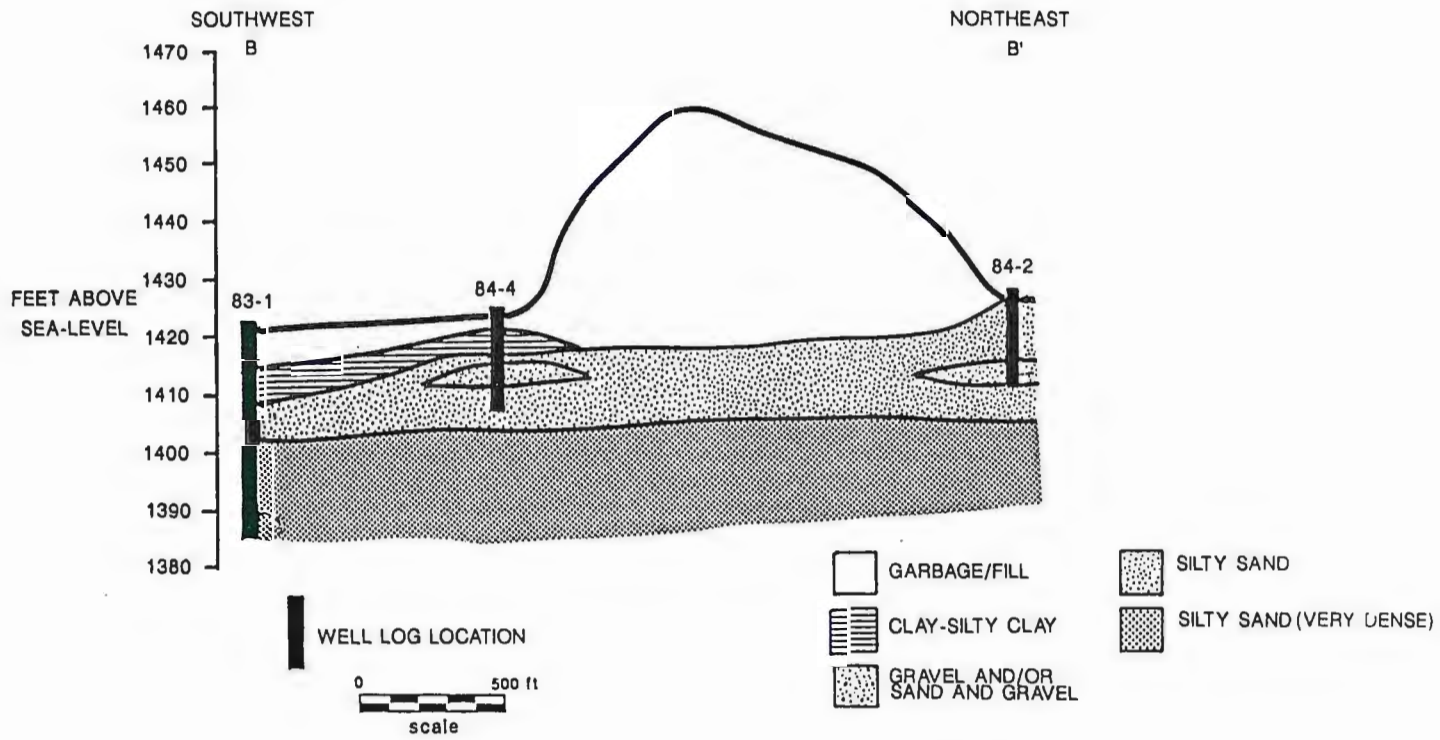

Figure 9: Cross-section B-B' showing geology and topographic expression.

should also be performed on selected sediment samples obtained during the drilling operations.

Resistivity Survey

Selected resistivity values obtained from the resistivity survey are shown in Figure 10. Table 3 shows the correlations between resistivity values and sediment types used for this study. The resistivity values indicate that a silty sand layer underlies a large portion of the site.

Lower resistivity values in the western and southwestern sections of the site suggest the presence of a finer grained material overlying the silty sand. Soil Exploration Company (1983) suggests that these lower resistivity values represent a silty clay layer.

Determining the lateral extent of the silty clay layer by the resistivity survey results is difficult. Refuse deposited on the southwestern side of the study site, unfortunately, exhibits similiar resistivity values to the silty clay layer.

The resistivity survey was only moderately useful in determining the stratigraphy of the surficial sediments at the site. Attempts to identify different units is usually only possible when they exhibit a clearly measurable difference in resistivity. Unfortunately, due to the

Figure 10: Location of resistivity survey lines and selected resistivity values (RREM, Inc., 1984).

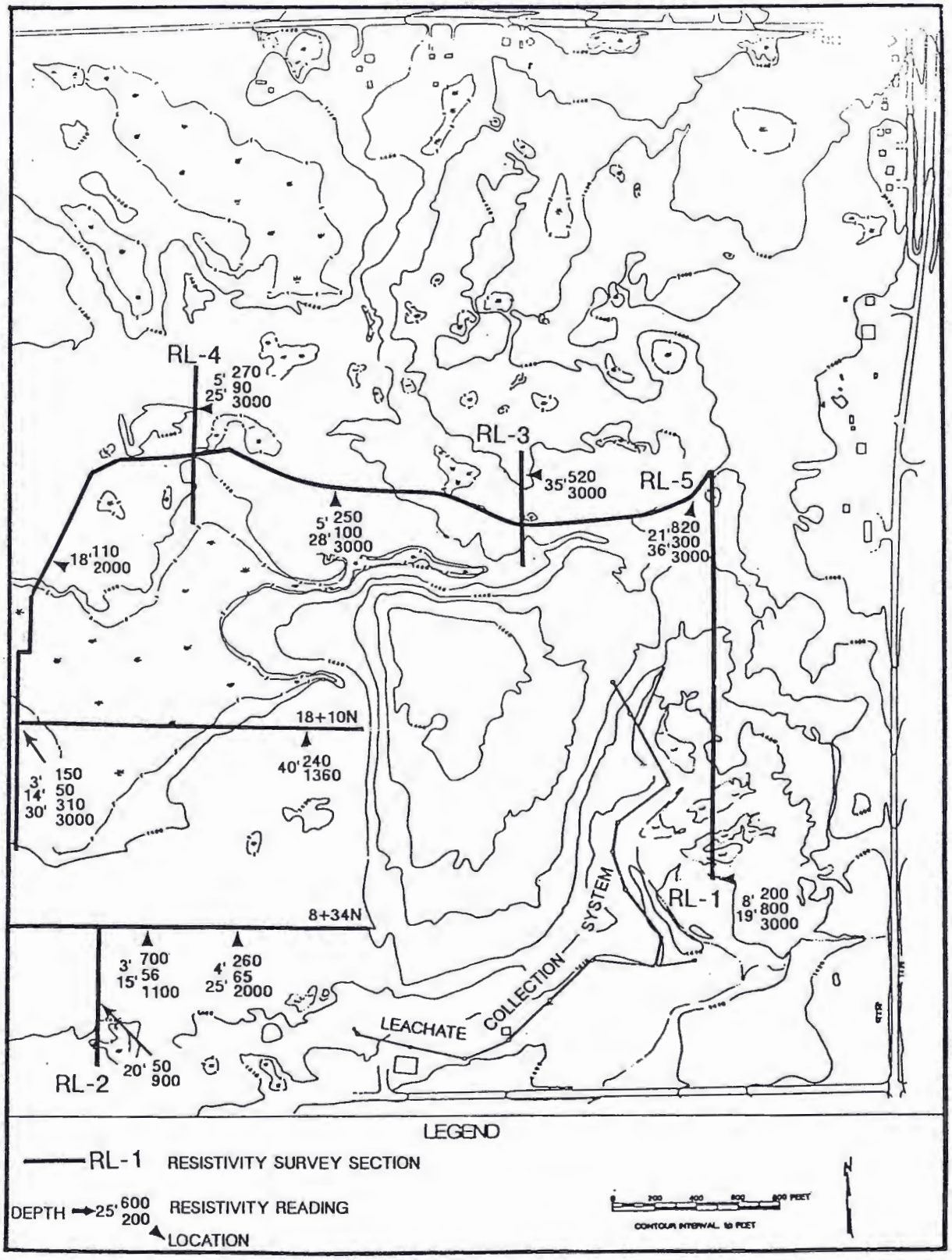
RL-4
5' 270
25' 90
3000
RL-3
35' 520
3000
RL-5
5' 250
28' 100
3000
21' 820
36' 300
3000
18' 110
2000
18+10N
40' 240
1360
3' 150
14' 50
30' 310
3000
8+34N
3' 700
15' 56
1100
4' 260
25' 65
2000
RL-1
8' 200
19' 800
3000
LEACHATE COLLECTION SYSTEM
RL-2
20' 50
900
LEGEND
RL-1 RESISTIVITY SURVEY SECTION
DEPTH → 25' 600
200 RESISTIVITY READING
LOCATION
CONTOUR INTERVAL 10 FEET
N

RESISTIVITY (Ohm-ft)	SOIL TYPE
<100	Primarily clay.
100 - 400	Increasing coarseness - sandy clay, clayey sand, silt and silty sand.
400 - 1500	Silty sand with gravel, coarse sand, sand and gravel with cobbles and boulders.
1500 - 2500	Very coarse gravel, cobbles and boulders, possible bedrock.
>2500	Bedrock (or very dry coarse gravel, cobbles and boulders).

Table 3: Correlations between resistivity values and sediment types.

heterogeneity of the surficial sediments, this was not the case here.

Sediment Analyses

The surficial material at the site can be best described as a silt-rich, light reddish-brown diamicton. The compactness of the material varies: at some locations the material is very dense, while at others it is easily disaggregated. Lithology of the gravel fraction is dominated by basalt, red sandstone, and gabbro. Clasts greater than 32 mm in diameter made up 0 to 25 percent of the total volume of sediment. Complex interbedding of different sediment types is common throughout the site. Small interbeds (1 to 15 cm in thickness) of gray to tan clay, along with interbeds of sand, and sand and gravel were present at most locations. Complex stratigraphic sequences such as this are common throughout the Highland Moraine (Moss, 1977). These small, complex sequences are indicative of the stagnation and melting of glacier ice. See Moss (1977) for a detailed discussion of ice disintegration features and their mode of deposition.

Sediment samples were collected from the eastern and northeastern portions of the study site for grain size analysis of the <2 mm fraction (Figure 11). The grain size distributions for the sediment samples are contained in Appendix B. The sediments ranged in textural class from a

Figure 11: Reference map for sediment sample locations and sample numbers.

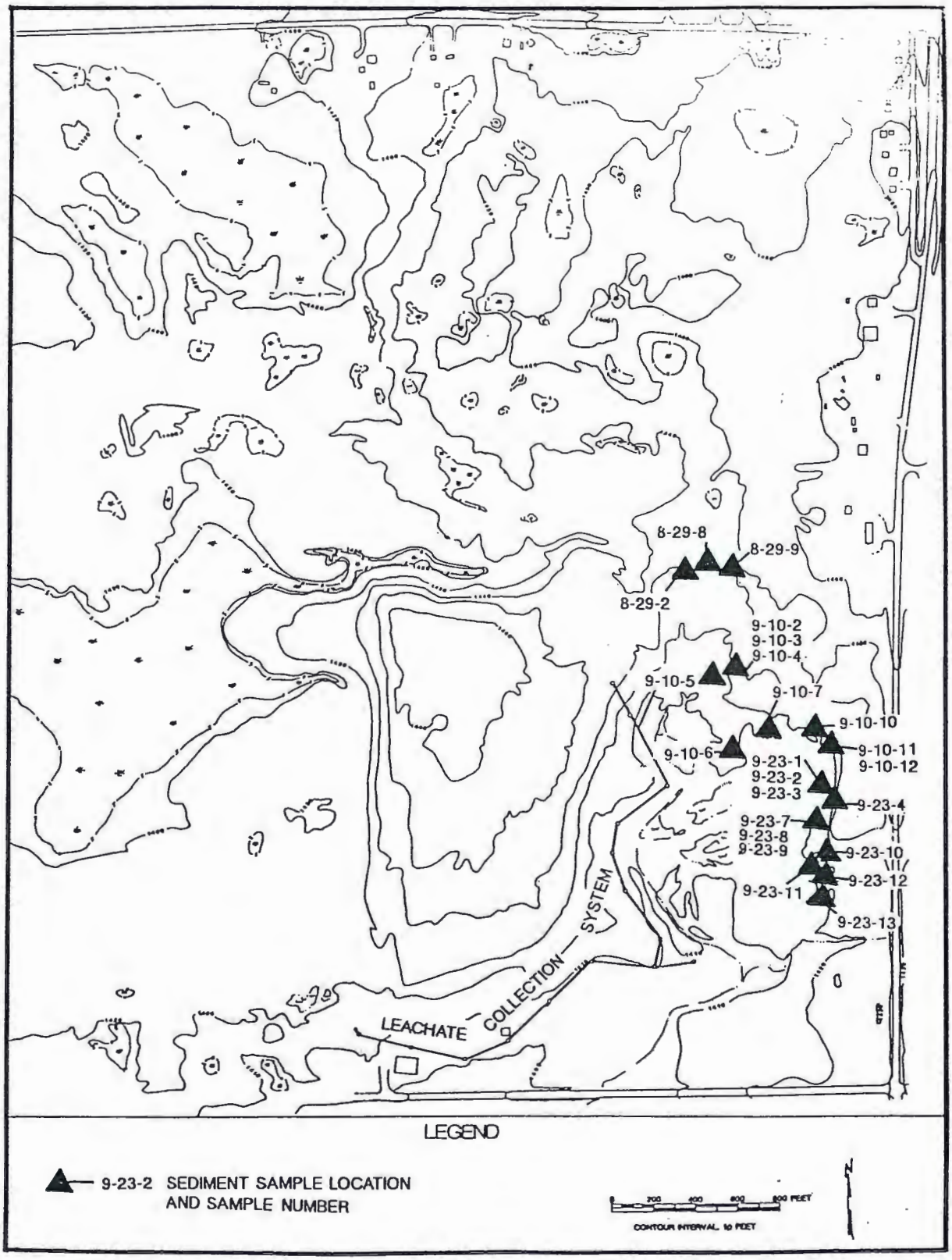
8-29-8
8-29-9
8-29-2
9-10-2
9-10-3
9-10-4
9-10-5
9-10-7
9-10-10
9-10-11
9-10-12
9-10-6
9-23-1
9-23-2
9-23-3
9-23-4
9-23-7
9-23-8
9-23-9
9-23-10
9-23-12
9-23-11
9-23-13
LEACHATE COLLECTION SYSTEM
LEGEND
9-23-2 SEDIMENT SAMPLE LOCATION AND SAMPLE NUMBER
CONTOUR INTERVAL 10 FEET

sandy loam, to loam, to a silt loam (Figure 12). The average sand/silt/clay ratio was 45/46/9 (average of 23 samples). The average sand/silt/clay ratio was considerably less clay-rich than Lannon's (1986) and Moss's (1977) results, but more clay and silt-rich than Gross's (1981) results for the supraglacial facies of the Upper Cromwell Formation (Figure 13). The grain size variations within the supraglacial facies of the Upper Cromwell Formation may be attributed to minor differences in the amount of sediment that the stagnant ice had available to deposit, and/or the relative abundance of the glacier ice at each location.

The grain size distribution of the sediment does not appear to vary laterally. The sediment does, however, become slighty coarser (greater amounts of sand) with depth at some locations. Figure 14 is a diagrammatic representation of the bank where sediment samples 9-23-7, 9-23-8, and 9-23-9 were taken. The figure shows the progressive coarsening of the sediment with depth. This trend is also observed where samples 9-10-2, 9-10-3, and 9-10-4 were located.

Bedrock Geology

The bedrock that underlies the study site is a massive intrusive rock assigned to the Duluth Complex, which intruded the lower part of the Middle Keweenawan Volcanic

Figure 12: Textural data for sediment samples collected at at the study site.

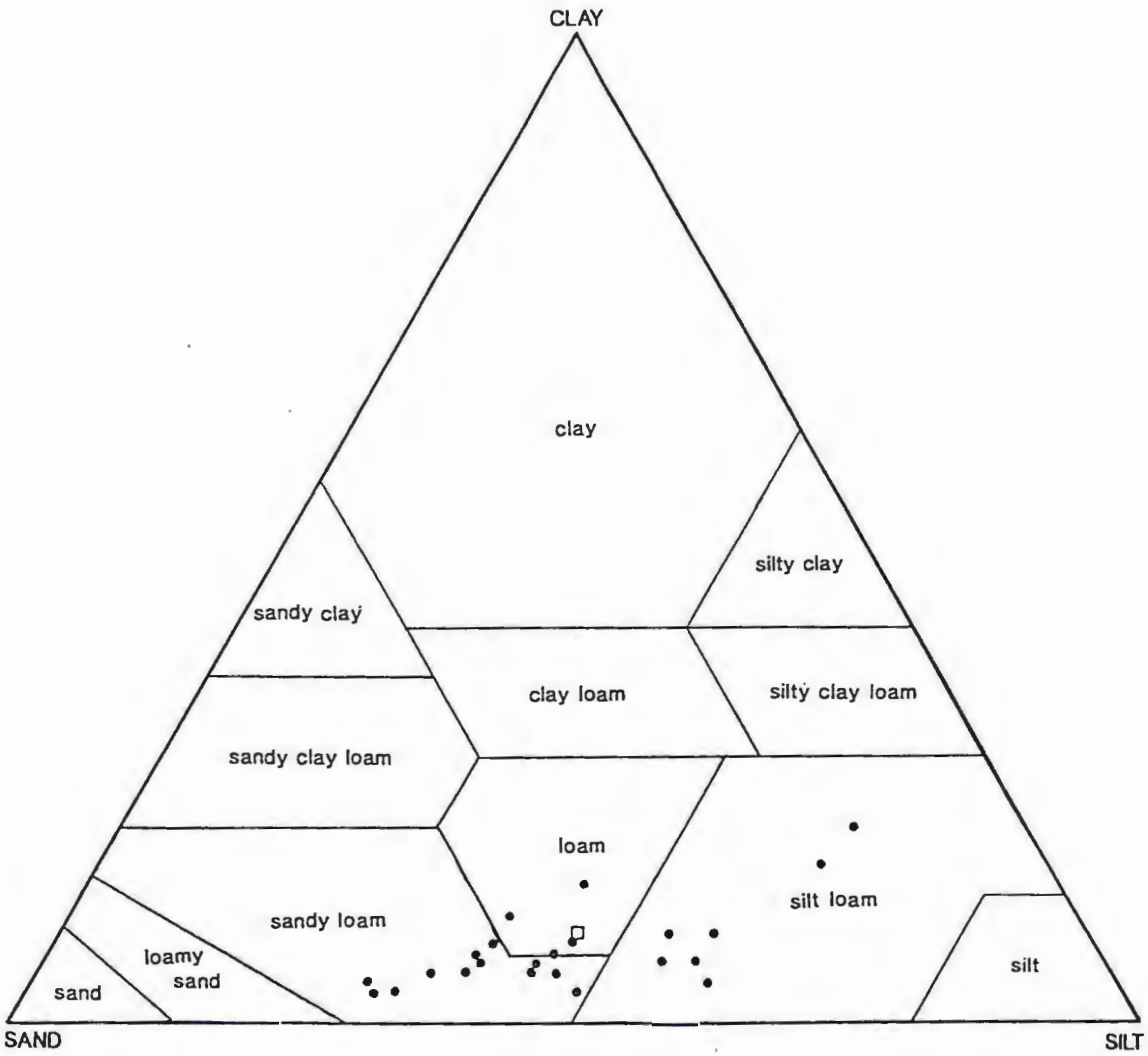

□ AVERAGE SAND/SILT/CLAY = 45/46/9 (N:23)

Figure 13: Upper Cromwell textural averages.

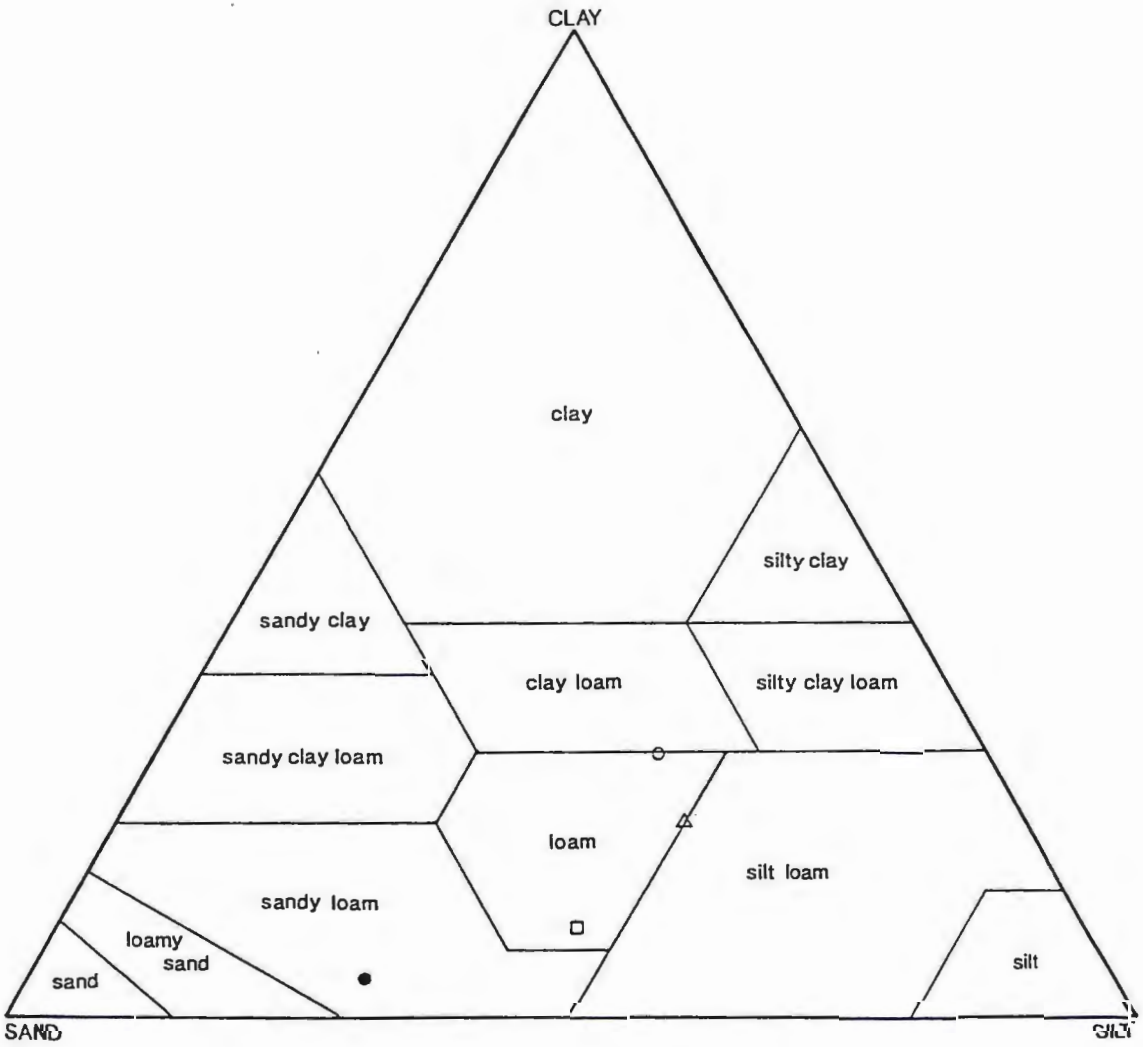

UPPER CROMWELL SAND/SILT/CLAY AVERAGES

△ 30/50/20 (Moss, 1977)
○ 29/44/27 (Lannon, 1986)
● 66/30/04 (Gross, 1981)
□ 45/46/9 (this study)

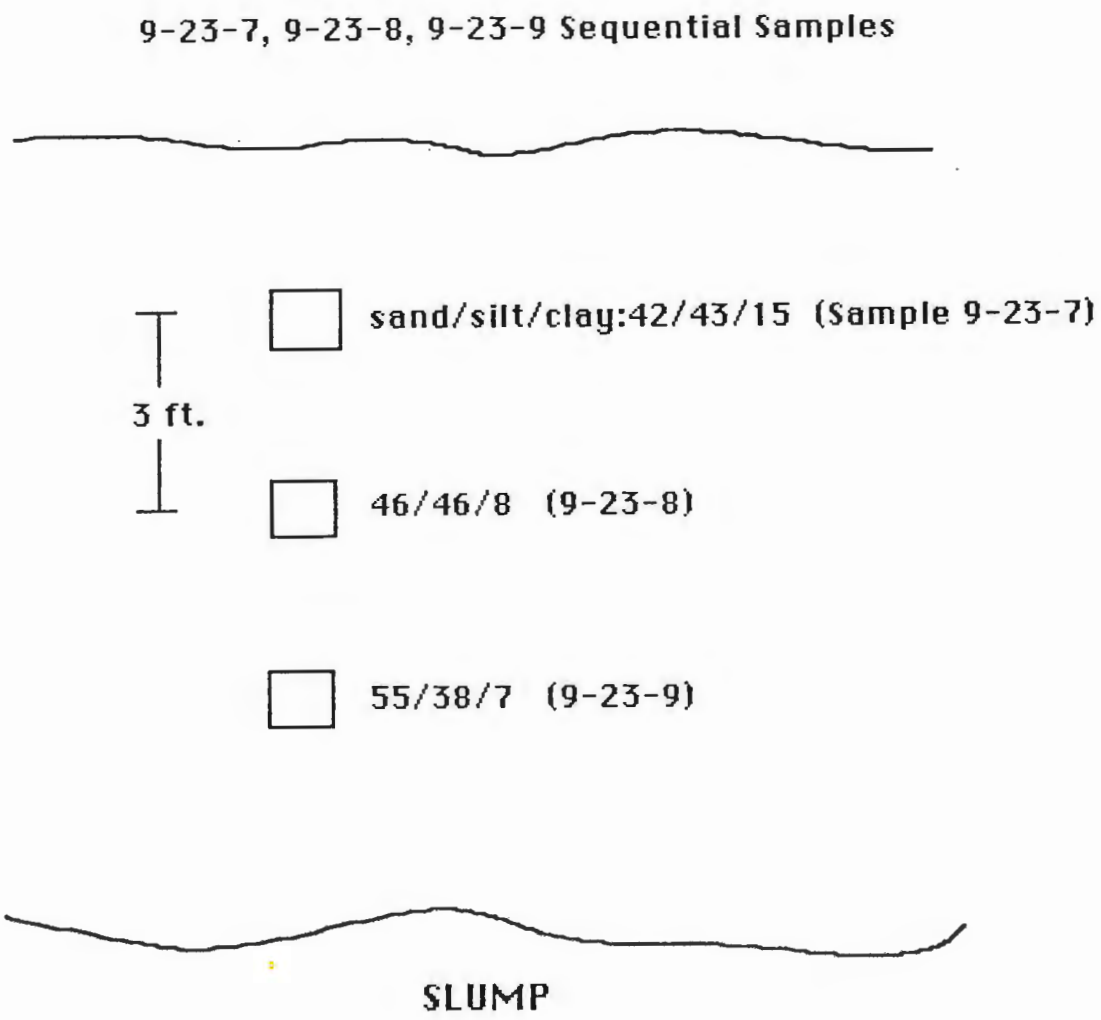

Figure 14: Stratigraphic section showing progressive coarsening of the sediment with depth.

sequence (Craddock, 1972) about 1100 m.y. ago (Van Schmus and others, 1982). The Duluth Complex consists of anorthositic, troctolitic, gabbroic, granodioritic, and granitic intrusive rocks.

Depth to bedrock varies from surface outcrops found at the northern edge of the landfill, to 40 to 50 feet (12.2 - 15.2 m) in the south and southwest portions of the site. Figures 15a - 15b compiled from resistivity sounding data give profile views of the bedrock surface at various locations within the study site. Figure 10 gives the location of the profiles.

Figure 16 is a generalized bedrock contour map based on outcrop elevations, resistivity survey results, well logs, and previous bedrock contours reported by Rogers (1962). Resistivity data indicate the bedrock surface is somewhat irregular in the central portion of the study site. The data also indicate a decrease in bedrock elevations to the south. This decrease in elevation is consistent with the presence of a bedrock valley sloping towards the southwest as reported by Rogers (1962).

Site Hydrogeology

Introduction

Rogers (1962) performed one of the earliest detailed hydrogeologic investigations of the area surrounding the

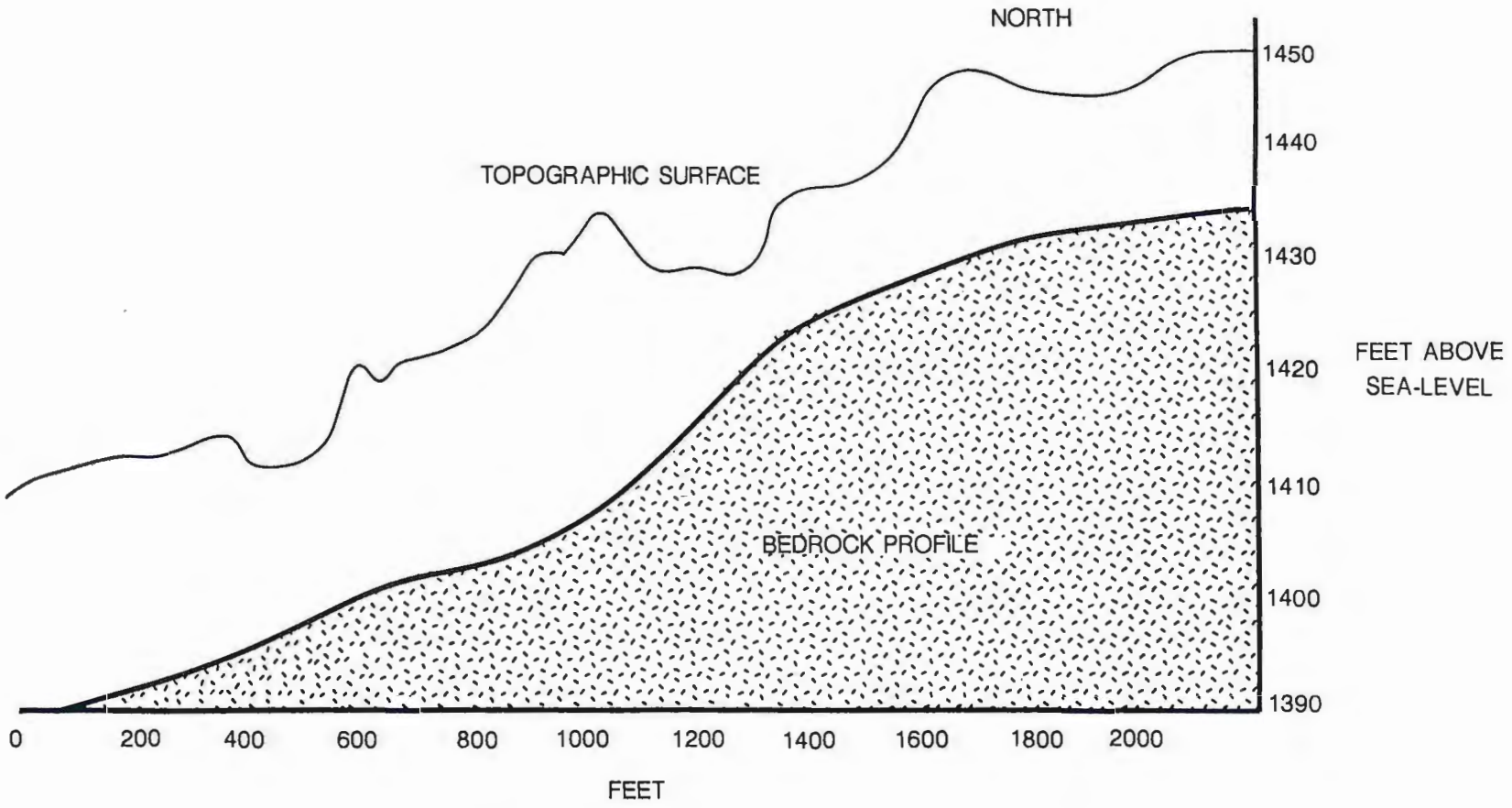

Figure 15a: Bedrock profile for section RL-1

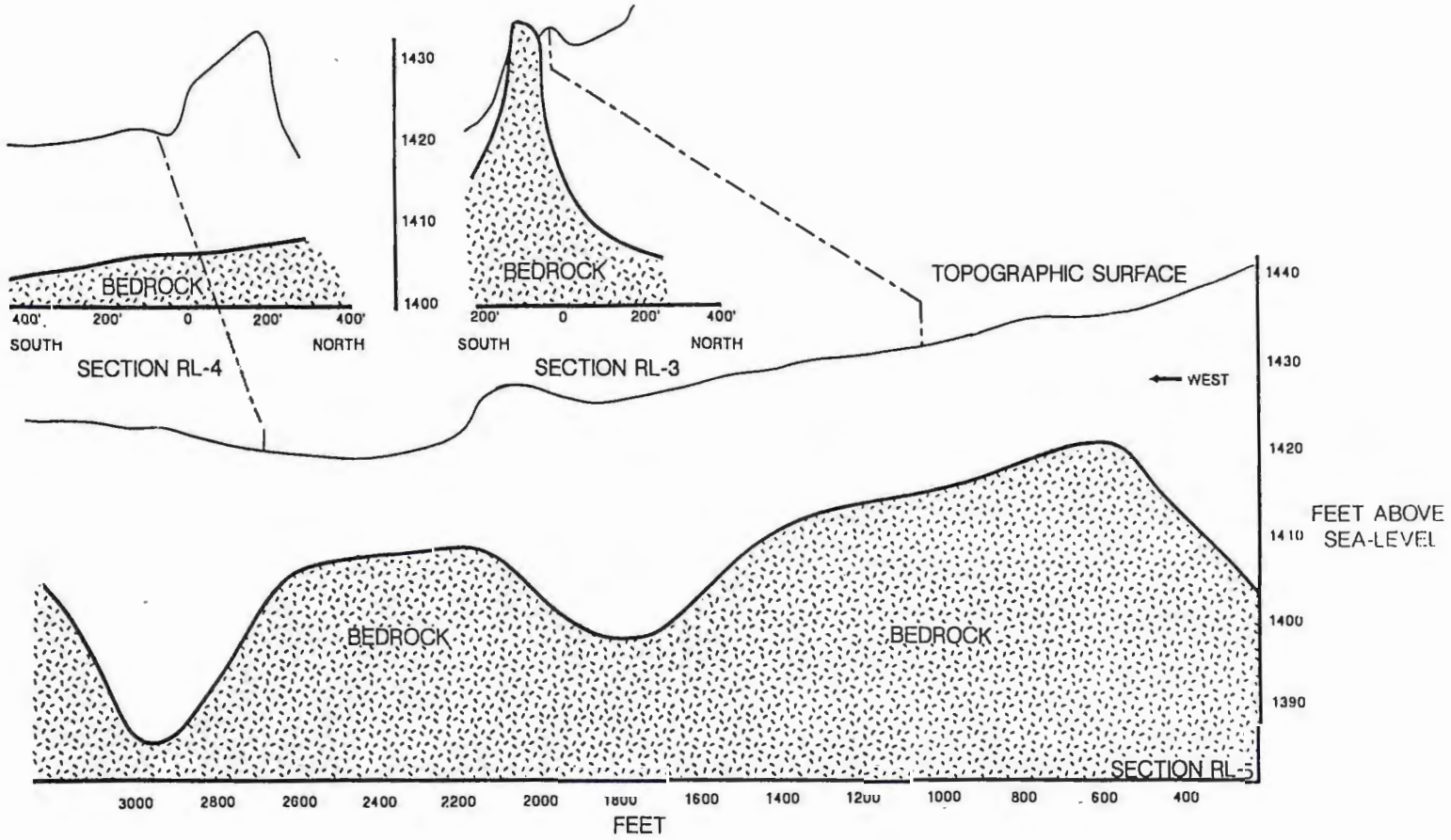

Figure 15b: Bedrock profiles for sections RL-3, RL-4, and RL-5 (After RREM, Inc., 1984).

Figure 16: Generalized bedrock contour map based on outcrop elevations, resistivity survey results, well logs, and previous bedrock contours reported by Rogers (1962).

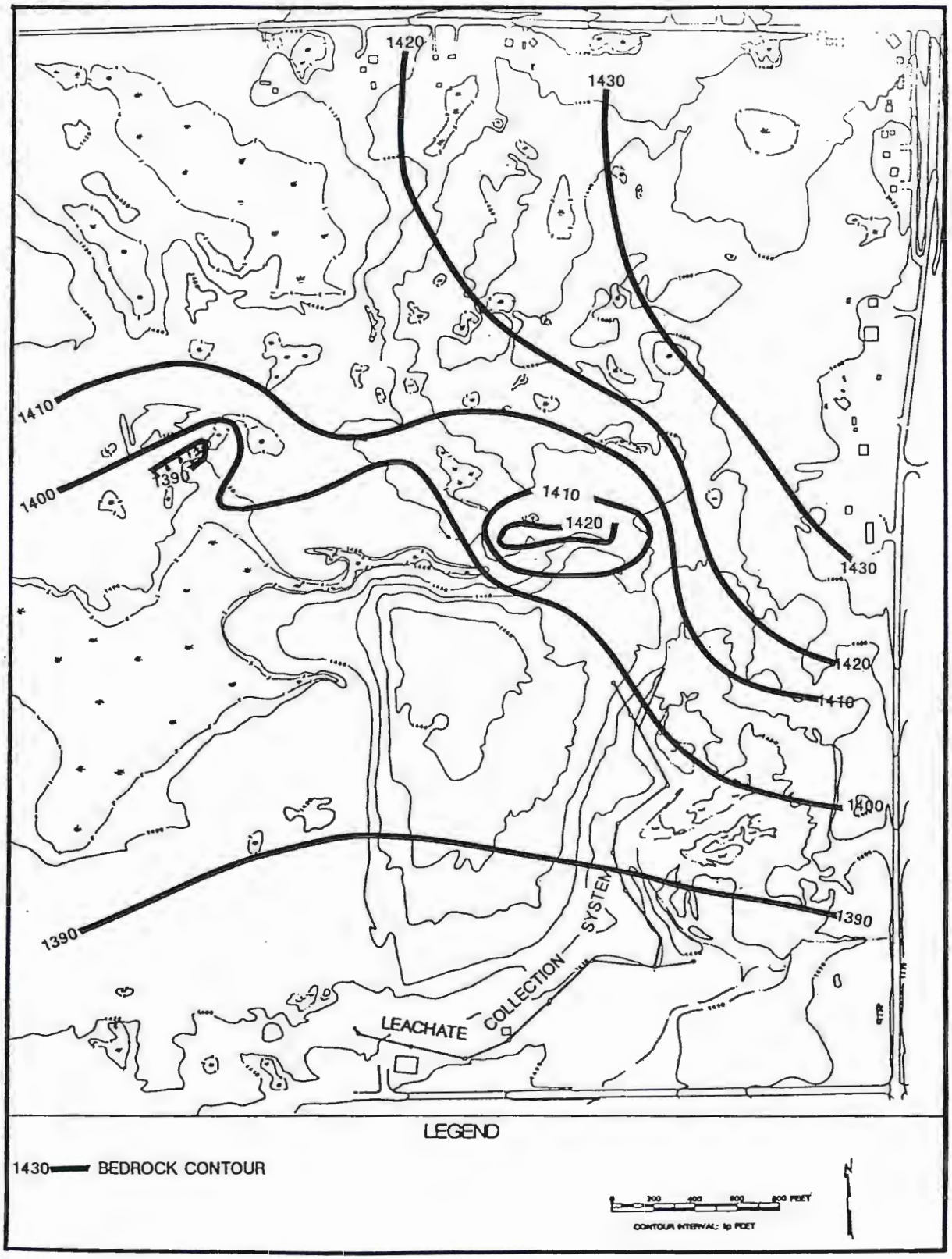
1420
1430
1410
1400
1390
1410
1420
1430
1420
1410
1400
1390
LEACHATE COLLECTION SYSTEM
LEGEND
1430 BEDROCK CONTOUR
CONTOUR INTERVAL: 10 FEET

study site. He reported great differences in the water-bearing characteristics of the glacial deposits. Two main water-bearing units were recognized by Rogers: kames composed of outwash sand and gravel; and a reddish-brown sandy till. At most locations, however, these units are only capable of supplying water for domestic supplies due to the limited areal extent of an individual kame, and the limited permeability and thickness of the reddish-brown sandy till (Rogers, 1962).

Recent detailed geologic and hydrogeologic investigations have focused on the landfill situated within the study area. Most of the recent investigations have been performed by engineering firms to determine the environmental impact of the landfill on the hydrologic environment.

One recent site-specific investigation was started in 1979 when Barr Engineering Co. was retained by WLSSD to investigate a leachate problem and design a retrofitted leachate collection system (Knight and others, 1983). In the study, Barr Engineering Co. placed several monitoring wells at the landfill to determine the groundwater gradient. Conclusions based on data obtained from these observation wells were: (1) the groundwater gradient is towards the south-southeast part of the landfill; and, (2) that a large groundwater mound had developed in the middle of the landfill as a result of the

deposition of refuse (Barr Engineering Co., 1979). To protect Miller Creek and to protect the quality of the groundwater downgradient of the landfill, a leachate collection system was constructed to intercept the contaminated groundwater and numerous toe seeps (Knight and others, 1983).

In 1984 RREM Inc. performed a two-phase study to examine the possibility of expanding the landfill. In their investigation RREM, Inc. analyzed resistivity survey results, observation well logs, and water level data.

Based on data collected at the site it was concluded that there was a groundwater divide extending in a northeast-southwest direction through the middle of the landfill (RREM, Inc., 1984). Water level data collected at the western edge of the site also indicated that a silty clay layer is acting as a semi-confining layer, placing a slight pressure on the underlying water-bearing silty sand unit.

Current investigations involve WLSSD personnel taking quarterly water level measurements and selected water samples for contaminant analyses. Soil samples are also periodically taken to determine the grain size distribution of the cover material.

Steady State Groundwater Elevations

Most of the tables and graphs in this section are shown with the Julian date, rather than the more familiar

day and month format. Table 4 is provided to compare day of the month dates to Julian dates.

Groundwater measurements were made in 15 observation wells during the late spring, summer, and early fall of 1985. Figure 17 shows the location of the observation wells. All of the observation wells terminated in the surficial sediment. Logs of wells P-4, 84-2, 84-4, 83-1, and 83-1 are included in Appendix A. Logs of wells 82-1, 82-2, 82-3, 82-4, 82-5, and 82-6 were not recorded during the drilling operation. These later wells all terminated in peat/organic silt (Barr Engineering Co., 1981). Logs for wells C-1, C-2, and W-6 were not available.

Fluctuation of the water levels within the observation wells, and the amount of precipitation recorded at the Duluth Municipal Airport are shown in Figures 18a - 18m. Water level measurements for each well are contained in Appendix C. Precipitation data are contained in Appendix D.

Water level fluctuations are usually seasonal with the highest water levels typically in the spring and fall. Factors contributing to the increase in water level during these seasons include: heavier precipitation; the presence of snow meltwater in the spring; and lower evapotranspiration rates than in the summer. Well hydrographs from the study site show this general trend.

JULIAN DATE CALENDAR
1985

DAY	MAY	JUNE	JULY	AUG	SEPT	OCT
1	121	152	182	213	244	274
2	122	153	183	214	245	275
3	123	154	184	215	246	276
4	124	155	185	216	247	277
5	125	156	186	217	248	278
6	126	157	187	218	249	279
7	127	158	188	219	250	280
8	128	159	189	220	251	281
9	129	160	190	221	252	282
10	130	161	191	222	253	283
11	131	162	192	223	254	284
12	132	163	193	224	255	285
13	133	164	194	225	256	286
14	134	165	195	226	257	287
15	135	166	196	227	258	288
16	136	167	197	228	259	289
17	137	168	198	229	260	290
18	138	169	199	230	261	291
19	139	170	200	231	262	292
20	140	171	201	232	263	293
21	141	172	202	233	264	294
22	142	173	203	234	265	295
23	143	174	204	235	266	296
24	144	175	205	236	267	297
25	145	176	206	237	268	298
26	146	177	207	238	269	299
27	147	178	208	239	270	300
28	148	179	209	240	271	301
29	149	180	210	241	272	302
30	150	181	211	242	273	303
31	151		212	243		304

Table 4: Table for comparing Julian dates to day of the month dates.

Figure 17: Observation well locations.

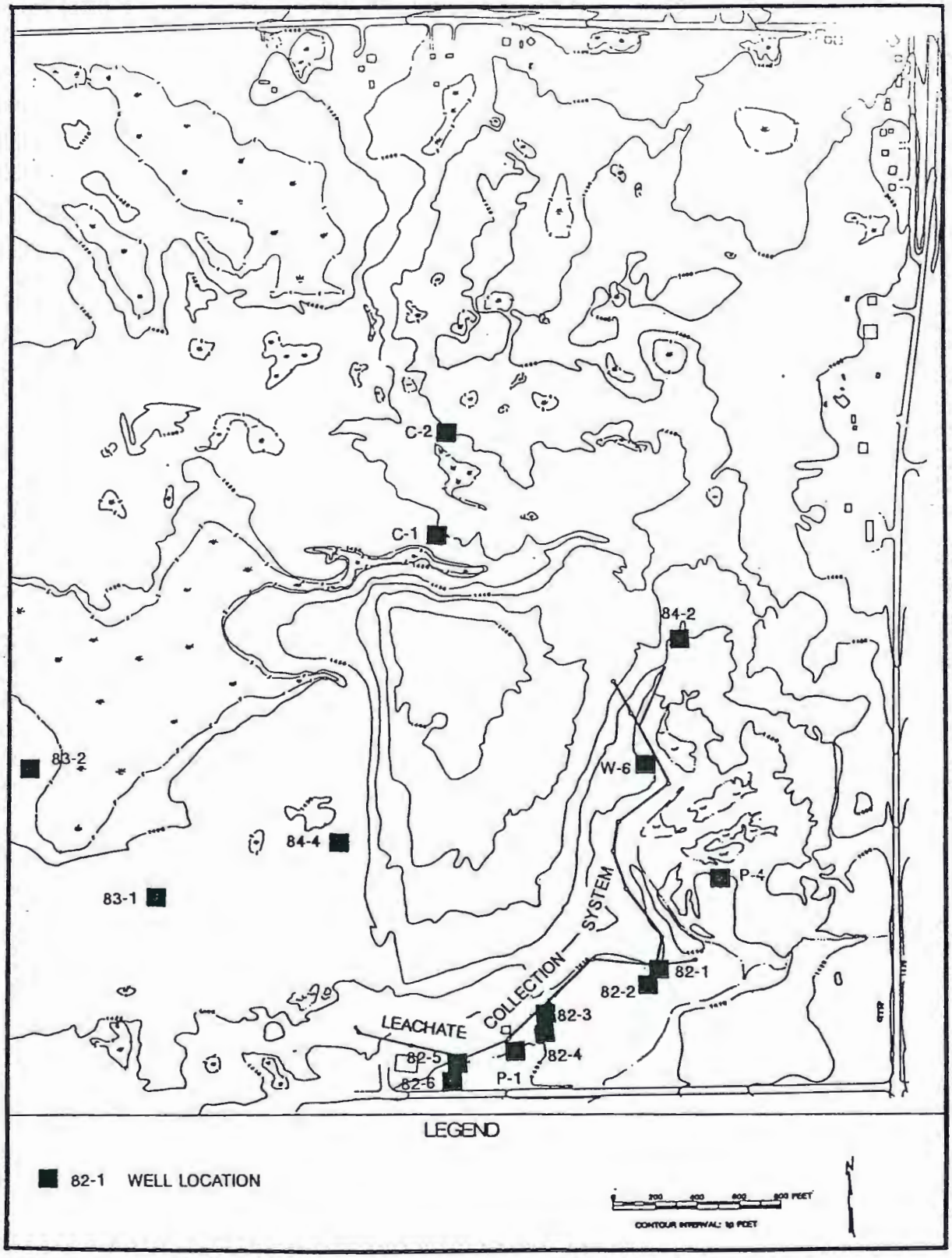
C-2
C-1
84-2
W-6
83-2
84-4
83-1
P-4
SYSTEM
COLLECTION
82-1
82-2
LEACHATE
82-3
82-4
82-5
82-6
P-1
LEGEND
82-1 WELL LOCATION
CONTOUR INTERVAL: 10 FEET

Figure 18a - 18m: 1985 precipitation events and water level fluctuations for observation wells located at the site.

82-1 WATER TABLE ELEVATION
WATER TABLE ELEVATION
1400
1401
1402
1403
1404
1405
PRECIPITATION (inches)
0
1
2
3
4
JULIAN DATE
150
170
190
210
230
250
270
290

Figure 18a

82-2 WATER TABLE ELEVATION
PRECIPITATION (inches)
WATER TABLE ELEVATION
JULIAN DATE
0
1
2
3
4
1400
1401
1402
1403
1404
1405
150
170
190
210
230
250
270
290

Figure 18b

82-3 WATER TABLE ELEVATION
PRECIPITATION (inches)
WATER TABLE ELEVATION
JULIAN DATE
1397
1398
1399
1400
1401
1402
150
170
190
210
230
250
270
290
0
1
2
3
4

Figure 18c

82-4 WATER TABLE ELEVATION
PRECIPITATION (inches)
WATER TABLE ELEVATION
JULIAN DATE
1397
1398
1399
1400
1401
1402
150
170
190
210
230
250
270
290
0
1
2
3
4

Figure 18d

82-5 WATER TABLE ELEVATION
PRECIPITATION (inches)
WATER TABLE ELEVATION
JULIAN DATE
0
1
2
3
4
1397
1398
1399
1400
1401
1402
150
170
190
210
230
250
270
290

Figure 18e

82-6 WATER TABLE ELEVATION
PRECIPITATION (inches)
WATER TABLE ELEVATION
JULIAN DATE
1397
1398
1399
1400
1401
1402
150
170
190
210
230
250
270
290
0
1
2
3
4

Figure 18f

P-1 WATER TABLE ELEVATION
WATER TABLE ELEVATION
1399
1400
1401
1402
1403
1404
PRECIPITATION (inches)
0
1
2
3
4
JULIAN DATE
150
170
190
210
230
250
270
290

Figure 18g

P-4 WATER TABLE ELEVATION
WATER TABLE ELEVATION
1408
1409
1410
1411
1412
1413
JULIAN DATE
150
170
190
210
230
250
270
290
PRECIPITATION (inches)
0
1
2
3
4

Figure 18h

83-2 WATER TABLE ELEVATION
WATER TABLE ELEVATION
1415
1416
1417
1418
1419
1420
JULIAN DATE
150
170
190
210
230
250
270
290
PRECIPITATION (inches)
0
1
2
3
4

Figure 18i

C-1 WATER TABLE ELEVATION
WATER TABLE ELEVATION
1417
1418
1419
1421
1422
1423
PRECIPITATION (inches)
0
1
2
3
4
JULIAN DATE
150
170
190
210
230
250
270
290

Figure 18j

C-2 WATER TABLE ELEVATION
WATER TABLE ELEVATION
1423
1424
1425
1426
1427
1428
JULIAN DATE
150
170
190
210
230
250
270
290
PRECIPITATION (inches)
0
1
2
3
4

Figure 18k

84-2 WATER TABLE ELEVATION
PRECIPITATION (inches)
4
3
2
1
0
290
270
250
230
210
190
170
150
JULIAN DATE
1419
1421
1422
1424
1425
1427
WATER TABLE ELEVATION

Figure 18l

84-4 WATER TABLE ELEVATION
PRECIPITATION (inches)
WATER TABLE ELEVATION
JULIAN DATE
4
3
2
1
0
1425
1424
1423
1422
1421
1420
290
270
250
230
210
190
170
150

Figure 18m

The amount of water that recharges an unconfined aquifer is determined by a number of factors such as the amount of precipitation that is not lost by evapotranspiration and runoff, the vertical hydraulic conductivity of the surficial deposits, and the transmissivity and potentiometric gradient of the aquifer (Fetter, 1980). If the water-bearing unit is overlain by a unit of lower permeability (typically a silt or clay-rich unit) the amount of water that percolates to the water table can be retarded or even diverted. Visual inspection of the hydrographs shows significant variations in the water level response of different wells to the same precipitation event. Wells 83-1, 83-2, W-6, C-1, and 82-1 showed little water level fluctuation during the monitoring period. The water levels in P-1, P-4, 84-2, 84-4, 82-5, and 82-6, however, changed markedly. These variations can be attributed to stratigraphic heterogeneity, and subtle differences in the hydraulic conductivity of the surficial sediments.

The mild variations in water levels observed for wells 83-1, 83-2, and 84-4 may be due to the presence of a silt and clay-rich layer overlying the water-bearing silty sand. The silt and clay-rich layer, which exhibits a slight confining pressure on the silty sand (RREM, 1984), may slow the downward leakage of water, thereby dampening the response of the water table to precipitation.

Water levels in wells 84-2, P-1, and P-4 show the opposite relationship. These wells are located in areas devoid of the silt and clay-rich semi-confining layer.

Wells 82-1, 82-2, 82-3, 82-4, 82-5, and 82-6 were constructed to permit monitoring of the leachate collection system installed in 1981. The leachate collection system was designed to intercept toe seeps and contaminated groundwater migrating to Miller Creek. The system consists of permeable filler materials in a trench, and slotted collection pipe used to transfer the contaminated groundwater by gravity to a lift station where it is pumped to a treatment facility. Figure 19 shows a generalized cross-section of the system.

To effectively intercept the toe seeps and the contaminated groundwater, it was essential to reverse the groundwater gradients in the area opposite the landfill (Knight and others, 1983). Reversal in the groundwater gradients can be observed by comparing water levels in the observation wells installed on the southern and southeastern sides of the collection system. When the collection system is operating properly, the water level in 82-1 is lower than 82-2, the water level in 82-3 is lower

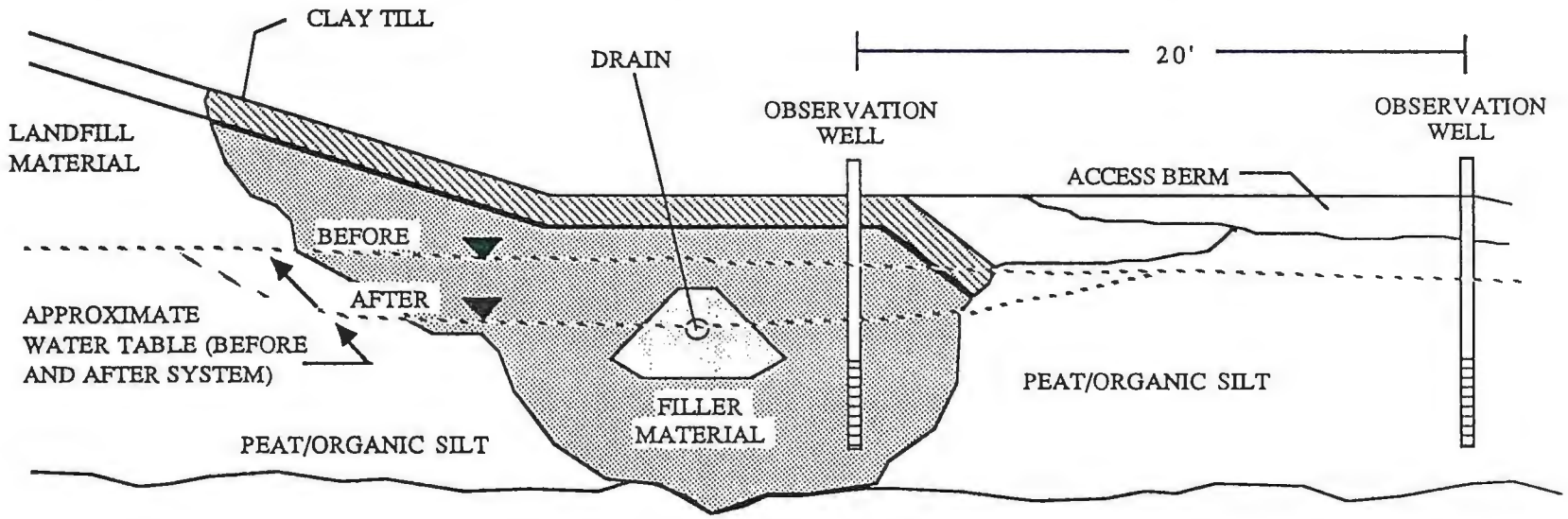

Figure 19: Generalized cross-section of the leachate collection system. (After Knight and others, 1983.)

than 82-4, and the water level in 82-5 is lower than 82-6. Hydrographs of wells 82-5 and 82-6 suggest that the reversed gradient at the southwestern arm of the collection system was not maintained for much of the monitoring period (Figure 20). The reasons for the gradient fluctuations are not clear at this time.

Flow Directions

The water level map for the study area was constructed from water level measurements made on July 31, 1985. The water level map (Figure 21) shows water level contours, the location of a suspected groundwater and surface water divide, and groundwater flow directions.

The local flow system in the study area is a subdued expression of the topography. Flow is from topographically high recharge areas toward the Wild Rice Lake Basin to the northwest, and the Miller Creek Basin to the southeast (Figure 22). The groundwater divide extending in a southwest to northeast direction appears to coincide generally with the surface water divide reported by RREM, Inc. (1984).

Figures 21 and 22 indicate the presence of a large groundwater mound located in areas where refuse is deposited. This mound developed early in the landfill's history. When the landfill was originally built, very little runoff occurred due to improper slope gradients.

Figure 20: Hydrograph showing water level relationship between wells 82-5 and 82-6.

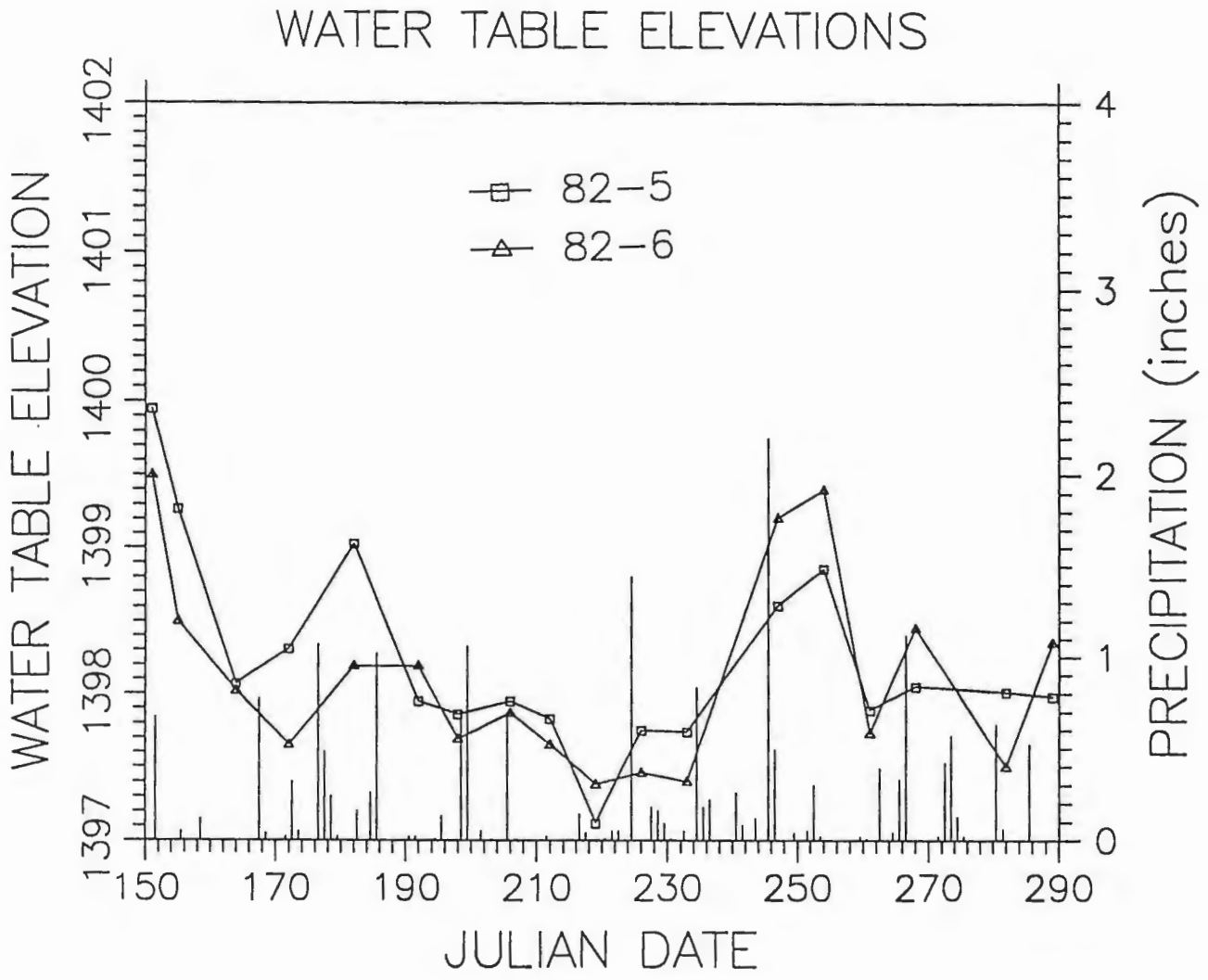
WATER TABLE ELEVATIONS
82-5
82-6
WATER TABLE ELEVATION
1397
1398
1399
1400
1401
1402
PRECIPITATION (inches)
0
1
2
3
4
150
170
190
210
230
250
270
290
JULIAN DATE

Figure 21: Water level map for study site.

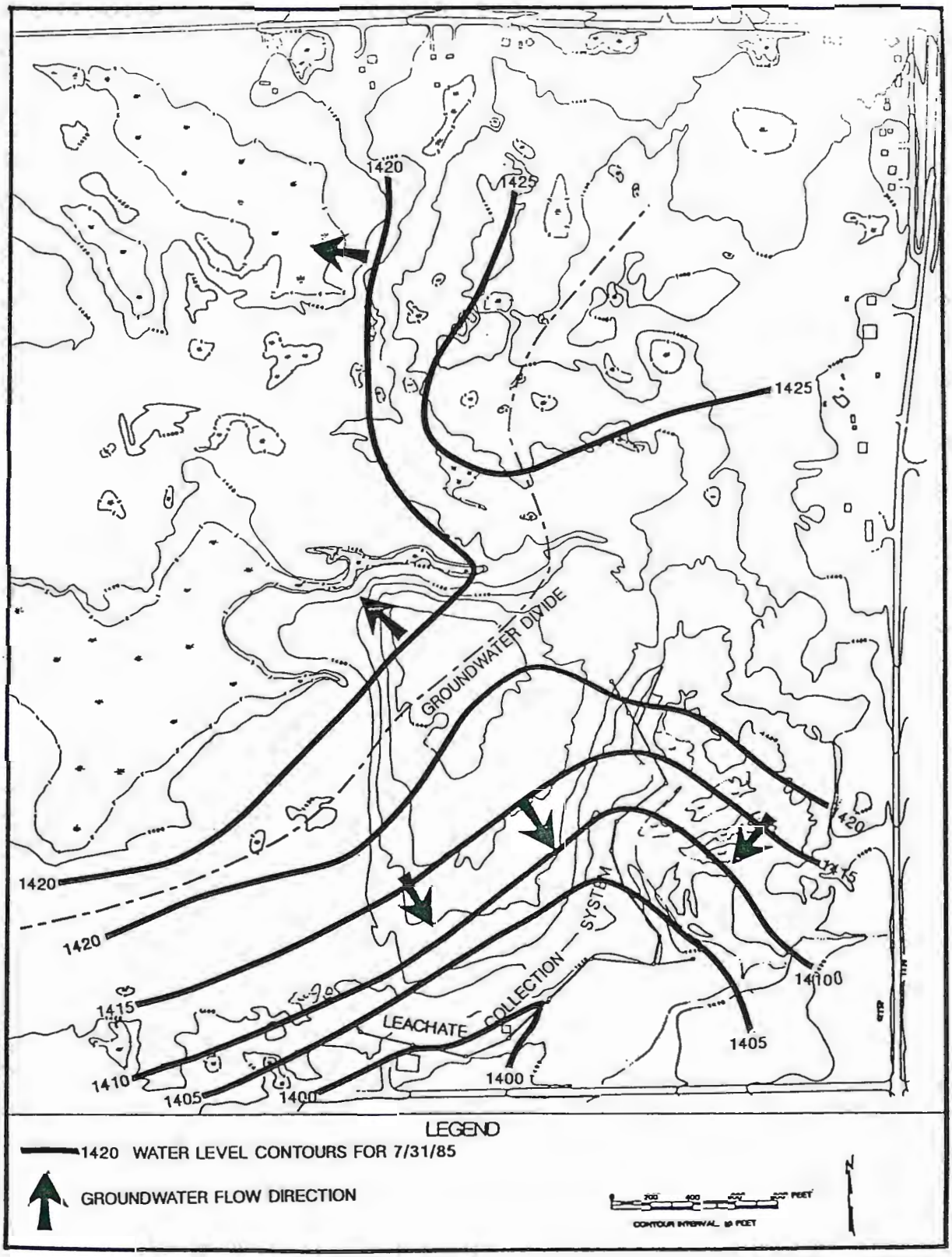
1420
1425
1425
GROUNDWATER DIVIDE
1420
1420
1420
1415
1410
1405
1400
1400
1405
LEACHATE COLLECTION SYSTEM
LEGEND
1420 WATER LEVEL CONTOURS FOR 7/31/85
GROUNDWATER FLOW DIRECTION
CONTOUR INTERVAL 5 FEET
N

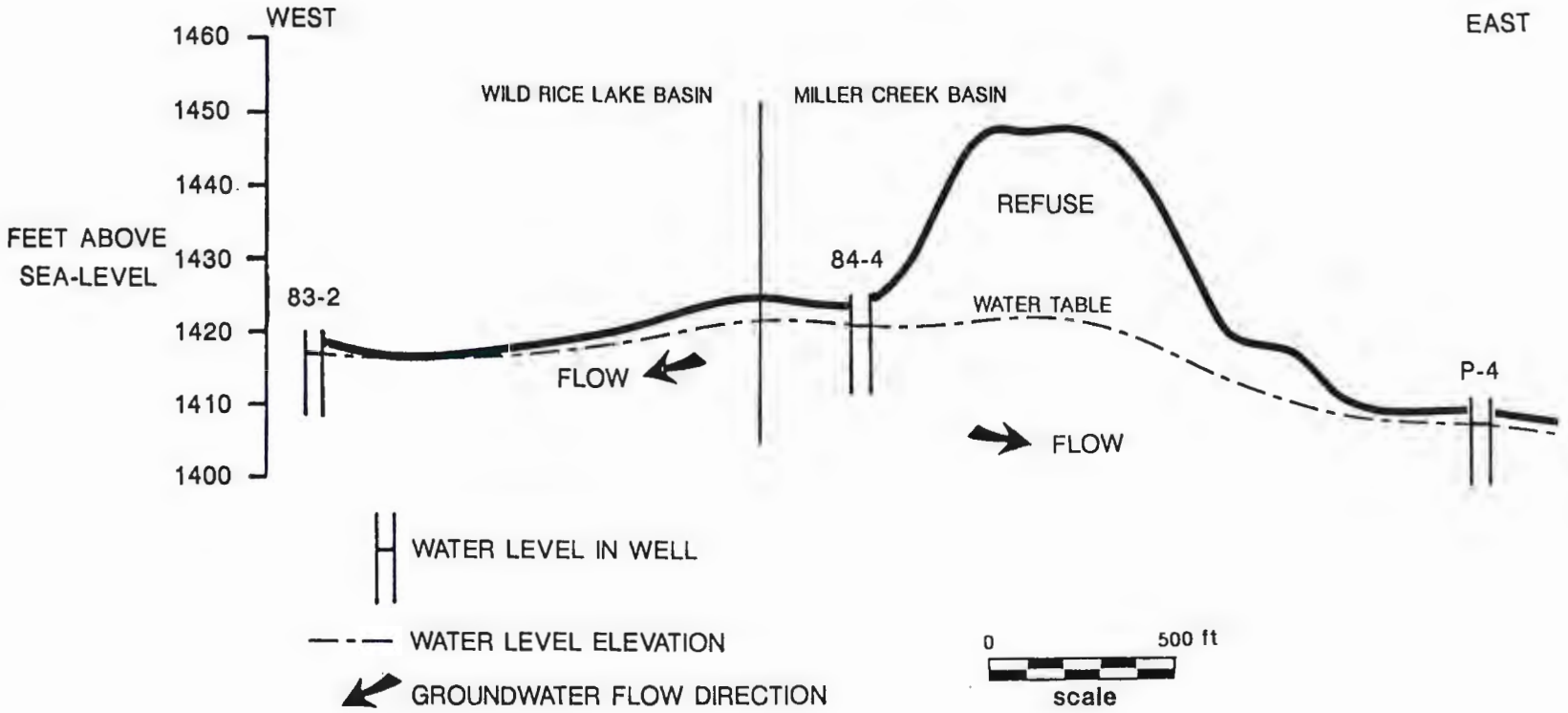

Figure 22: Cross-section showing groundwater flow directions.

Because of the amount of silt and clay in the cover material, water moved laterally through the refuse along the surface of the soil more easily than it moved through the soil. This caused the percolating precipitation to raise the water table and eventually form a mound within the deposited refuse.

Groundwater flow directions indicate that the water from the recharge zone moves through the refuse and discharges to the southeast. It was determined by WLSSD personnel that groundwater flowing through the refuse was leaching chemicals from the waste and discharging into Miller Creek, significantly affecting the creek's water quality (Knight and others, 1983).

To collect and treat the contaminated groundwater, WLSSD installed a leachate collection system in areas downgradient of the refuse. For the system to work properly the contaminated groundwater must flow towards the collection system. Flow lines constructed perpendicular to lines of equal water table elevations indicate that at least some of the groundwater flowing through the refuse is intercepted by the leachate collection system.

Groundwater Gradients and Flow Rates

Groundwater flows from areas of higher hydraulic head to areas of lower hydraulic head. The slope of the water table is the hydraulic gradient under which groundwater

movement takes place in unconfined (water table) aquifers. The water table elevations show that the groundwater surface has a gradient towards the leachate collection system (southeast) on the southeastern side of the groundwater divide; and towards the west and northwest, on the opposite side of the groundwater divide.

Visual inspection of the groundwater contours indicates that the slope (or gradient) of the water table is not the same on both sides of the groundwater divide. To quantify the hydraulic gradient, the differences of head between two wells are divided by the distance along the flow path where the heads were measured:

$$[1] \qquad i = \frac{h_1 - h_2}{L}$$

where

i = hydraulic gradient (m/m)
$h_1 - h_2$ = difference in head (m)
L = distance between points h_1 and h_2 (m)

Table 5 contains the difference in elevation and the groundwater gradients between three locations in the study area. The average gradient is given in percent (the drop of groundwater surface in meters per 100 meters of horizontal distance). These gradients are only average values: the leachate collection system undoubtedly affected the differences in the groundwater gradients between wells

FROM	TO	DROP IN WATER LEVEL ELEVATION ($h1 - h_2$)	LENGTH BETWEEN h_1 and h_2	AVERAGE GRADIENT (percent)
84-2	W-6	8.11 ft 2.47 m	620 ft 189 m	1.31
84-4	P-1	22.49 ft 6.86 m	1240 ft 378 m	1.81
**	83-2	7.74 ft 2.36 m	660 ft 201 m	1.17

** - Groundwater divide between 83-1 and 83-2

Table 5: Average groundwater gradients.

84-4 and P-1, and wells 84-2 and W-6. The value for the gradient on the northwestern side of the divide could only be estimated using the location of the groundwater divide as a head reference. This was necessary due to the lack of wells on the northwestern side of the divide.

As indicated by the spacing of the water level contours, the calculated hydraulic gradient is higher on the southeastern side of the groundwater divide than on the northwestern side of the divide. The gradients ranged from 1.17% on the western side of the groundwater divide to 1.81% on the eastern side of the divide.

Since the groundwater flow velocity is related to the hydraulic gradient by Darcy's Law:

$$[2] \qquad V = \frac{K * i}{n}$$

where

V = velocity (m/day)
K = hydraulic conductivity (m/day)
i = hydraulic gradient (m/m)
n = porosity

the horizontal groundwater velocity can easily be calculated if the porosity and hydraulic conductivity of the unconsolidated sediment are known.

Using an average hydraulic conductivity of 6.63×10^{-2} m/day (the average of 4 hydraulic conductivity values determined by Scholl (1984) for the silty sand at the

site), assuming a porosity of 0.3 (Fetter, 1980), and the hydraulic gradients in Table 5, the groundwater flow rates were calculated for 4 locations at the study site.

The calculated flow velocity (Table 6) indicates that the groundwater flows about 3.5 times faster on the eastern side of the groundwater divide than on the western side. The calculated groundwater flow rates are low for a silty sand in this area, according to previous studies (RREM, 1985). This may be due to the the high density of the silty sand which significantly impedes the movement of the groundwater.

These groundwater flow rates are not to be taken as absolute values. They are presented only to give a general indication of the expected flow rates in the study area.

Summary and Conclusions

The study site is situated in a complicated ice-stagnation complex known as the Highland Moraine. From geomorfic and sediment analyses it was determined that the site is located in the silt-rich Upper Cromwell Formation.

Subsurface exploration data reflect the heterogeneity of the glacial deposits at the study site. Well logs and resistivity surveys indicate that the study site is underlain by a silty sand layer that contains interbeds of gravel, and sand and gravel. Overlying this silty sand

FROM	TO	K m/day	AVERAGE FLOW RATE m/day	m/year	ft/year
84-2	W-6	.0663	.0029	1.05	3.34
84-4	P-1	.0663	.0040	1.46	4.79
**	83-2	.0663	.00078	0.28	0.93

** - Groundwater divide between 83-1 and 83-2

Table 6: Average groundwater flow rates.

unit in the western part of the study site is a silty clay layer.

Sediment samples collected from the eastern edge of the site ranged in textural class from a sandy loam to loam to silt loam. The average sand/silt/clay ratio was 45/46/9 (average of 23 samples).

The bedrock that underlies the study site is gabbro. Depth to bedrock varies from surface outcrops in the north-central region of the site, to 40 to 50 feet (12.2 - 15.2 m) in the south and southwest parts. Resistivity data indicate that the irregular bedrock surface slopes to the south-southwest.

Groundwater measurements made in 15 observation wells from May 31, 1985 to October 16, 1985 indicate that the water level fluctuations were seasonal: the highest water levels were during the spring and fall. Well hydrographs for the observation wells showed that the wells had different responses to the same precipitation events. Wells in the western section of the site showed smaller fluctuations during the monitoring period. This is due to the presence of a silty clay layer overlying the water-bearing silty sand unit. The silty clay layer may have inhibited downward leaking of the percolating precipitation. Wells located in areas devoid of the semi-confining silty clay layer showed greater responses to precipitation events.

Hydrographs of wells on the southwestern arm of the leachate collection system indicate that during part of the monitoring period the reversed gradient, needed to effectively intercept contaminated groundwater, was not maintained. The reasons for the gradient fluctuations are not apparent at this time.

The flow of the groundwater at the site is from topographically high recharge areas toward the Wild Rice Lake Basin to the northwest, and the Miller Creek Basin to the southeast. The groundwater divide extends in a southwest to northeast direction through the western edge of the landfill. Groundwater flow directions indicate that at least some of the groundwater flowing through the refuse is being intercepted by the leachate collection system.

Groundwater gradients at the study site range from 1.17% on the western side of the divide to 1.81% on the eastern side of the divide. Using a permeability of 6.63×10^{-2} m/day and a porosity of 0.3 the groundwater flow velocity was estimated using the calculated hydraulic gradients. The flow velocity for the western side was calculated to be about .28 m/year, whereas the flow velocity for the eastern side was calculated to range from 1.05 to 1.46 m/year.

HEAVY-METAL TRANSPORT STUDY

Introduction

This chapter centers on the utilization of a one-dimensional transport model for the movement of Cd, Pb, Ni, Zn, and Cu through unconsolidated sediments under steady state saturated moisture flow. This model was based, in part, on experimentally determined breakthrough curves for the heavy metals listed above. This chapter also discusses the results of a batch equilibrium study performed to help describe the kinetics of the heavy metal adsorption with the sediment.

A goal in the land disposal of wastes is to minimize the contact of toxic pollutants with the environment. Because sediment/soil (unconsolidated sediment, regolith) is the main controlling factor in the maximization of pollutant containment, numerous studies have been undertaken to describe the complex relationship between sediment and pollutants. As a result of these studies user-oriented equations have been developed to help predict the extent of pollutant migration. Once functional data are obtained for the soil and pollutant(s), these equations can be employed to help determine the degree of action that is necessary to prevent or halt groundwater contamination.

Lapidus and Amundson (1952) have presented one such

equation, which describes the movement of adsorbed pollutants through porous media under steady state soil water conditions:

$$[3] \qquad \frac{\partial C}{\partial t} + \frac{\partial X}{\theta_v \, \partial t} = D \frac{\partial^2 C}{\partial z^2} - V \frac{\partial C}{\partial z}$$

where

C = concentration of pollutant in soil solution (units M/L^3)
V = convective (pore water) velocity (L/T)
D = apparent diffusion coefficient (L^2/T)
θ_v = volumetric water content of soil (L^3/L^3)
X = amount of pollutant adsorbed per unit volume of soil (M/L^3)
z = vertical distance (L)
t = time (T)

The adsorption rate (i.e., X/t) is assumed to be described as a first order reaction:

$$[4] \qquad \partial X/\partial t = K_1 C - K_2 X$$

where K_1 and K_2 are forward and backward reaction terms. This implies that the rate of adsorption of the pollutant by soil is finite. Equation [3] has been solved and models utilizing forms of this equation have been utilized by Enfield and Shew (1975) for phosphorus movement in soils, and van Genuchten and others (1974) for pesticide movement in soils. Amoozegar-Fard and others (1984), have developed a simplified equation based on the Lapidus-Amundson model for which apparent diffusion and forward and reaction

coefficients are best fitted to whatever experimental data are available. A problem with many of these models is that they require the use of high-speed digital computers which often limit their use to a small group of theoreticians (Amoozegar-Fard and others, 1984).

The thrust of recent modeling studies has been to develop equations that require little or no main-frame computer time. Amoozegar-Fard and others (1983) presented such a user-oriented error-function model for the movement of an ion through soil. This error-function model that fits a sigmoidal breakthrough curve is presented with two unknown parameters that can be estimated explicitly by a small calculator. The error-function model for one-dimensional flow for a step input of salt is described by:

$$[5] \qquad C/C_0 = (0.5)\,\mathrm{erfc}[(Rz-vt)/(4DRt)^{0.5}]$$

where

C = concentration in soil water (M/L^3)
C_0 = concentration in input solution (M/L^3)
z = depth (L)
t = time (T)
v = pore water velocity (L/T)
R = retardation factor (dimensionless)
D = diffusion-dispersion coefficient (L^2/T)
erfc = complementary error function

Because of the simplicity of Equation [5], the two parameters R and D can be estimated explicitly and easily

as follows (Amoozegar-Fard, Warrick, and Fuller, 1983). With t in terms of pore volume P, length of interest L, and pore water velocity v,

$$[6] \qquad t = PL/v$$

Equation [5] yields

$$[7] \qquad (RLv/4DP)^{0.5} - (LvP/4DR)^{0.5} = \text{erfc}^{-1}(2C/C_0)$$

in which $\text{erfc}^{-1}(2C/C_0)$ is the inverse complementary error function of $2C/C_0$. Assuming that C_i/C_0 and P_i are the measured values of the relative concentration and pore volume displacement for the i^{th} point, and n is the total number of experimental points, minimization of the sum of the squares of the differences between calculated $\text{erfc}^{-1}(2C/C_0)$ and experimental values of $\text{erfc}^{-1}(2C/C_0)$ results in explicit relationships for R and D:

$$[8] \qquad R = a/b,$$

$$[9] \qquad D = Lv/(4ab),$$

with

$$[10] \quad a = \frac{n\ P_i^{0.5}[\text{erfc}^{-1}(2C_i/C_o)] - P_i[\text{erfc}^{-1}(2C_i/C_o)/P_i^{0.5}]}{n^2 - P\ (1/P_i)}$$

and

$$[11] \quad b = (a/n)(1/P_i) - (1/n)[\text{erfc}^{-1}(2C_i/C_0)/P_i^{0.5}]$$

where the sums are taken over the n points.

Table 7 presents the values of $\text{erfc}^{-1}(2C_i/C_0)$ for 19 values of C_i/C_0 from 0.05 to 0.95. If necessary, other values can be calculated by interpolation. Table 7 is useful to find $\text{erfc}^{-1}(2C_i/C_0)$ for the n experimental values. Substitution of corresponding values of P_i and $\text{erfc}^{-1}(2C_i/C_0)$ in Equation [10] gives a. Use of Equation [11] and the calculated value of a with corresponding values of P_i and $\text{erfc}^{-1}(2C_i/C_0)$ gives b, from which R and D are defined.

It is useful to describe the adsorptive characteristics of a pollutant when performing modeling studies. Batch equilibrium studies have been used to help interpret the kinetics of adsorption. A batch equilibrium study uses a system where a known volume of solid particles is put in contact with a known volume of solution and the change in concentration of the solution phase is measured

C/C_0	$erfc^{-1}(2C/C_0)$
0.05	1.1610
0.10	0.9062
0.15	0.7329
0.20	0.5951
0.25	0.3708
0.30	0.4770
0.35	0.2725
0.40	0.1791
0.45	0.0889
0.50	0.0000
0.55	-0.0889
0.60	-0.1791
0.65	-0.2725
0.70	-0.3708
0.75	-0.4770
0.80	-0.5951
0.85	-0.7329
0.90	-0.9062
0.95	-1.1610

Table 7: Relative concentration C/C_0 and corresponding values of inverse complementary error function of $2C/C_0$ (From Amoozegar-Fard, and others, 1983).

either as a function of time or after a set contact period (Fuller and Warrick, 1985). Caution must be used when applying data obtained from a batch adsorption test to a field situation since batch study results do not fully take into consideration the effects of diffusion-dispersion, pore-water velocity and volumetric water content.

The adsorption process is generally described as being thermodynamic (instantaneous) or kinetic (time-dependent). Instantaneous adsorption for phosphate (Fitter and Sutton, 1975), pesticides (Rao and others, 1979), cadmium, copper and zinc (Sidle, 1976) and cadmium (Christensen, 1984) have been described by the Freundlich relationship, which has the form:

[12] $$X = K_f C^{1/n}$$

where

X = amount of constituent adsorbed per gram of sediment (M/M)
C = concentration of adsorbate at equilibrium (M/L^3)
K_f = constant
1/n = constant

Estimating the constants is possible by transforming the equation into the form:

[13] $$\log X = \log K + (1/n) \log C$$

Problems with the Freundlich equation include the failure

to express X as a linear function of C at low concentrations, and the failure to provide for a maximum value of X (Adamson, 1967). Moreover, application of the Freundlich equation is limited to ranges of intermediate surface coverage at infinite concentration, a condition that does not often occur (Anderson and Rubin, 1981).

Kinetic adsorption for zinc (Udo and others, 1970), cadmium (John, 1972), lead (Griffen and Shimp, 1976), and heavy metals (Wong and others, 1983) has been described by the Langmuir adsorption equation which has the form

$$[14] \qquad X = X_m C/K_L + C$$

where

C = equilibrium concentration of adsorbate (M/L^3)
X = amount of adsorbate adsorbed per gram of soil (M/L^3)
X_m = adsorption maxima
K_L = constant related to bonding energy

Estimating the constants is then possible by transforming the equation into the form:

$$[15] \qquad C/X = C/X_m + K/X_m$$

Langmuir (1918) developed the equation to describe the adsorption of gas molecules by homogeneous crystalline materials. After modification the equation has been widely used to describe the adsorption of constituents from

solution by heterogeneous solids (Anderson and Rubin, 1981). The main disadvantage to this equation is that it assumes adsorbent heterogeneity, and that adsorbents have only one elementary type of adsorption site with a single adsorption energy potential.

Materials and Methods

Adsorption Study

Sediment samples used in the batch equilibration study were taken at depth from locations within the landfill to avoid the high organic matter content near the surface which is atypical of the sediment below the site (Fuller and Warrick, 1985). The soil samples were air-dried, screened through a 2 mm sieve and stored in plastic bags. The sand/silt/clay ratio for the soil was 10/80/10.

Six solutions were prepared containing the hydrated nitrate salts of Pb, Zn, Cd, Cu, and Ni. The initial pH levels of the batch solutions were adjusted to 3.5 by the addition of HNO_3 or KOH. Concentration of the heavy metals for each batch solution are shown in Table 8.

Duplicate 5.000 g samples of sediment were weighed for each batch concentration and equilibration time. Soils were placed into 250 ml acid-washed centrifuge bottles with 50 ml of the equilibration solution. The bottles were then placed on a mechanical shaker and agitated for periods of 0.3, 1, 3, 10, and 30 hours (Sidle, 1976). After shaking, the bottles were centrifuged at 7500 rpm for 10 minutes and the supernatant was filtered through .45 um filter paper. The filtrate was analyzed for Pb, Ni, Cu, Cd, and Zn by atomic absorption spectrophotometry.

	BATCH SOLUTION NUMBER				
CATION	1	2	3	4	5
Copper	2 mg/l	4 mg/l	8 mg/l	16 mg/l	32 mg/l
Zinc	1 mg/l	2 mg/l	4 mg/l	8 mg/l	16 mg/l
Nickel	3 mg/l	6 mg/l	12 mg/l	24 mg/l	48 mg/l
Cadmium	1 mg/l	2 mg/l	4 mg/l	8 mg/l	16 mg/l
Lead	15 mg/l	30 mg/l	60 mg/l	120 mg/l	240 mg/l

Table 8: Initial concentration of heavy metals in batch solutions.

Column Study

The system used to study the transport of heavy metals through unconsolidated sediment, as shown in Figure 23, consisted of a 10.03 cm long PVC column (5.73 cm ID), a displacing-solution reservoir, and an automatic fraction collector.

The sediment samples were collected at depth from locations within the study area (Figure 24). Properties of the sediment used in the column study are shown in Table 9. The air-dried sediments were passed through a 2 mm sieve and gently spooned into the PVC column. The soil was spooned to a depth of 1-2 cm at a time and then packed with a rounded tamping device to minimize particle segregation and stratification (Fuller and Warrick, 1985). This procedure was repeated until the columns were tightly packed to the pre-determined height of 10 cm. PVC caps containing acid-washed porous plates were then connected to the ends of the column.

After packing, the columns were saturated with distilled-deionized water while inverted to exclude air and

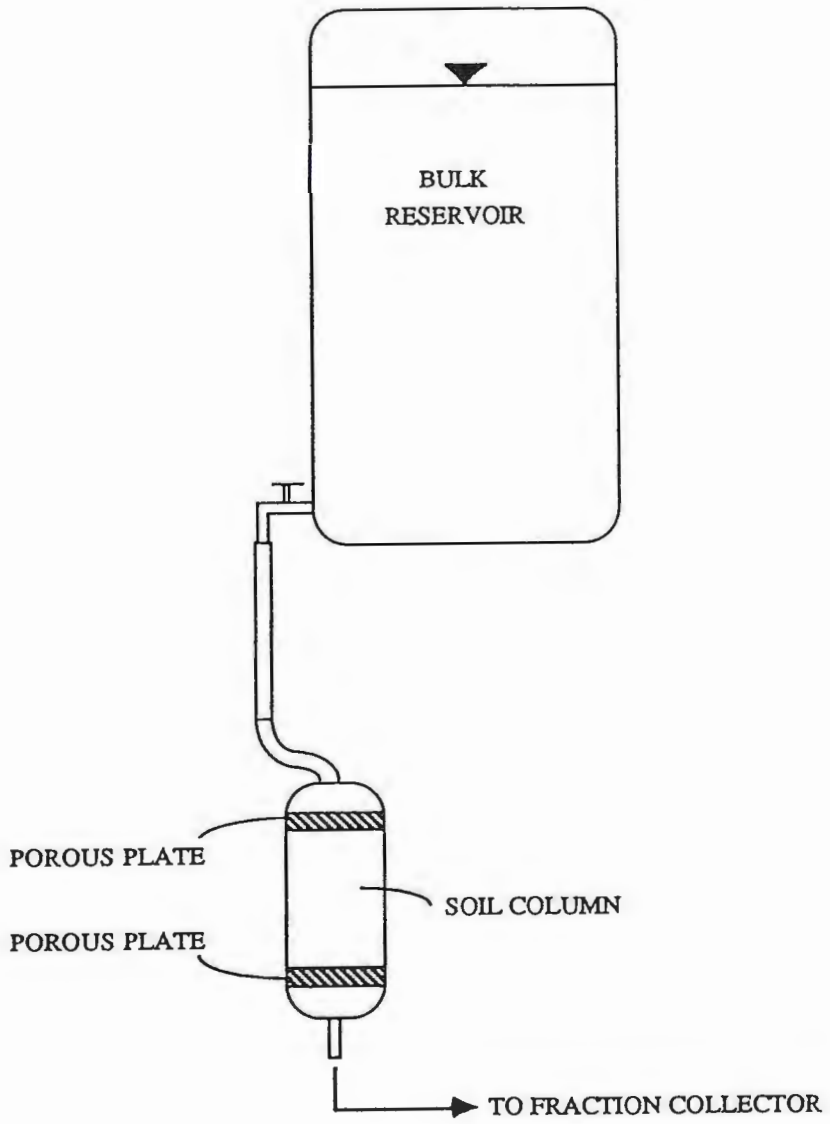

Figure 23: Simplified diagram of column apparatus.

Figure 24: Sediment sample locations for Column 1 and Column 2.

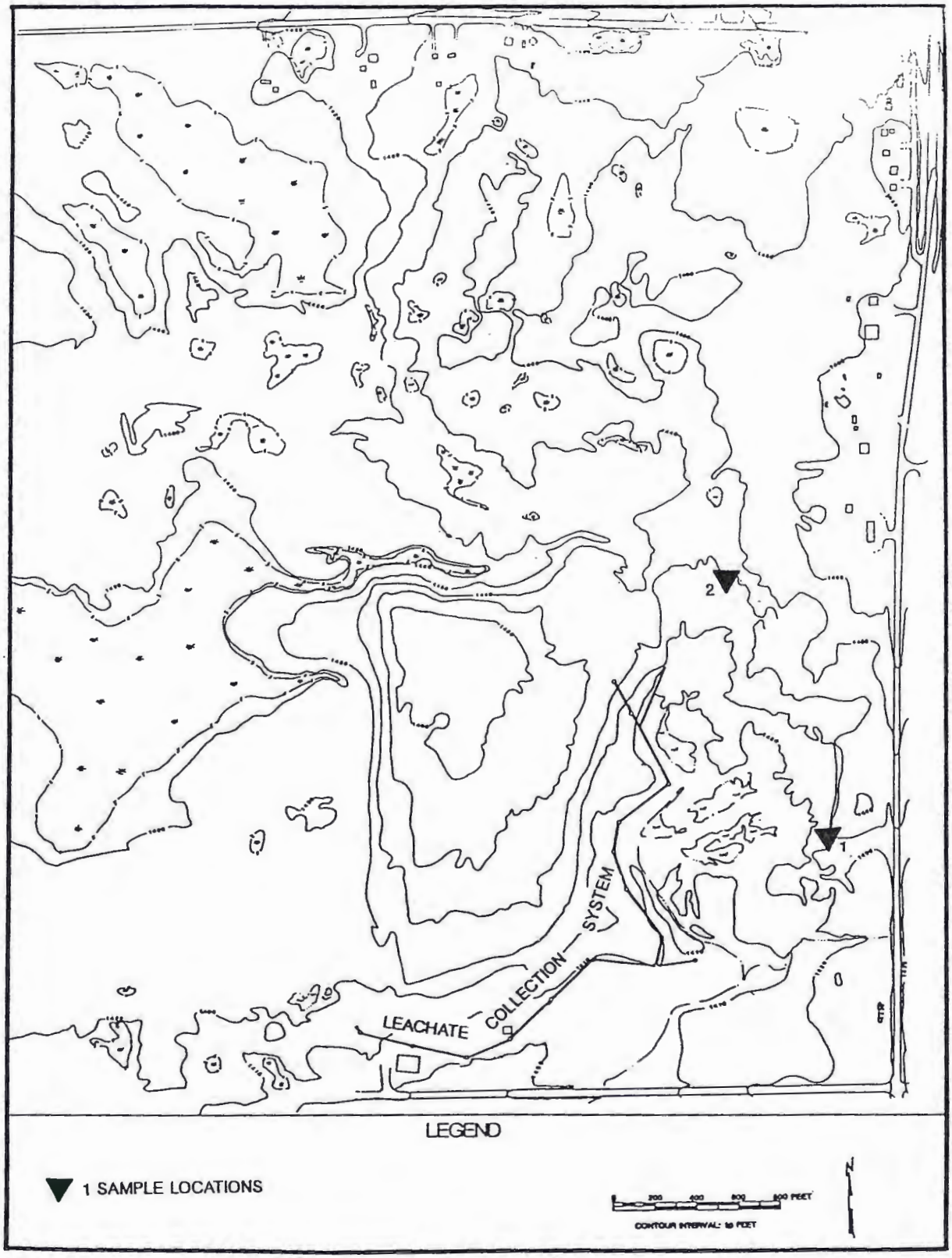
2
1
LEACHATE COLLECTION SYSTEM
LEGEND
1 SAMPLE LOCATIONS
CONTOUR INTERVAL: 10 FEET

PARAMETER	COLUMN 1	COLUMN 2
Soil Paste pH	6.7	7.0
(%) Iron	4.03	5.49
(%) Manganese	0.09	0.09
Column Bulk Density (g/cm^3)	1.65	1.77
Porosity (%)	38	33
% Sand	10	41
% Silt	80	42
% Clay	10	17
Surface Area (m^2/g)	10.09	7.75
Predominant Clay Minerals	Mont., Kaol.	Mont., Kaol.

** - Mont. = montmorillonite
Kaol. = kaolinite

Table 9: Characteristics of sediments used in the Column Study.

to provide uniform wetting (Korte and others, 1976). Column height was adjusted to maintain as uniform a flow rate as possible. Immediately after saturation, the columns were examined for channeling or piping. If any channels were observed, the column was taken apart and repacked. Once steady state flow was observed with distilled-deionized water, the heavy metal solution was introduced to the column and allowed to flow through at a rate of .75 to 1.5 pore volumes (PV) (the total volume of pores in the soil column is equal to 1 pore volume) per day. The heavy metal solution consisted of distilled-deionized water spiked with the hydrated nitrate salts of Cd, Cu, Ni, Zn, and Pb to concentrations of 90-150 mg/l. The characteristics of the displacing solutions are summarized in Table 10.

After leaching was initiated, the soil effluent was collected in acid-washed test tubes within the fraction collector. Two drops of HNO_3 were added and the samples were refrigerated until they were analyzed by atomic absorption spectrophotometry. Leaching was continued until breakthrough (effluent concentration = influent concentration) was observed for Cu, Cd, Ni, Zn and Pb.

Once breakthrough was observed for Cu, Cd, Ni, Zn, and Pb, the soil was extruded from the PVC column, oven dried, and segmented into 1 cm sections. The sections were weighed and then mixed and 1.000 g splits were taken for

PARAMETER	COLUMN 1	COLUMN 2
pH	3.5	3.5
Lead (mg/l)	150	150
Nickel (mg/l)	105	105
Cadmium (mg/l)	90	90
Copper (mg/l)	90	90
Zinc (mg/l)	90	90
Sodium (mg/l)	0.1	7.3
Potassium (mg/l)	1	1
Calcium (mg/l)	0.05	0.05
Magnesium (mg/l)	0.04	0.08

Table 10: Characteristics of displacing solutions used in the Column Study.

soil digestion. The 1.000 g splits were transferred to 400 ml acid-washed beakers and 20 ml of fresh aqua regia were added (Houle and others, 1981). The beaker was covered with a watch glass and the soil sample was digested by boiling to incipient dryness. After cooling, the watch glass and beaker wall were washed with distilled-deionized water and the volume was adjusted to 25-30 ml. Two ml of concentrated HNO_3 were added and the sample was brought to a slow boil for 15 minutes. The cooled sample was filtered through Whatman 40 filter paper and into a 100 ml volumetric flask. The resulting residue was washed with 1 N HNO_3, and then washed five times with distilled-deionized water. The filtrate was diluted to 100 ml and analyzed by atomic absorption spectrophotometry.

Instrumentation and Analytical Procedures

A model 360 Perkin-Elmer spectrophotometer was used to analyze for Cd, Cu, Ni, Zn, and Pb. The wavelength, slit, and acetylene to air mixture were set as recommended by the instruction manual. The cathode lamps were aligned to maximize the intensity of the light beam. The detection range for the metals is given in Table 11.

The soil surface area was determined by Quantachrome Corporation. The samples were first heated to drive out the impurities and then a single-point BET surface area analysis was performed by measuring the adsorbed helium on

ELEMENT	FLAMELESS AAS DETECTION RANGE (mg/l)
Copper	0.09 - 25
Lead	0.50 - 25
Zinc	0.018 - 5
Nickel	0.15 - 25
Cadmium	0.025 - 5

Table 11: Detection range of Atomic Adsorption Spectophotometer.

the solid surfaces of the soil.

X-ray diffraction analysis of the <.002 mm fraction of the soil samples was done on a Siemens diffractometer using Ni-filtered CuK (alpha) radiation. The <.002 mm clay fraction was prepared by pipetting 20 ml of the suspended <.002 mm fraction from a settling cylinder. The 20 ml fraction was filtered through a .45 um filter and allowed to dry at room temperature for 24 hours. The filters were then attached to a clean glass slide with double-sided tape which resulted in strongly oriented samples with {001} planes of the clay minerals parallel to the slide. The x-ray analysis was then performed on each sample at 2^{o}/minute from 4^{o} to 35^{o}.

Analysis of sodium, potassium, calcium and magnesium in the displacing solution, and iron (%) and manganese (%) in the soil was performed by methods approved by the U.S. Environmental Protection Agency.

Results and Discussion

Adsorption Study

Adsorption can be considered as the process in which a constituent entering the sediment/soil becomes physically or chemically bonded to the colloidal and mineral surfaces, thereby causing a net decrease in its concentration in the solution phase (John, 1972). Batch equilibrium studies

were performed with Pb, Zn, Cd, Ni, and Cu in order to describe the kinetics of the adsorption process. To accomplish this, data obtained from the batch equilibrium study were fitted to the Langmuir and Freundlich adsorption isotherms and plots of percent of adsorbed metal versus time were made.

Figures 25a - 25e are typical plots of percent of adsorbed metal versus time for the batch adsorption study. The data indicate that the adsorption of Pb, Cu, Cd, Zn, and Ni was rapid. This reflects the fact that the adsorption is predominantly a surface phenomenon, and that the colloid surfaces are accessible to the cations in solution (Anderson and Rubin, 1981). Concentrations of metal remaining in solution at various time intervals along with percent of metal removed from the initial batch solution are contained in Appendix E.

The results of the batch adsorption study indicate that the sediment had the highesty affinity for Pb, among the several metals tested. Nearly 91% of the Pb in solution is adsorbed within the first 0.3 hr of equilibration for the Batch 1 solution. Cu is the next most strongly adsorbed cation, with about 78% of the Cu in solution adsorbed within the first 0.3 hr, followed by Cd (53%), Zn (38%), and Ni (29%). Although the initial adsorption of the metals was nearly instantaneous (within minutes), the time for the metals in solution to reach

Figure 25a - 25e: Typical plots of adsorbed metal versus time for the Batch 1 Adsorption Study.

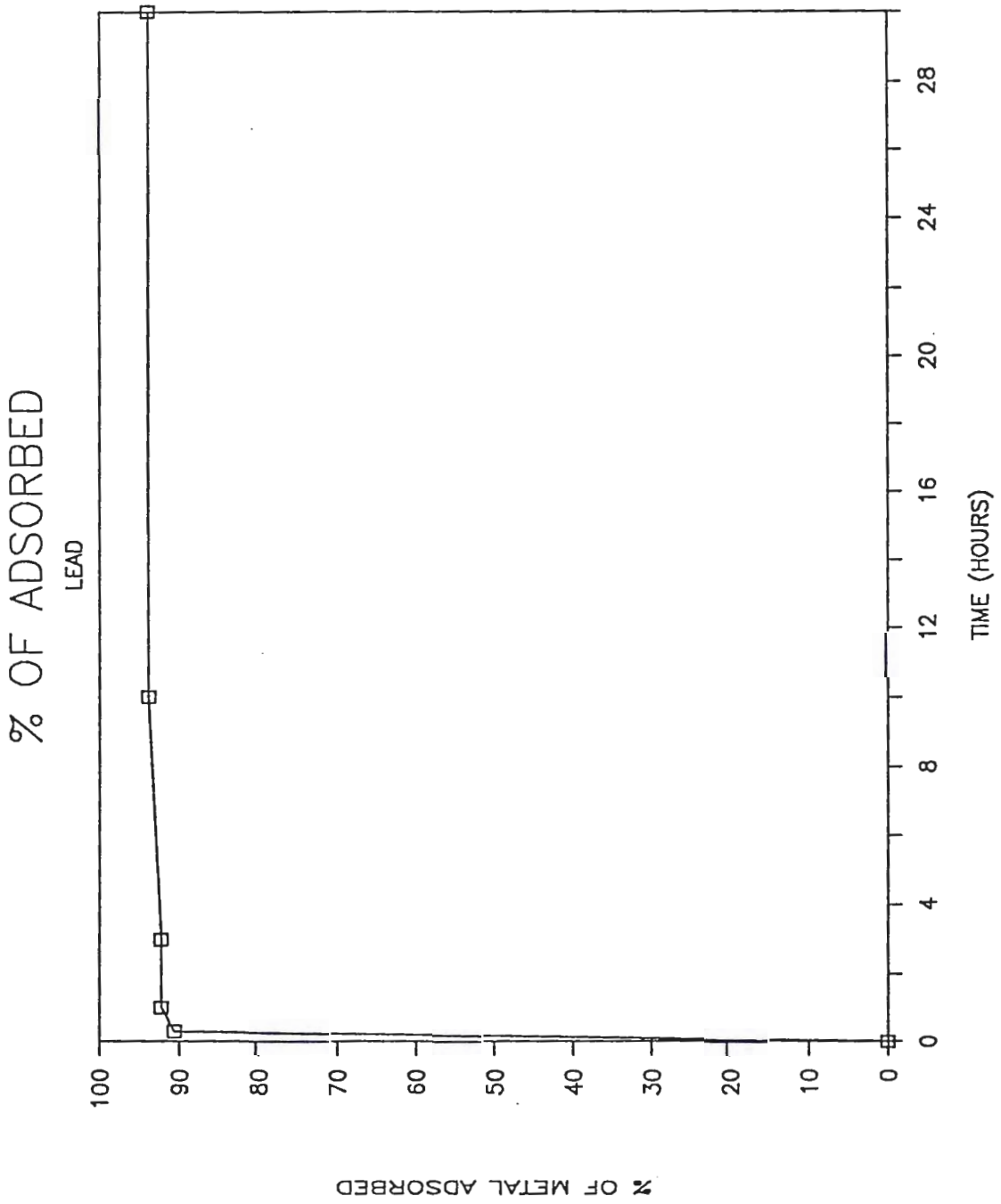
% OF ADSORBED
LEAD
100
90
80
70
60
50
40
30
20
10
0
% OF METAL ADSORBED
0
4
8
12
16
20
24
28
TIME (HOURS)

Figure 25a

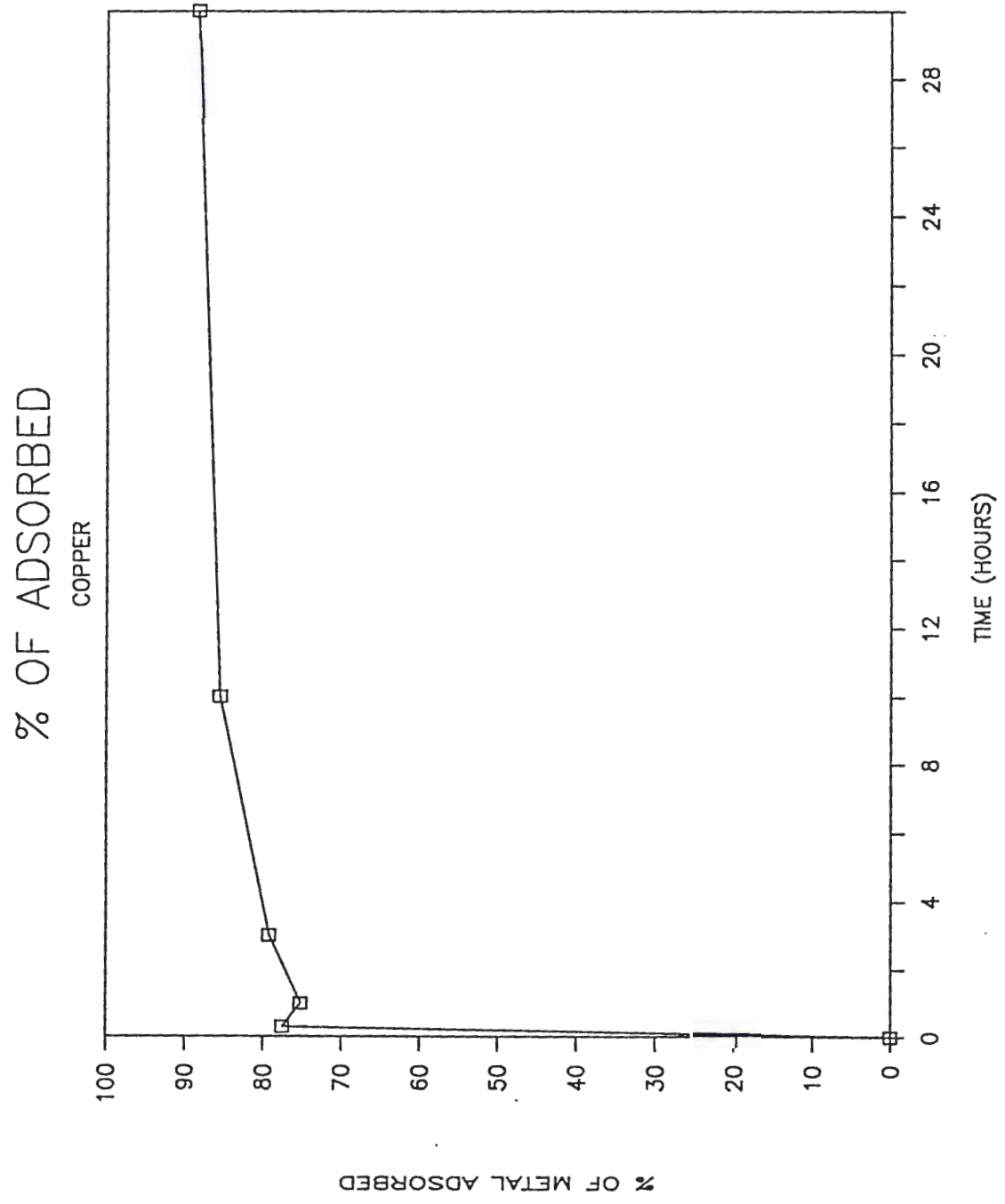
% OF ADSORBED
COPPER
% OF METAL ADSORBED
100
90
80
70
60
50
40
30
20
10
0
0
4
8
12
16
20
24
28
TIME (HOURS)

Figure 25b

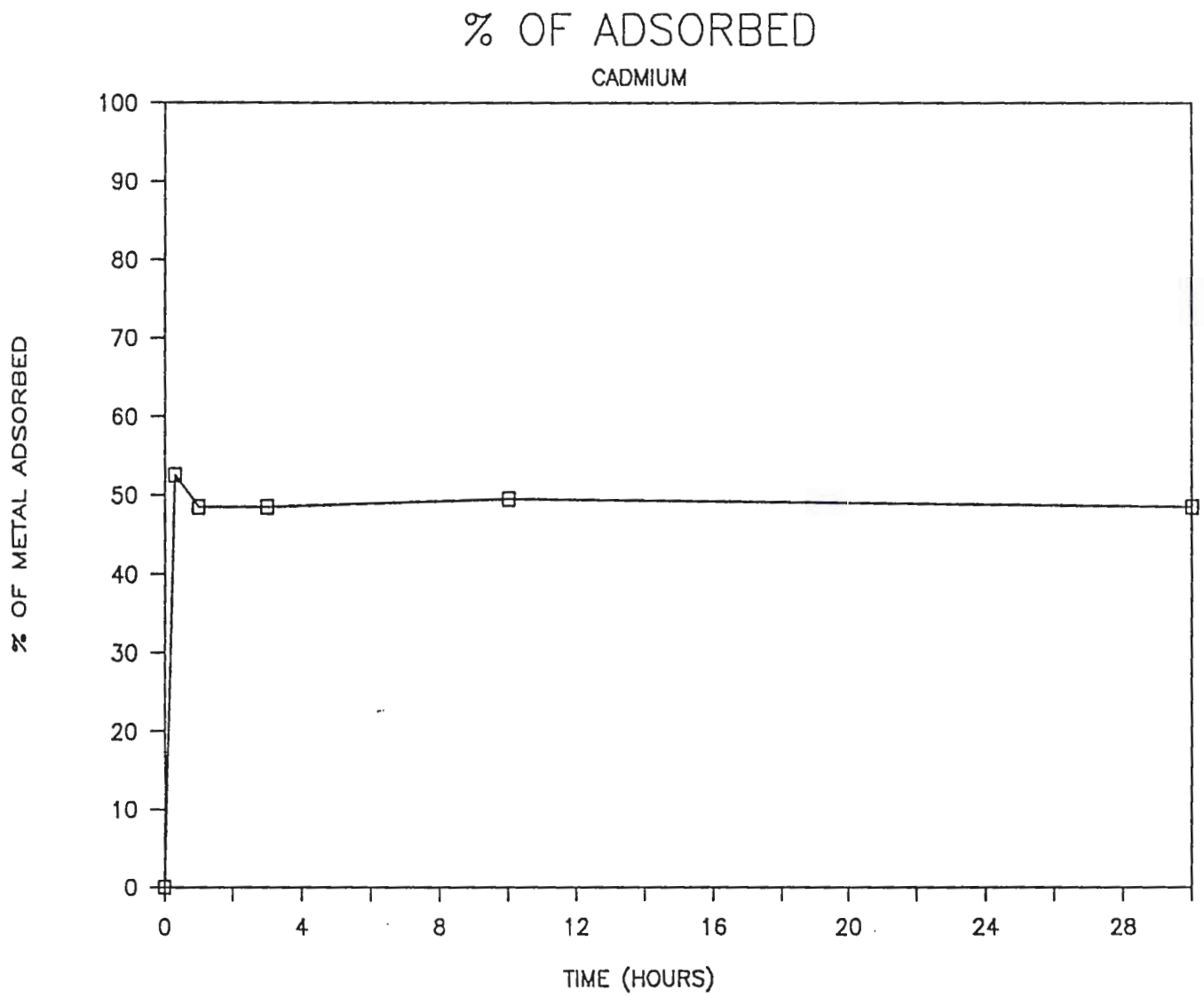
% OF ADSORBED
CADMIUM
% OF METAL ADSORBED
100
90
80
70
60
50
40
30
20
10
0
0
4
8
12
16
20
24
28
TIME (HOURS)

Figure 25c

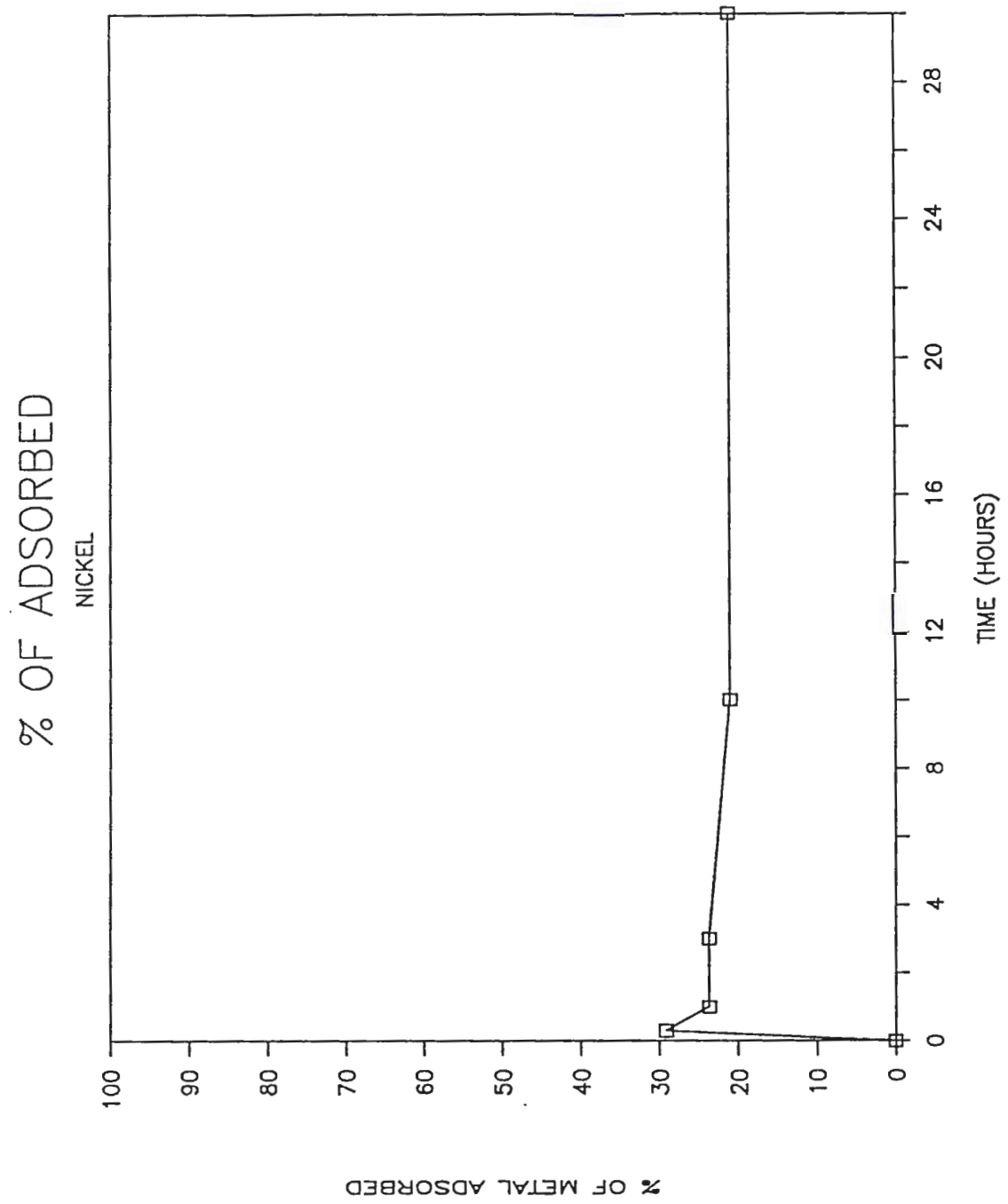
% OF ADSORBED
NICKEL
% OF METAL ADSORBED
TIME (HOURS)
0
10
20
30
40
50
60
70
80
90
100
0
4
8
12
16
20
24
28

Figure 25d

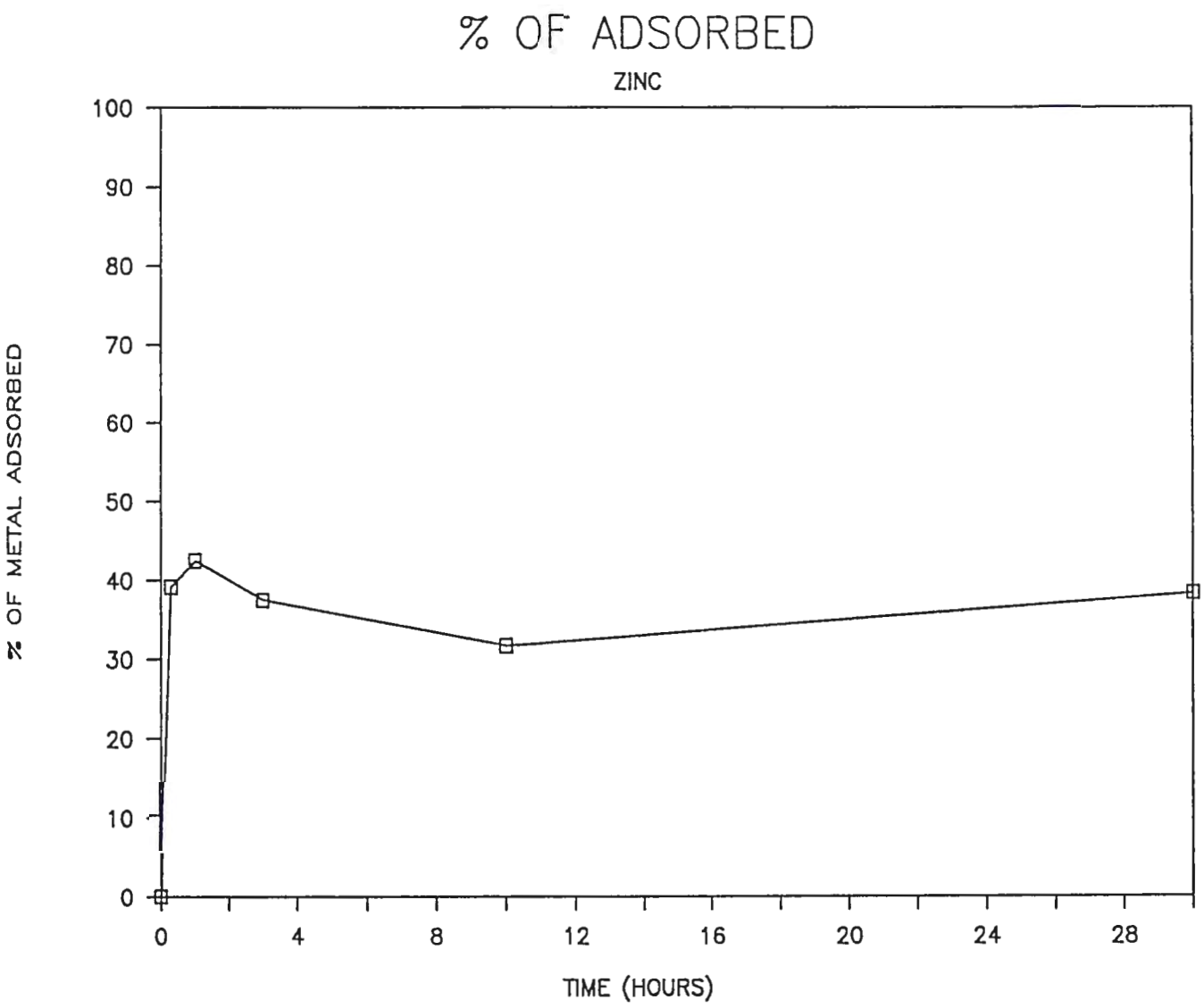
% OF ADSORBED
ZINC
% OF METAL ADSORBED
100
90
80
70
60
50
40
30
20
10
0
0
4
8
12
16
20
24
28
TIME (HOURS)

Figure 25e

equilibrium was not. This is apparent in Figures 25a - 25e. Pb and Cd reached equilibrium after about 1 hr of equilibration, Cu and Ni after about 10 hrs, and Zn not until after 30 hrs. The data also show that there is a considerable decrease in the percent of adsorbed metal after 0.3 hrs of equilibration for Cd, Ni, and Cu, and a considerable increase for Zn.

Many factors may have affected the time required for the metals to reach equilibrium. One explanation for this phenomenon is that there was some substitution between the heavy metal cations and colloid structural ions, as well as the expected adsorption.

The presence of simple hydrous oxides coating the soil colloids may have also affected the adsorption process. Adsorption of cations by simple hydrous oxides differs from that of clay colloids because for hydrous oxides the surface charge is largely controlled by the amount of adsorption of H^+ or OH^- from solution, rather than by the amount of isomorphous substitution within the clay structure (Anderson and Rubin, 1981).

Many studies have shown the importance of pH with regard to the extent of cation adsorption by soils. For most soils a decrease of heavy metal adsorption at low pH conditions is the result of an increase in competition by H^+ and the effect of the dissolution of ions (Al^{3+} for example) from the clay crystal lattice (Griffin and Shimp,

1976). There was a slight increase of about 0.4 pH units after 0.3 hrs of equilibration. This pH increase, however, was probably not the cause of the fluctuating adsorption, because with an increase of pH an increase in adsorption would be expected, not a decrease as was observed with Cd, Ni, and Cu. The fluctuation can be better attributed to complex exchange reactions occurring between the competing heavy metals and the clay colloids.

In order to further describe the adsorption kinetics, batch equilibrium data (30 hour) for Pb, Ni, Cd, Cu, and Zn were fitted to both the Freundlich adsorption isotherm (equation [12]) and Langmuir adsorption isotherm (equation [14]). Figures 26a - 26j are batch solution data for Pb, Ni, Cd, Cu and Zn fitted to the two isotherms. A least squares linear regression formula was used to determine the slope and intercept of the line of best fit for both isotherms. The coefficient of determination (r^2), which is the total variation in the Y values, was also calculated. An r^2 value of 1 indicates perfect correlation where an r^2 of 0 indicates no correlation. The correlation coefficients for 30 hr batch adsorption data fit to both isotherms are shown in Table 12.

The r^2 values for the heavy metals indicate that their adsorptions fit the Langmuir isotherm better than the Freundlich isotherm. The data fitted to the Langmuir isotherm yielded r^2 values for Pb, Zn, Cd, Cu, and Ni, of

Figure 26a - 26j: Freundlich and Langmuir adsorption isotherms for heavy metal adsorption after 30 hours of equilibration.

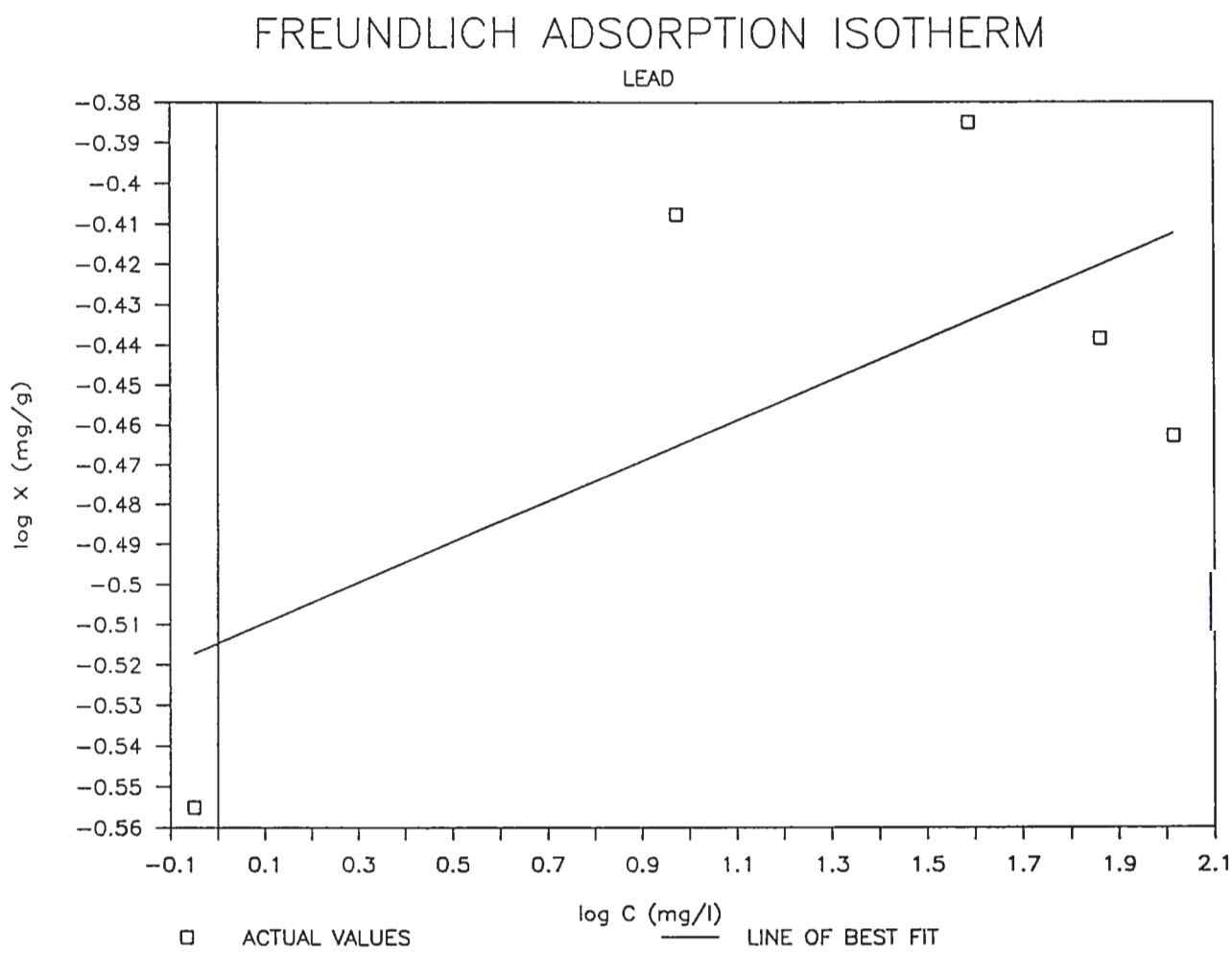
FREUNDLICH ADSORPTION ISOTHERM
LEAD
log x (mg/g)
−0.38
−0.39
−0.4
−0.41
−0.42
−0.43
−0.44
−0.45
−0.46
−0.47
−0.48
−0.49
−0.5
−0.51
−0.52
−0.53
−0.54
−0.55
−0.56
−0.1
0.1
0.3
0.5
0.7
0.9
1.1
1.3
1.5
1.7
1.9
2.1
log C (mg/l)
ACTUAL VALUES
LINE OF BEST FIT

Figure 26a

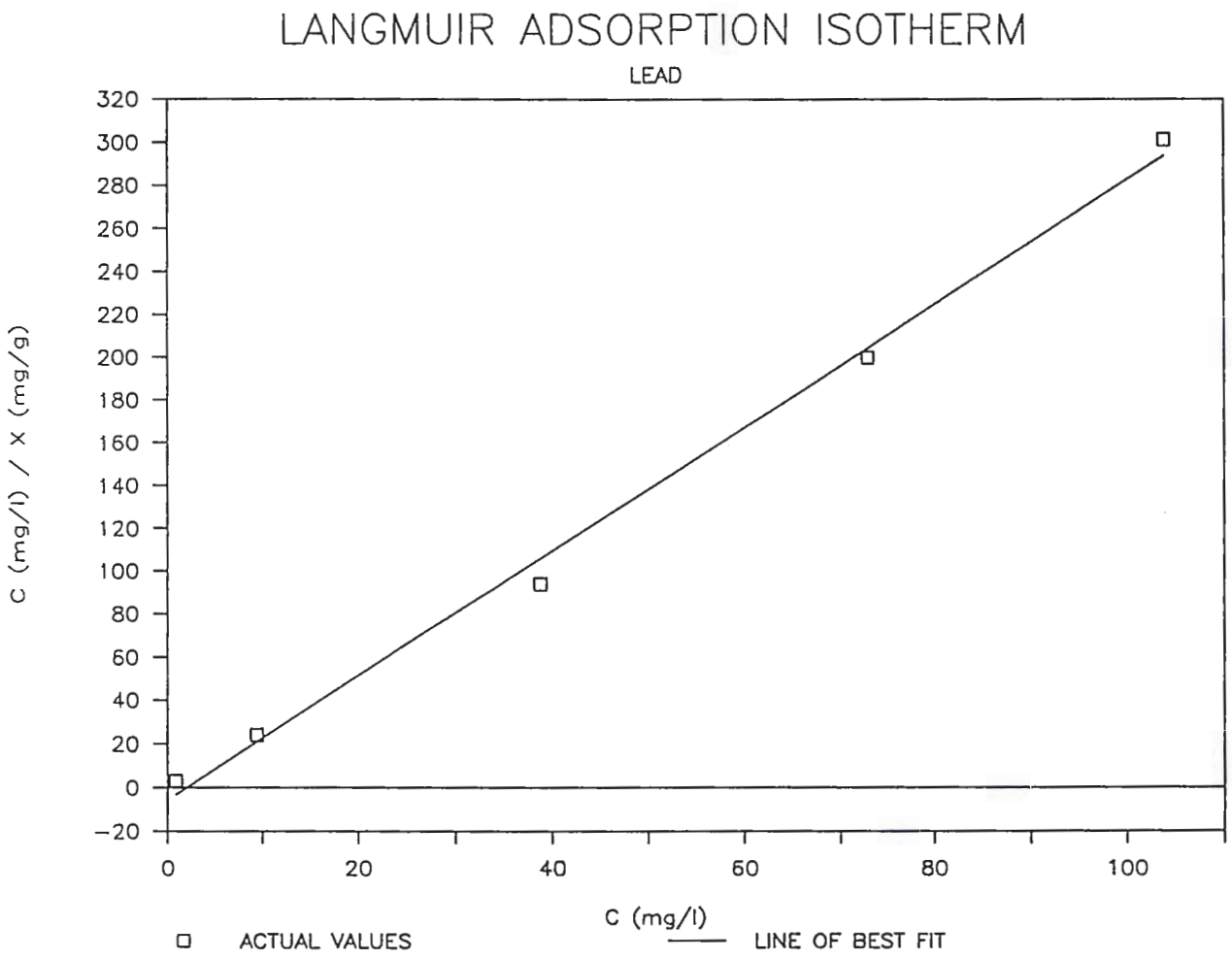
LANGMUIR ADSORPTION ISOTHERM
LEAD
C (mg/l) / X (mg/g)
320
300
280
260
240
220
200
180
160
140
120
100
80
60
40
20
0
-20
0
20
40
60
80
100
C (mg/l)
ACTUAL VALUES
LINE OF BEST FIT

Figure 26b

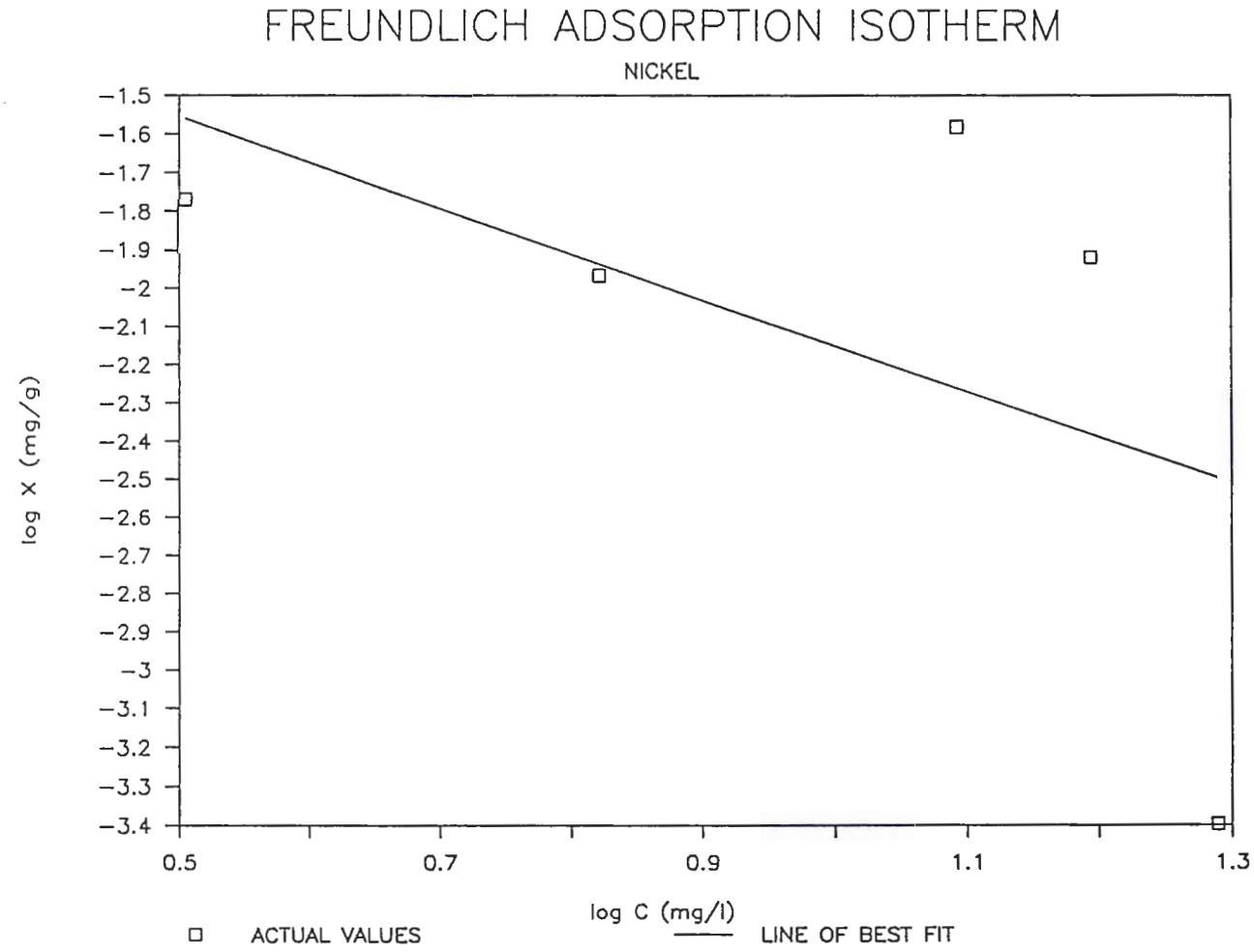
FREUNDLICH ADSORPTION ISOTHERM
NICKEL
log (x/m) (mg/g)
−1.5
−1.6
−1.7
−1.8
−1.9
−2
−2.1
−2.2
−2.3
−2.4
−2.5
−2.6
−2.7
−2.8
−2.9
−3
−3.1
−3.2
−3.3
−3.4
0.5
0.7
0.9
1.1
1.3
log C (mg/l)
ACTUAL VALUES
LINE OF BEST FIT

Figure 26c

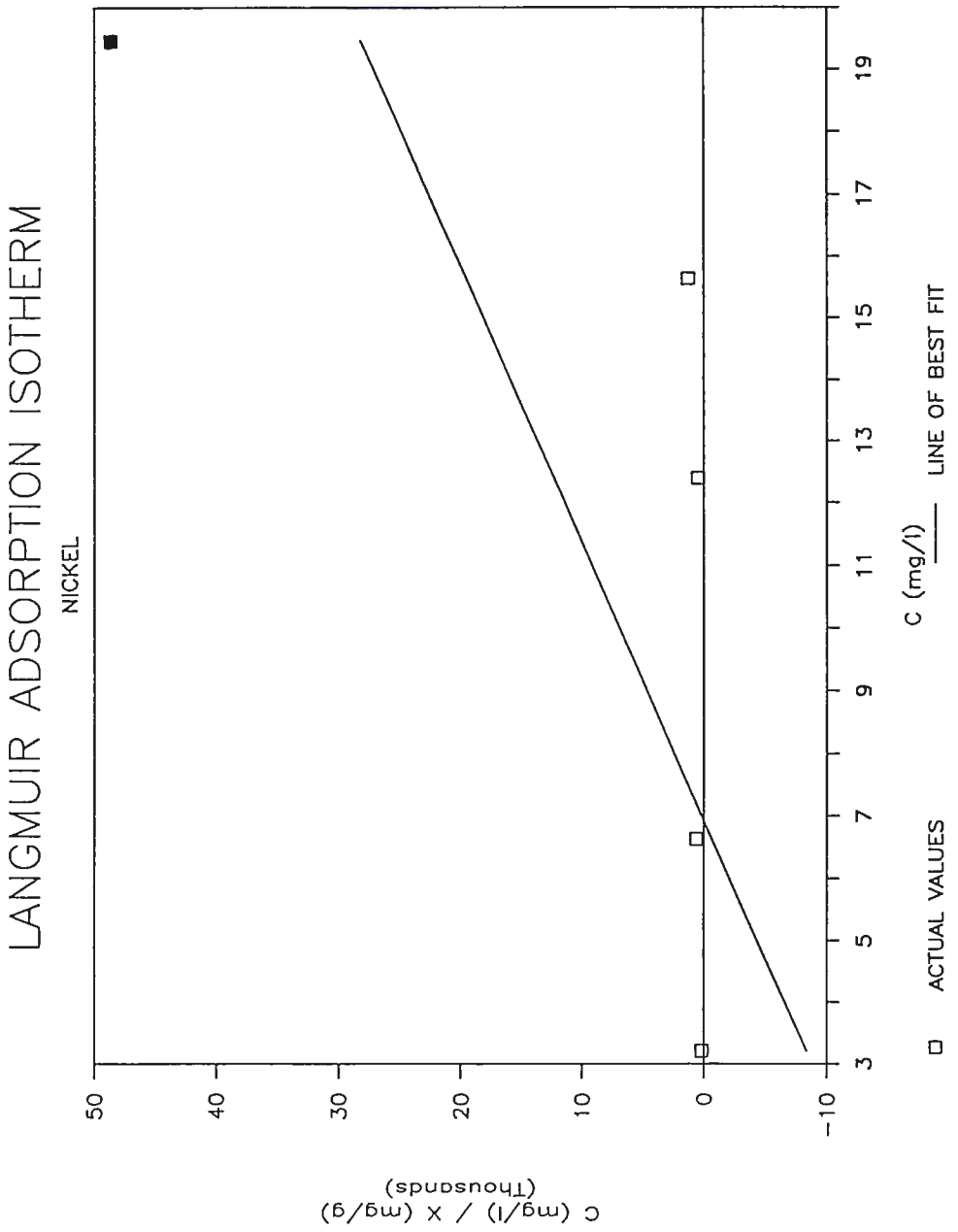
LANGMUIR ADSORPTION ISOTHERM
NICKEL
C (mg/l) / X (mg/g)
(Thousands)
50
40
30
20
10
0
-10
3
5
7
9
11
13
15
17
19
C (mg/l)
ACTUAL VALUES
LINE OF BEST FIT

Figure 26d

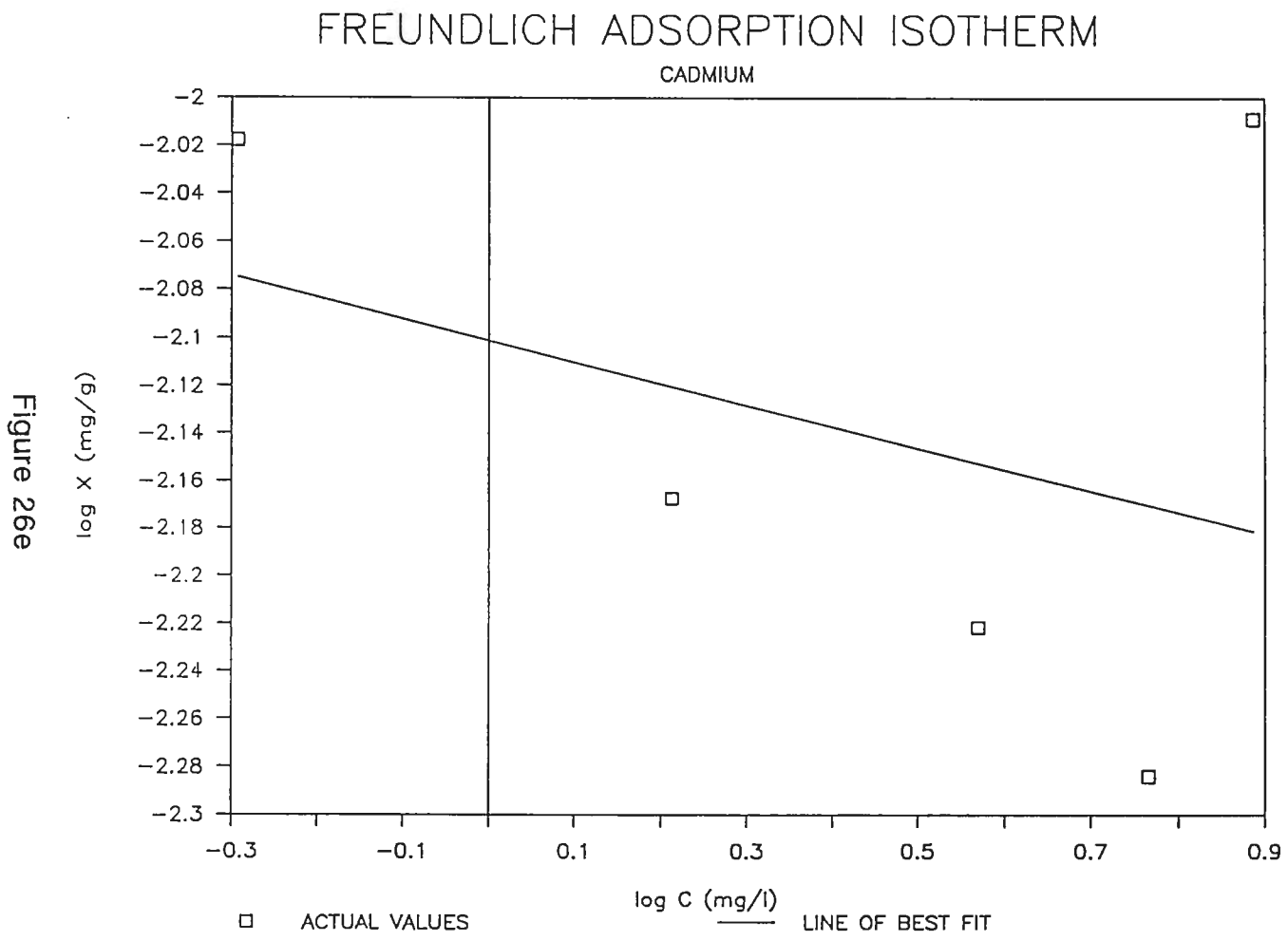
FREUNDLICH ADSORPTION ISOTHERM
CADMIUM
log x/m (mg/g)
-2
-2.02
-2.04
-2.06
-2.08
-2.1
-2.12
-2.14
-2.16
-2.18
-2.2
-2.22
-2.24
-2.26
-2.28
-2.3
-0.3
-0.1
0.1
0.3
0.5
0.7
0.9
log C (mg/l)
ACTUAL VALUES
LINE OF BEST FIT

Figure 26e

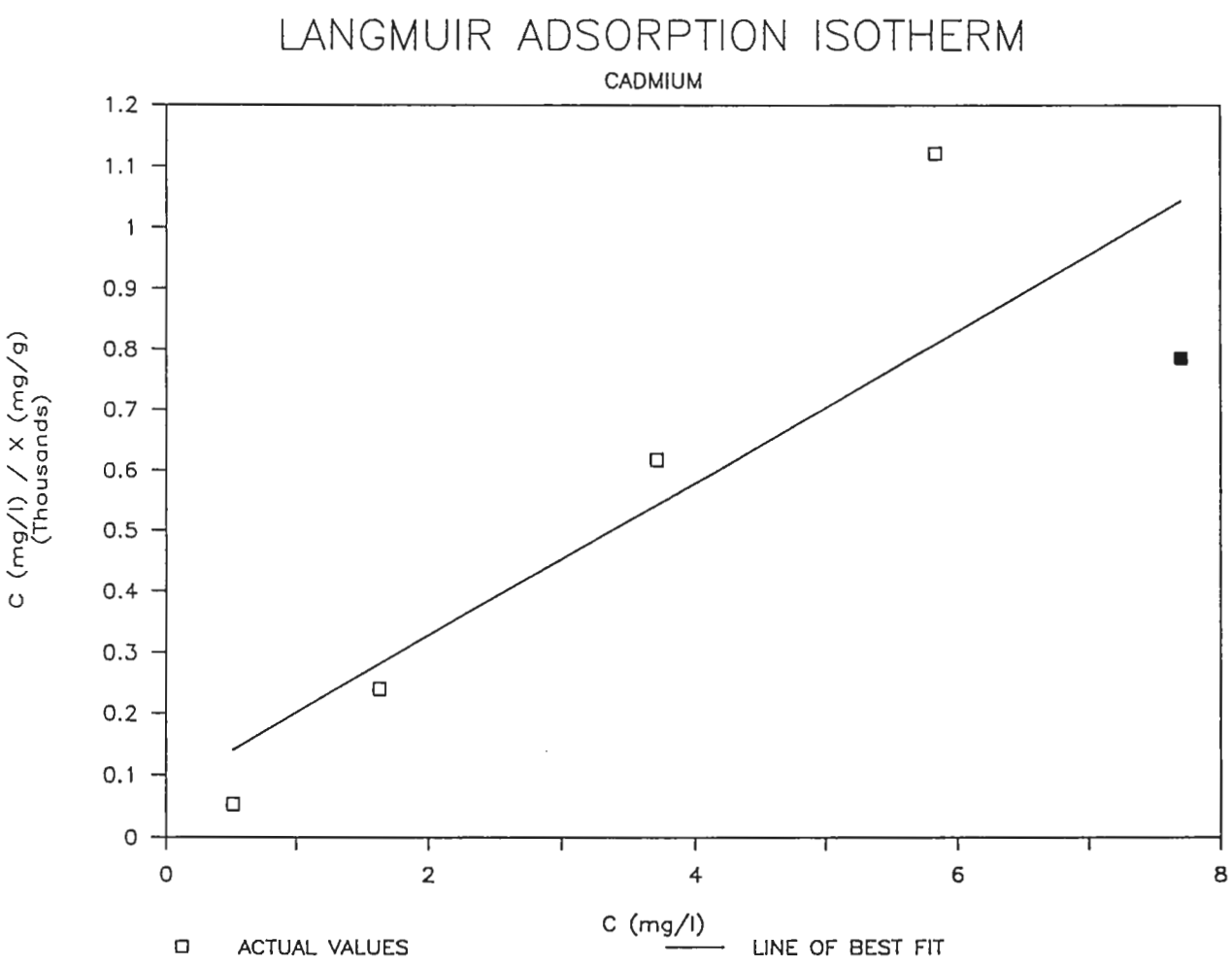
LANGMUIR ADSORPTION ISOTHERM
CADMIUM
C / (mg/l) x (mg/g) (Thousands)
1.2
1.1
1
0.9
0.8
0.7
0.6
0.5
0.4
0.3
0.2
0.1
0
0
2
4
6
8
C (mg/l)
ACTUAL VALUES
LINE OF BEST FIT

Figure 26f

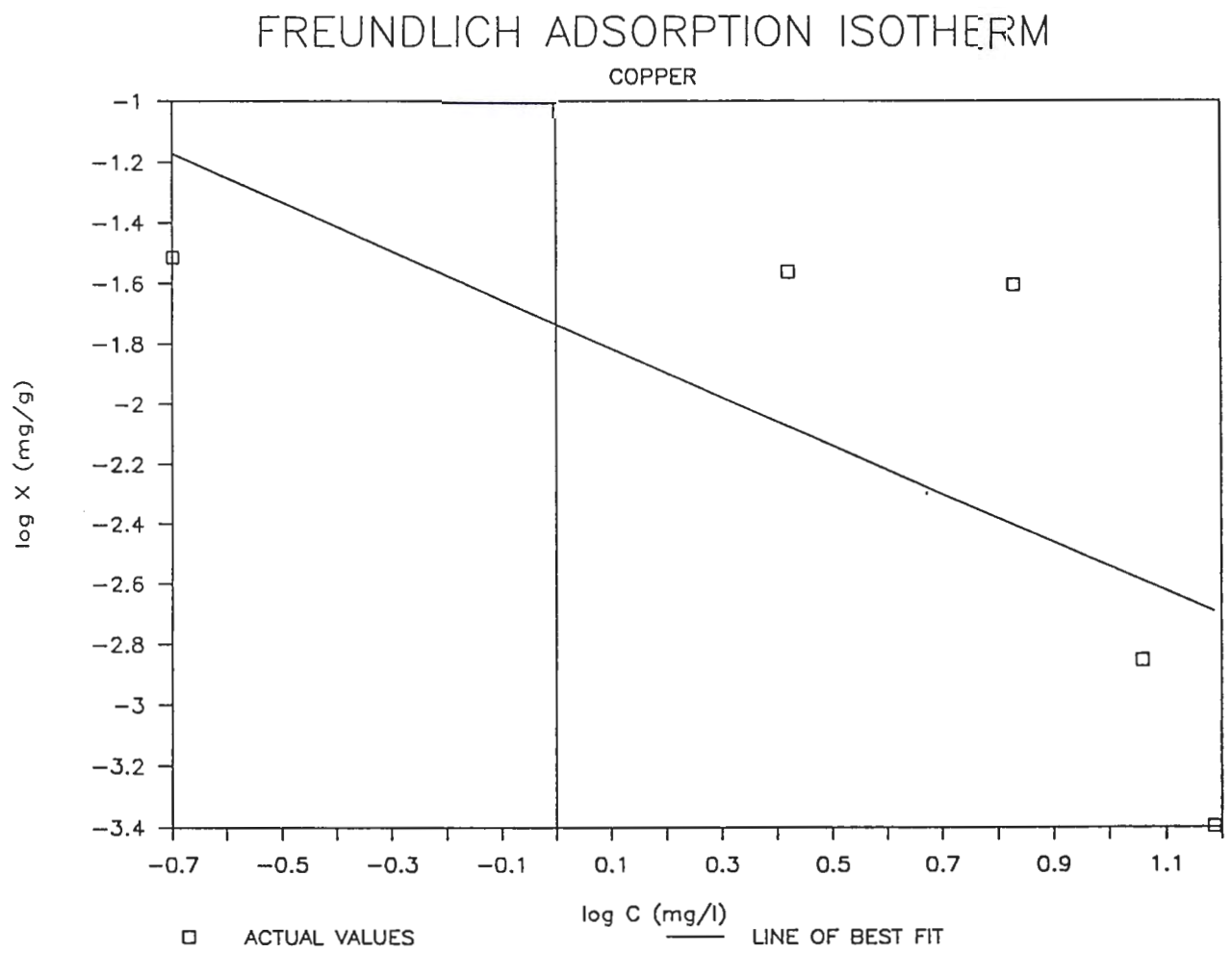
FREUNDLICH ADSORPTION ISOTHERM
COPPER
log X (mg/g)
−1
−1.2
−1.4
−1.6
−1.8
−2
−2.2
−2.4
−2.6
−2.8
−3
−3.2
−3.4
−0.7
−0.5
−0.3
−0.1
0.1
0.3
0.5
0.7
0.9
1.1
log C (mg/l)
ACTUAL VALUES
LINE OF BEST FIT

Figure 26g

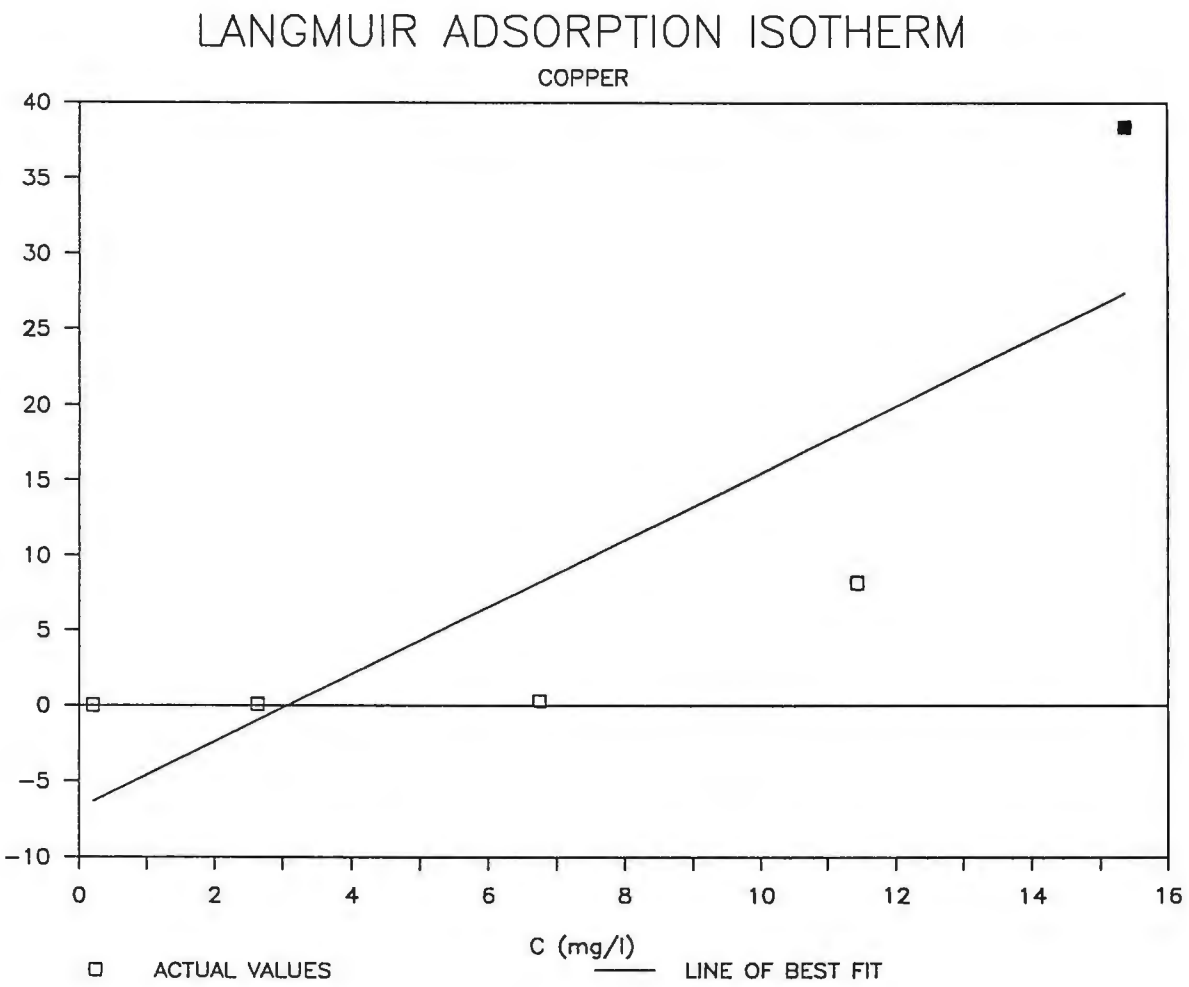
LANGMUIR ADSORPTION ISOTHERM
COPPER
C (mg/l) / X (mg/g)
(Thousands)
40
35
30
25
20
15
10
5
0
-5
-10
0
2
4
6
8
10
12
14
16
C (mg/l)
ACTUAL VALUES
LINE OF BEST FIT

Figure 26h

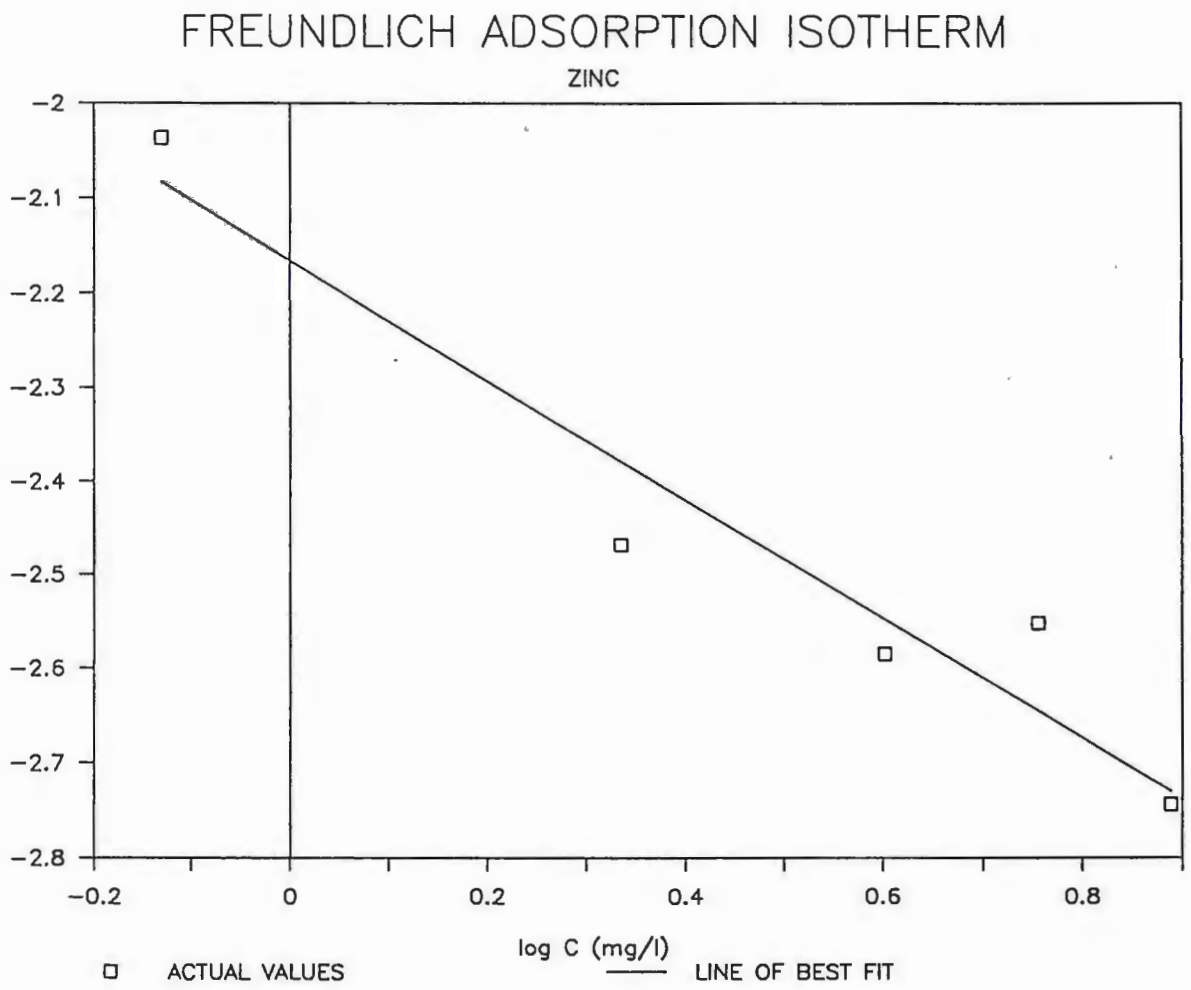
FREUNDLICH ADSORPTION ISOTHERM
ZINC
log x (mg/l)
−2
−2.1
−2.2
−2.3
−2.4
−2.5
−2.6
−2.7
−2.8
−0.2
0
0.2
0.4
0.6
0.8
log C (mg/l)
ACTUAL VALUES
LINE OF BEST FIT

Figure 26i

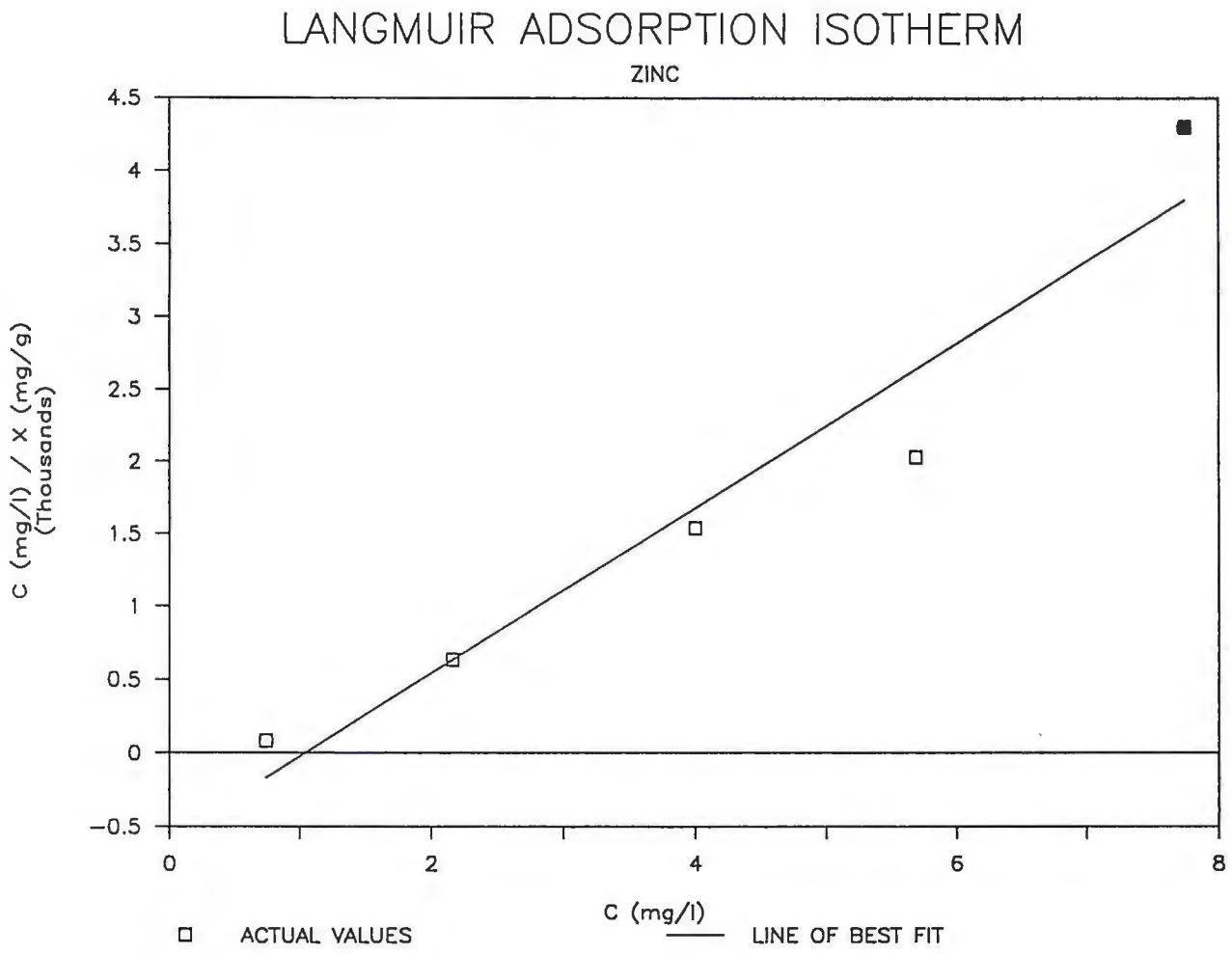
LANGMUIR ADSORPTION ISOTHERM
ZINC
C (mg/l) / X (mg/g)
(Thousands)
4.5
4
3.5
3
2.5
2
1.5
1
0.5
0
-0.5
0
2
4
6
8
C (mg/l)
ACTUAL VALUES
LINE OF BEST FIT

Figure 26j

HEAVY METAL	CORRELATION COEFFICIENT (r^2) LANGMUIR	FREUNDLICH
Copper	0.695	0.487
Lead	0.996	0.421
Zinc	0.934	0.928
Nickel	0.476	0.273
Cadmium	0.754	0.123

Table 12: Correlation coefficients (r^2) for 30 hour adsorption data fit to the Freundlich and Langmuir adsorption isotherms.

.996, .934, .754, .695, and .476 respectively. Zn, with an r^2 of .934, was the only heavy metal that fit the Freundlich isotherm. The low r^2 values for Cd, Cu, and Ni, (from data fit to the Langmuir isotherm) may be attributed to shortcomings of the Langmuir isotherm in describing the adsorption process. When using the Langmuir equation, an assumption is made that the adsorbent surface is homogeneous with respect to the energy of the adsorption sites (Griffin and Shimp, 1976). Griffin and Shimp (1976) contend that in a multicomponent cation system the adsorption sites are occupied by cations with various retention energies relative to a heavy metal cation. As an example, they discuss how Pb can displace certain cations such as Na^+ much more easily than it can replace cations such as Ca^{++}. They maintain that it is this type of reaction that changes the shape of the adsorption isotherm by filling the lower energy sites preferentially, i.e. Pb first exchanges with a cation or a group of cations of similiar energy. It is this phase of the adsorption that is then attributed to the initial slope of the Langmuir plot. As the metal concentration is increased, the chemical potential gradient is increased until it is sufficient to initiate exchange of the cation or group of cations with the next highest energy of retention relative to the metal of interest. This second energy level of exchange then produces the sharp slope changes on the

Langmuir plots observed with certain leachate solutions.

It is apparent in Figures 26a - 26j that if the "closed" data point for the Langmuir isotherm was eliminated for the calculations of r^2, the r^2 calculated for the remaining data points would be considerably higher. The deviance of this end point may be attributed to the onset of a two slope adsorption curve produced from the adsorption of the heavy metals to sites of distinctly different energy, or from competition between the other cations in solution. The reason Pb has such a high r^2 (.996) and does not display the start of a two-slope adsorption curve may be due to the similar retention energies between Pb and the exchangeable cations therefore allowing Pb to dominate the filling of the lower energy sites. This may also explain the sediment's high affinity for Pb (about 93 % of the Pb in solution was adsorbed from the Batch #1 solution) as compared to Cu (88%), Cd (48%), Zn (38%), and Ni (21%).

Column Study

Elution Curves

Elution curves for the migration of Pb, Ni, Cd, Cu, and Zn through a silt loam (column 1) and a sandy loam (column 2) are shown in Figures 27a - 27j. All data are plotted as C/C_0 versus pore volumes (time), where C/C_0 is the ratio of the effluent concentration to influent

Figure 27a - 27j: Elution curves for the migration of Pb, Ni, Cd, Cu, and Zn through a silt loam (Column 1) and sandy loam (Column 2).

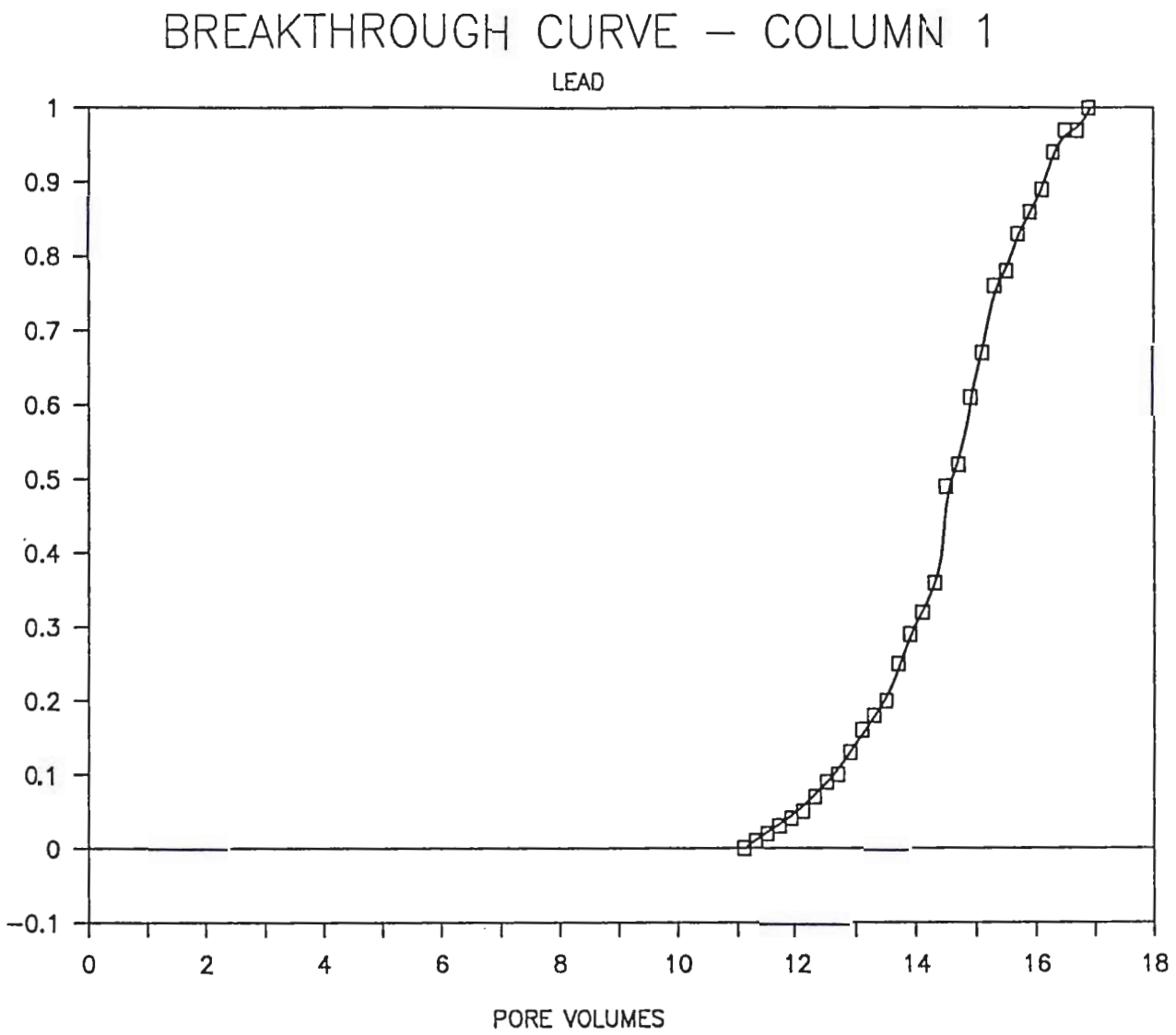
BREAKTHROUGH CURVE – COLUMN 1
LEAD
c/co
1
0.9
0.8
0.7
0.6
0.5
0.4
0.3
0.2
0.1
0
-0.1
0
2
4
6
8
10
12
14
16
18
PORE VOLUMES

Figure 27a

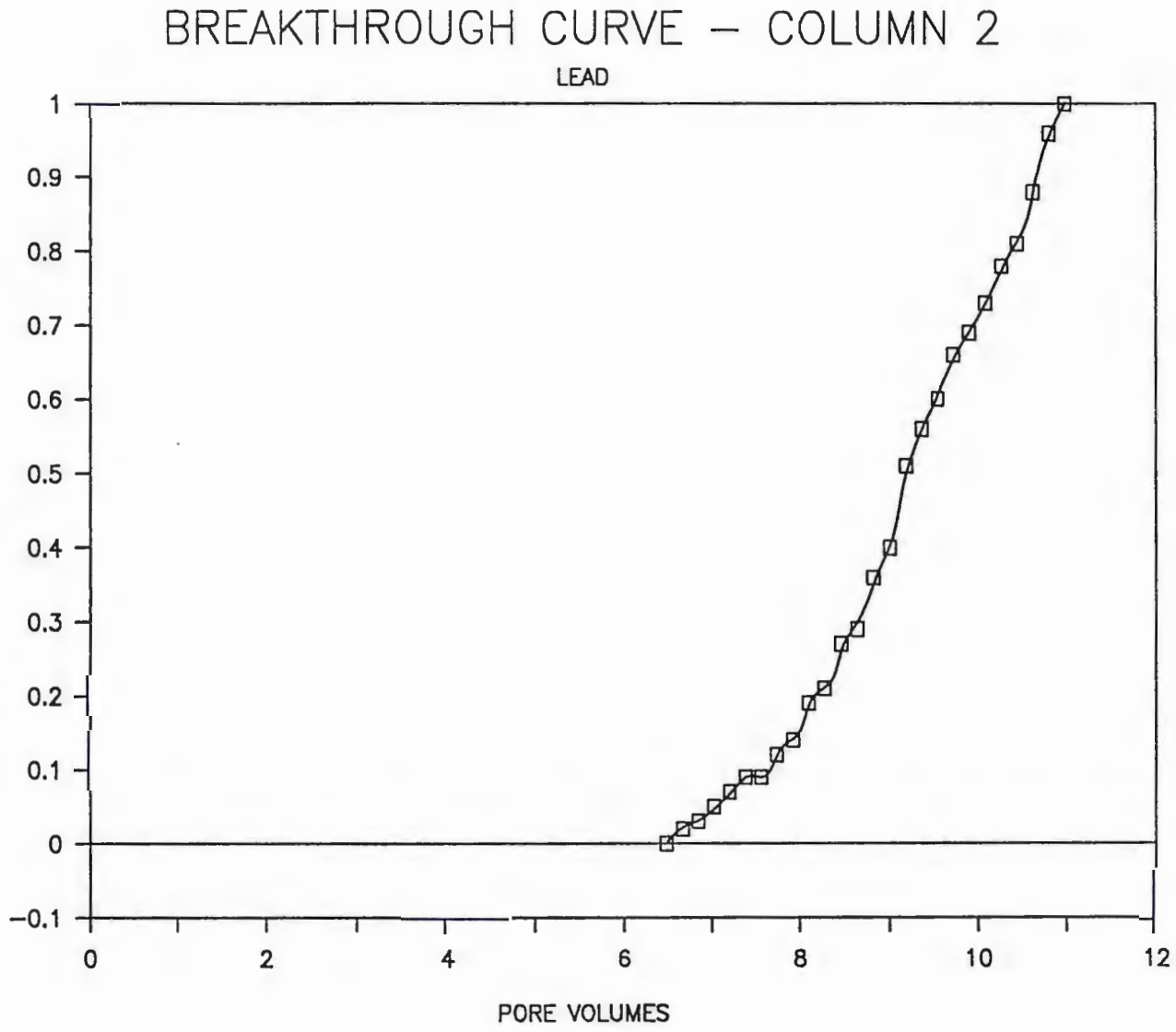
BREAKTHROUGH CURVE – COLUMN 2
LEAD
C/Co
1
0.9
0.8
0.7
0.6
0.5
0.4
0.3
0.2
0.1
0
-0.1
0
2
4
6
8
10
12
PORE VOLUMES

Figure 27b

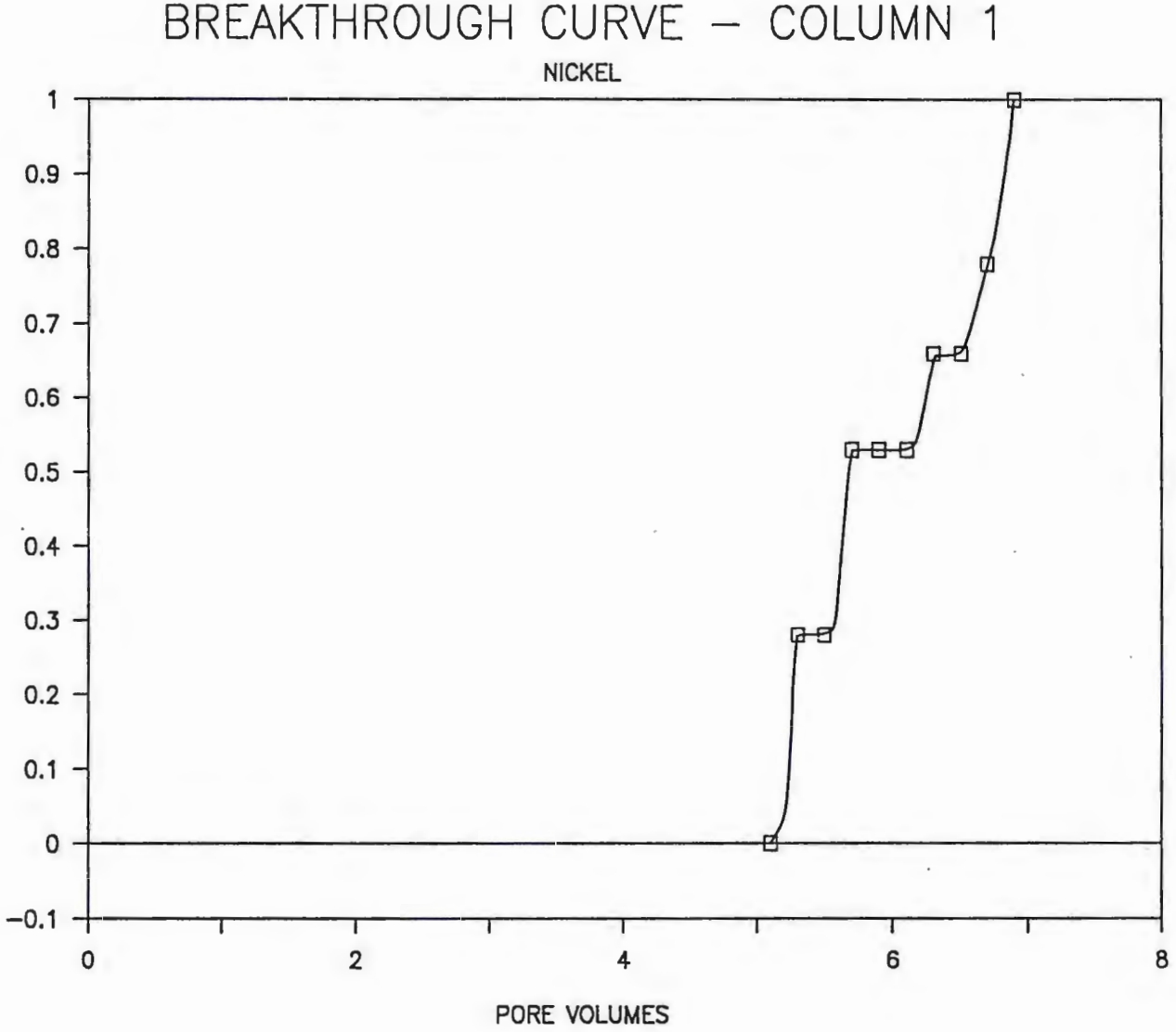
BREAKTHROUGH CURVE – COLUMN 1
NICKEL
C/Co
1
0.9
0.8
0.7
0.6
0.5
0.4
0.3
0.2
0.1
0
-0.1
0
2
4
6
8
PORE VOLUMES

Figure 27c

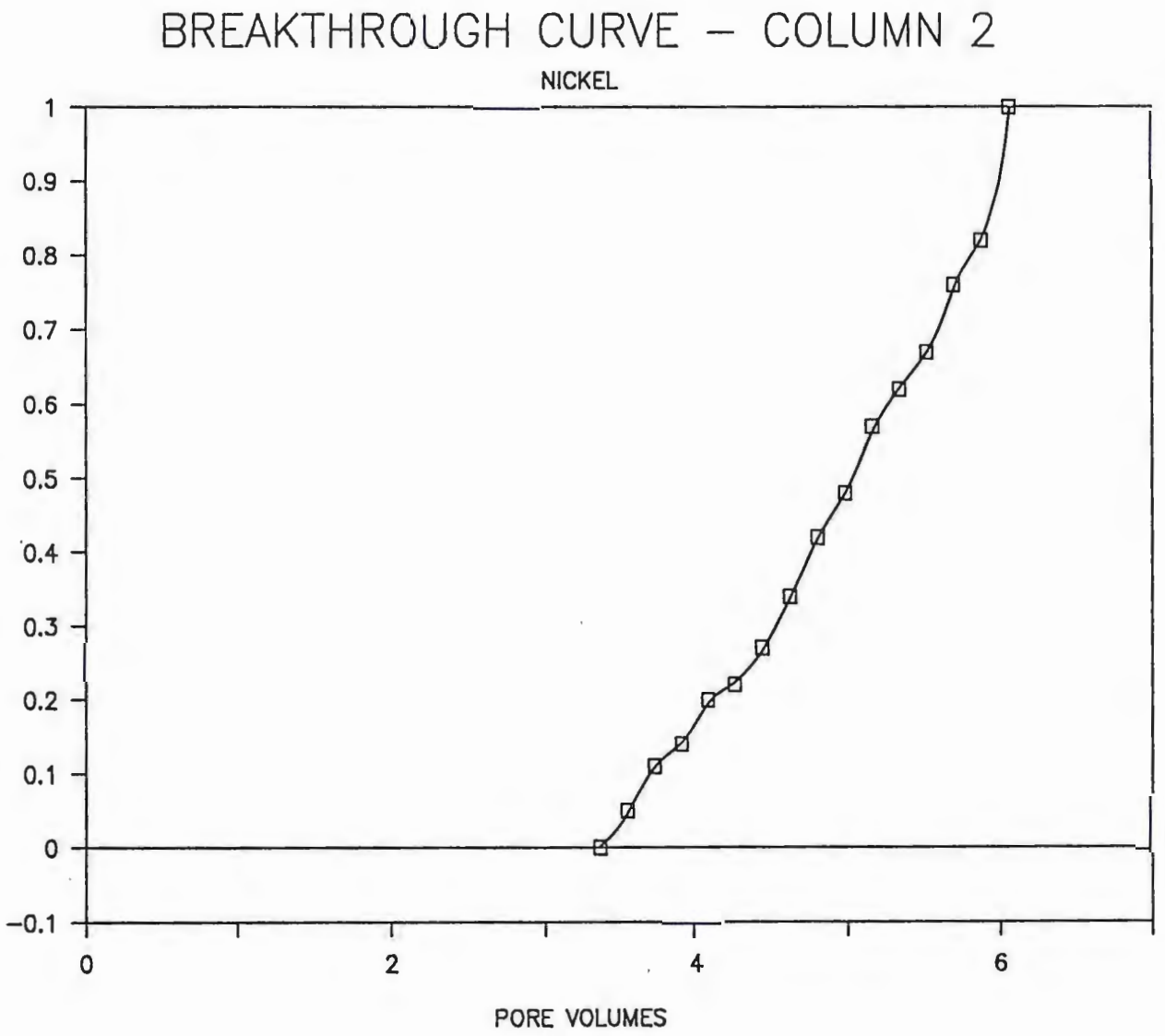
BREAKTHROUGH CURVE – COLUMN 2
NICKEL
C/Co
1
0.9
0.8
0.7
0.6
0.5
0.4
0.3
0.2
0.1
0
-0.1
0
2
4
6
PORE VOLUMES

Figure 27d

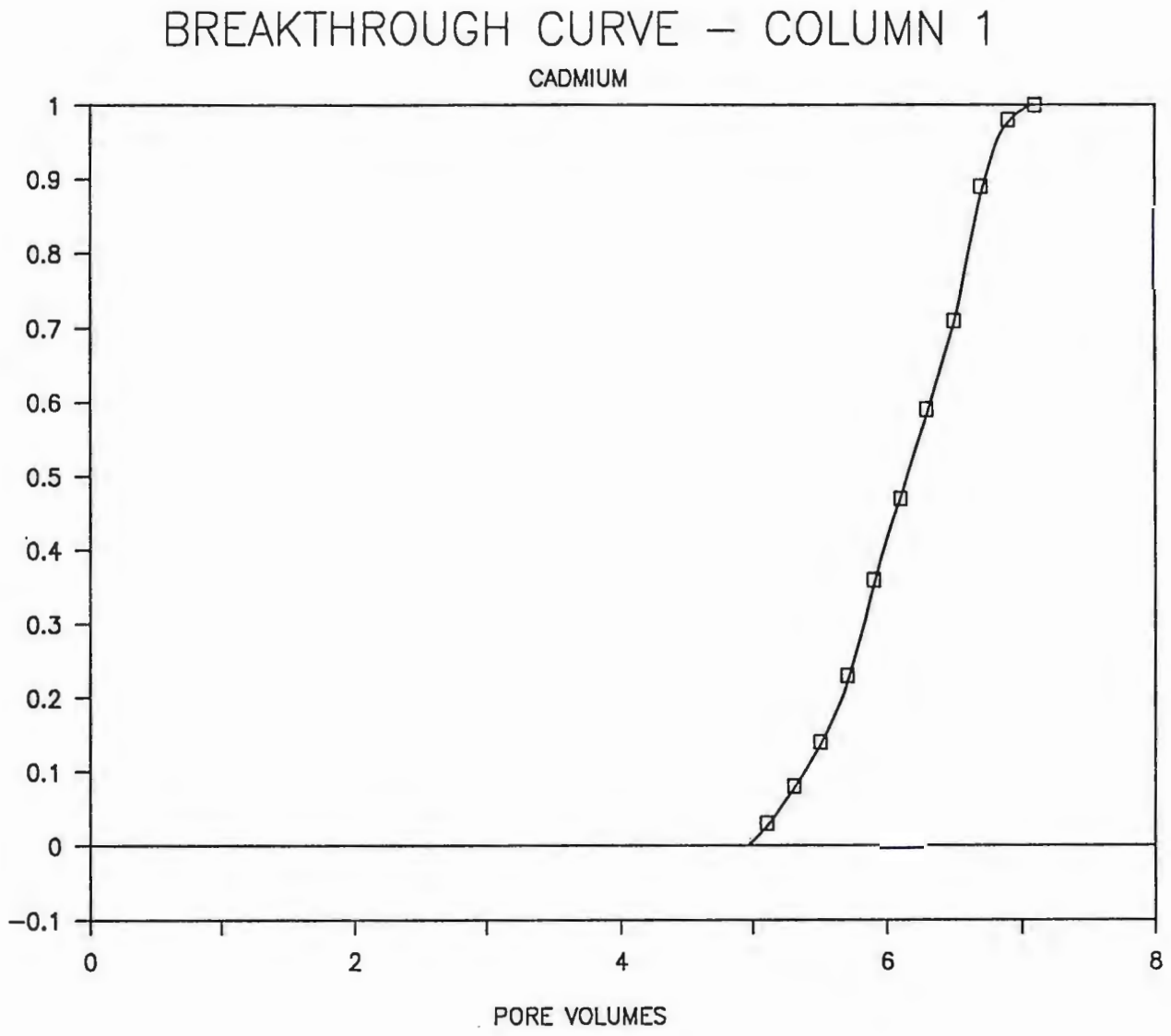
BREAKTHROUGH CURVE – COLUMN 1
CADMIUM
C/Co
1
0.9
0.8
0.7
0.6
0.5
0.4
0.3
0.2
0.1
0
-0.1
0
2
4
6
8
PORE VOLUMES

Figure 27e

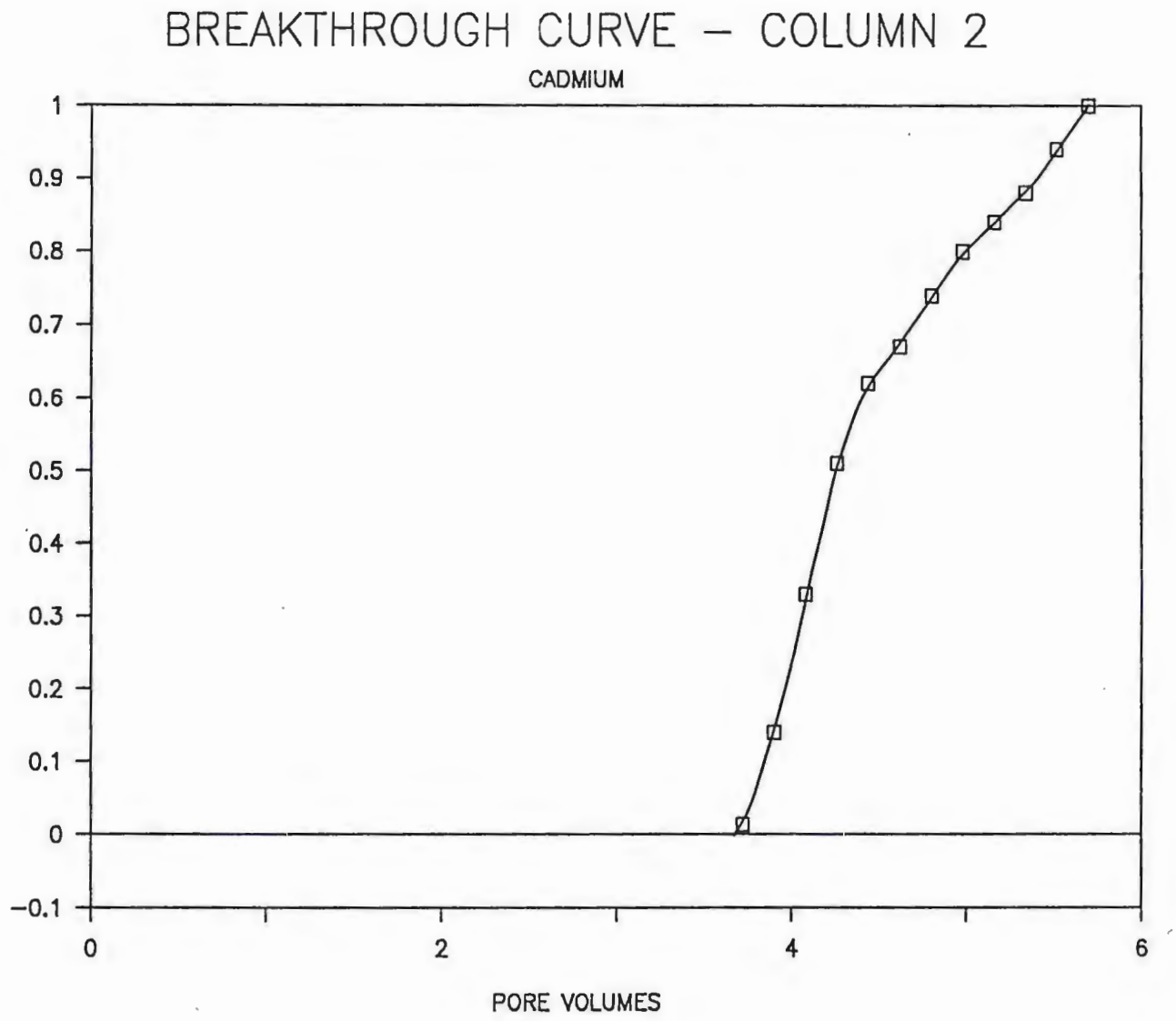
BREAKTHROUGH CURVE – COLUMN 2
CADMIUM
C/Co
1
0.9
0.8
0.7
0.6
0.5
0.4
0.3
0.2
0.1
0
-0.1
0
2
4
6
PORE VOLUMES

Figure 27f

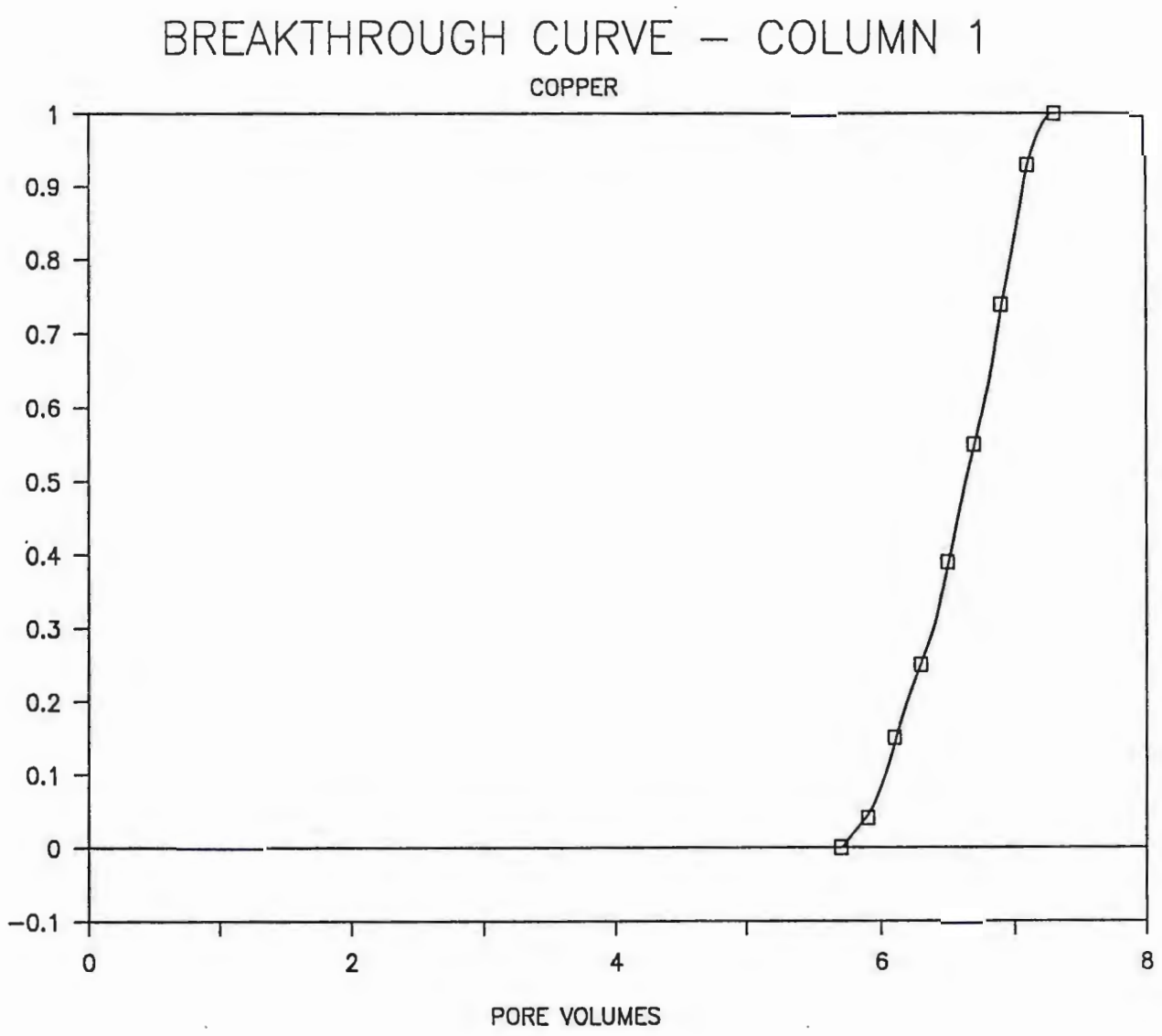
BREAKTHROUGH CURVE – COLUMN 1
COPPER
C/Co
1
0.9
0.8
0.7
0.6
0.5
0.4
0.3
0.2
0.1
0
-0.1
0
2
4
6
8
PORE VOLUMES

Figure 27g

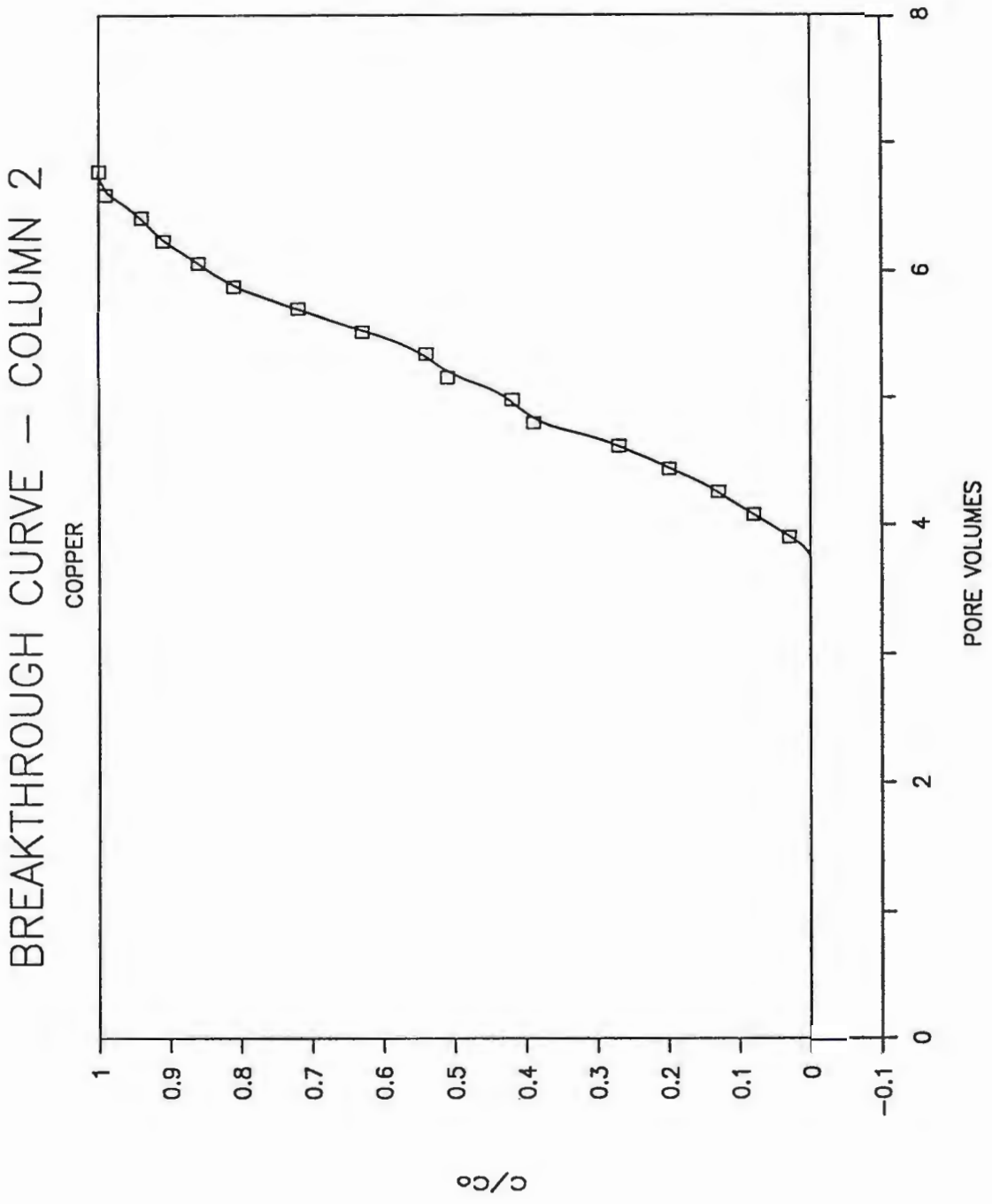
BREAKTHROUGH CURVE – COLUMN 2
COPPER
C/Co
1
0.9
0.8
0.7
0.6
0.5
0.4
0.3
0.2
0.1
0
-0.1
0
2
4
6
8
PORE VOLUMES

Figure 27h

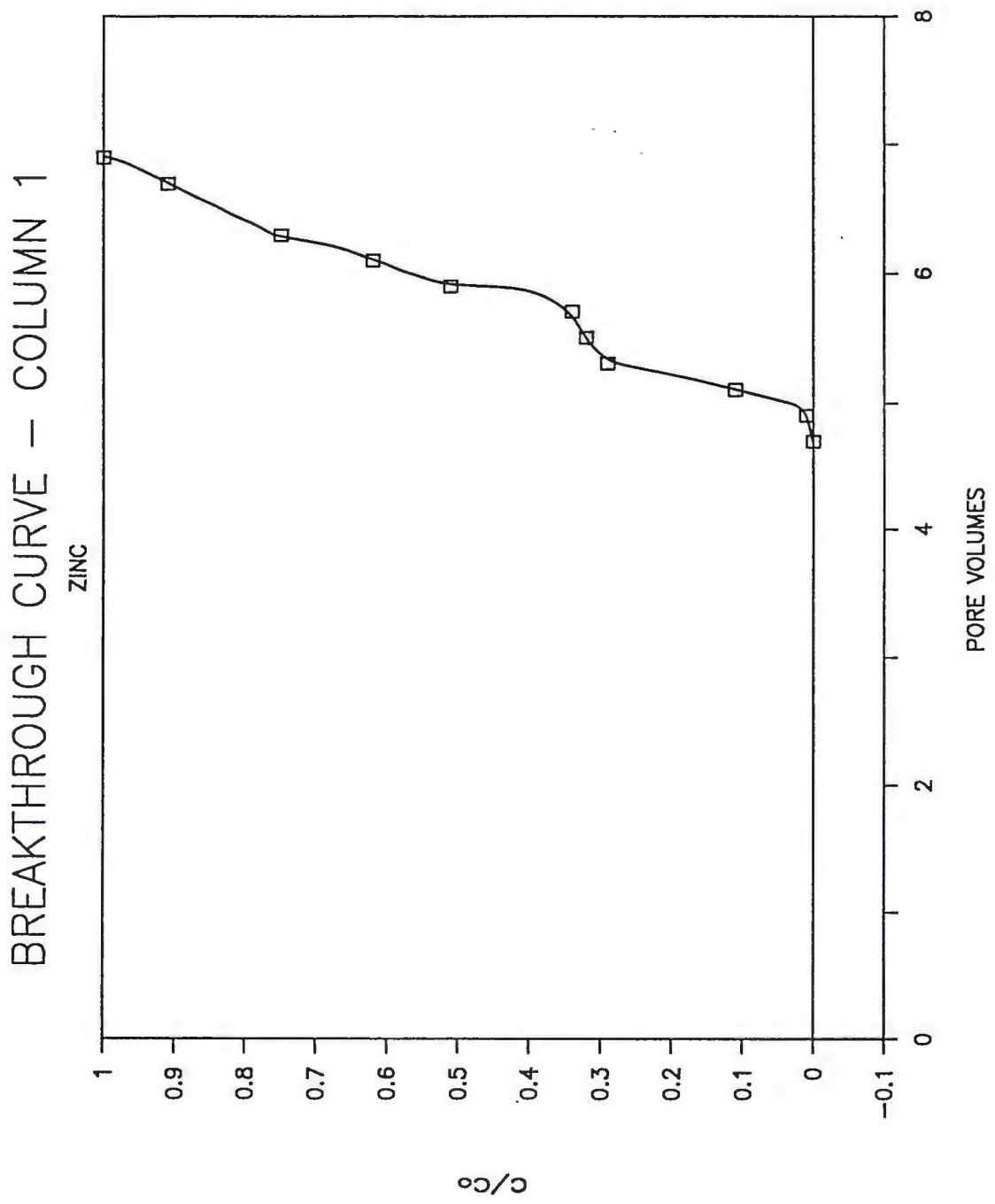
BREAKTHROUGH CURVE – COLUMN 1
ZINC
C/Co
1
0.9
0.8
0.7
0.6
0.5
0.4
0.3
0.2
0.1
0
-0.1
0
2
4
6
8
PORE VOLUMES

Figure 27i

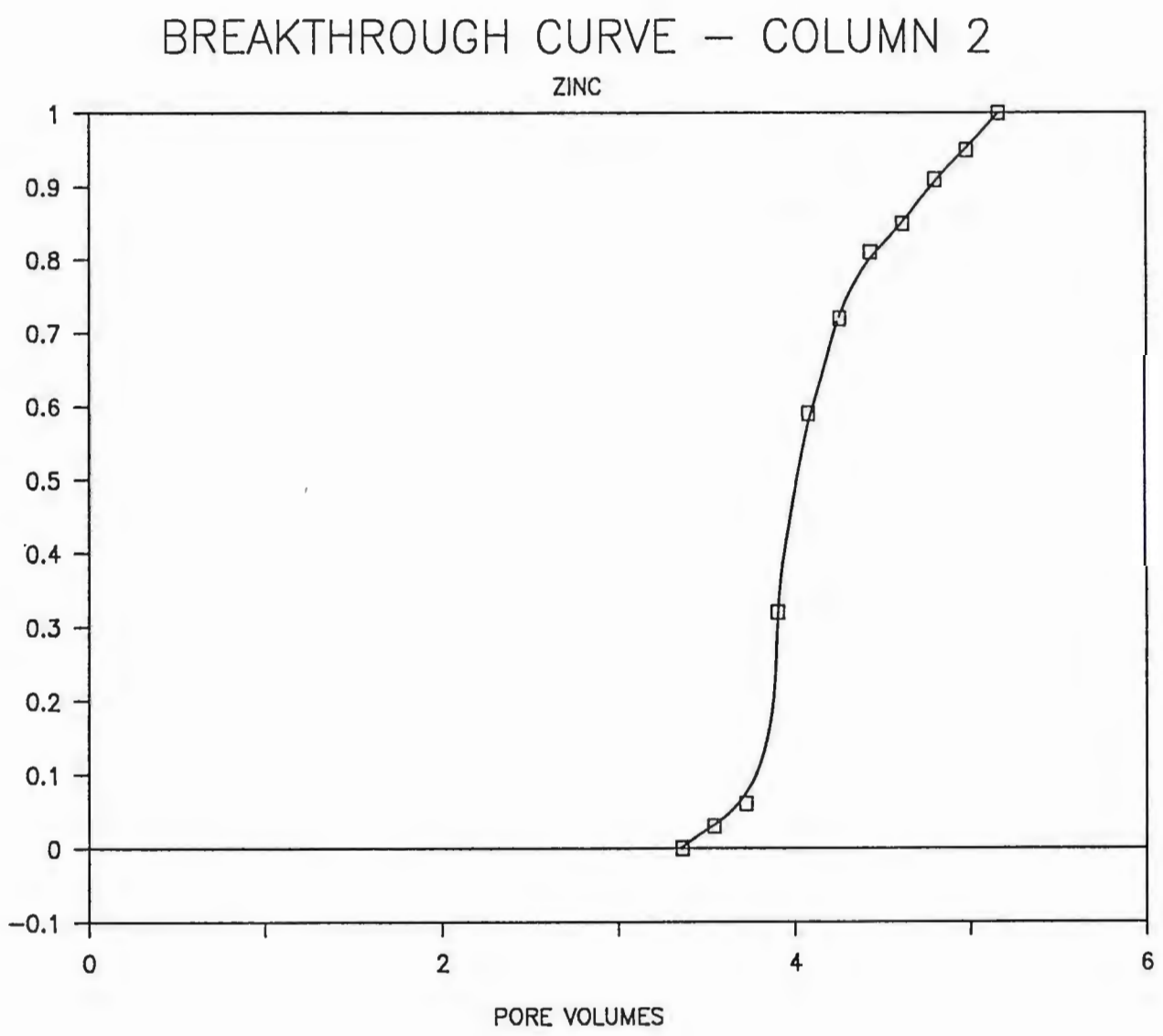
BREAKTHROUGH CURVE – COLUMN 2
ZINC
C/Co
1
0.9
0.8
0.7
0.6
0.5
0.4
0.3
0.2
0.1
0
-0.1
0
2
4
6
PORE VOLUMES

Figure 27j

concentration Soil column elution data are contained in Appendix F.

The elution curves indicate that Cu, Zn, Cd and Ni exhibit similiar migration behavior within each sediment type. The relative sharpness of the elution curves, and the early detection of Cu, Zn, Cd, and Ni in the effluent suggests that these metals were only weakly to moderately retained by the sediments. The elution curves for Pb, however, are significantly delayed and more sigmoidal in shape. This implies that Pb, in contrast to Cu, Zn, Cd, and Ni, was more strongly retained (attenuated) by the sediments.

The elution data further verify the results obtained in the batch adsorption study: that the unconsolidated sediment at the landfill has a much greater affinity for Pb than for Cu, Cd, Ni, or Zn. The reasons why Cd, Cu, Ni, and Zn exhibited similiar behavior in the column study, in contrast to the batch adsorption study, are not clear. The answer to this problem is beyond the scope of this study due to the complexity of the various mechanisms governing the migration behavior of heavy metals in a multicomponent system.

Visual inspection of Figures 27a - 27j indicates that the heavy metals migrated through the two columns at different rates. Differences in heavy metal migration rates are usually attributed to variations in the

sediment's physical and chemical properties and/or differences in the leachate's chemical properties. According to Fuller and Warrick (1985), physical and chemical properties of the soil/sediment that can influence pollutant migration include particle size distribution, sediment type, bulk density, porosity, pH, particle surface area, amount of soluble salts, and percentage of free iron oxides. Leachate chemical and physical properties that can influence pollutant migration include pH, concentration of soluble salts, concentration of pollutant in solution, concentration of associated potential pollutants in solution, and solution flux.

The above properties were compared for column 1 and column 2 to determine what mechanisms were responsible for the differences in attenuation. Upon inspection it was determined that only particle size distribution (texture), and solution flux played a major role in controlling the migration rates of the metals. The other properties exhibited no significant difference between the two columns.

Differences in solution flux between column 1 (flux = 5.4 ml/hr) and column 2 (flux = 9.4 ml/hr) are a possible attenuation mechanism. Bigger and Nielson (1960) have shown that solution flux can influence the migration rates for some ions. Heavy metals, in particular Cd (Korte and others, 1976; Alesii and others, 1980), Ni and Zn (Alesii

and others, 1980), however, do not appear to be influenced by solution flux. Even though the differences in solution flux were significant, in light of previous studies it was concluded that solution flux was not an important attenuation mechanism in this study.

Recent studies (Griffin and Shimp, 1976; Korte and others, 1976; Alesii and others, 1980), have shown that sediment texture is a significant controlling factor in the migration rates of heavy metals. The reason for this is not apparent at this time, but it is probably due to surface effects such as adsorption and ion exchange (Korte and others, 1976).

Although the column studies were not initially designed to study the effect of grain size distribution on the migration rates of heavy metals, the data suggest that even small differences in the grain size distribution can alter the attenuation capability of a sediment. In other words, the more fine-grained a sediment (especially an increase in the percent clay) the more effective the sediment is in reducing heavy metal mobility.

Model Application

The error function model was fitted to the elution curve data points for the movement of the heavy metals through the two sediments. Equations [8] - [11] were used to calculate the retardation factor, R (dimensionless), and

the diffusion-dispersion coefficient, D (cm^2/hr) for the two sediments (Table 13).

The calculated values of R and D provide a quantitative method for describing the migration rates of the heavy metals in the sediment columns. Table 13 shows that the calculated values of R and D describe the elution curves observed in Figures 27a - 27j. As expected, the values of R calculated for the migration of heavy metals through the silt loam (column 1) are higher than those calculated for the silty sand (column 2). This reflects the fact that R and D, for a particular heavy metal and sediment type, are calculated from their experimentally determined elution curves. Therefore, the earlier the breakthrough, the smaller the retardation factor. The same interpretation can be made for the diffusion-dispersion coefficient. The less sigmoidal the elution curve, the smaller the diffusion-dispersion coefficient.

To utilize the Error Function Model, the estimated values of R and D for each metal and soil type were substituted into Equation [5]. The equation was then solved for depth (z) using a time (t) of 250, 300, and 350 days, and a pore-water velocity (v) of 4.0 cm/day. The resulting profiles for Cu, Cd, Ni, Pb, and Zn were plotted as a function of depth (z) versus relative concentration (C/C_0) (Figures 28a - 28j).

The profiles estimate how far a solute front will

HEAVY METAL	COLUMN 1				COLUMN 2			
	a	b	R	D	a	b	R	D
Cadmium	18.56	3.04	6.10	.58	9.50	2.18	4.36	3.19
Copper	29.38	4.47	6.57	.25	10.60	2.25	4.71	2.77
Nickel	9.48	1.61	5.89	2.17	7.06	1.42	4.97	6.58
Zinc	15.78	2.72	5.81	.77	14.23	3.44	4.13	1.35
Lead	28.28	1.96	14.43	.60	-4.99	-.67	7.51	19.89

Table 13: Calculated values of a, b, R, and D, for column 1 and column 2.

Figure 28a - 28j: Estimated depth to which the heavy metals will migrate to in a silt loam (column 1) and a sandy loam (column 2) using a pore water velocity of 4.0 cm/day.

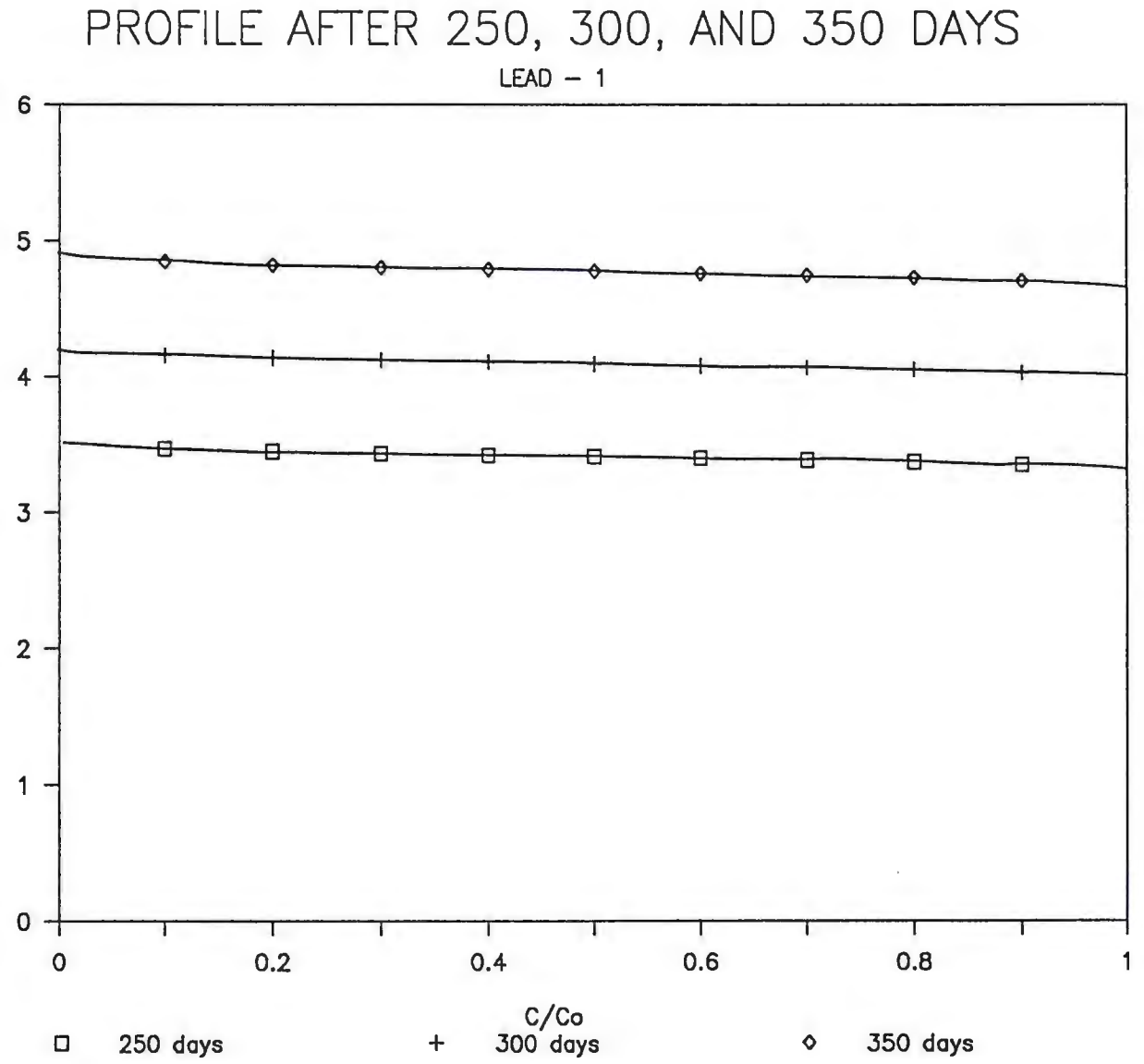
PROFILE AFTER 250, 300, AND 350 DAYS
LEAD – 1
DEPTH (M)
6
5
4
3
2
1
0
0
0.2
0.4
0.6
0.8
1
C/Co
250 days
300 days
350 days

Figure 28a

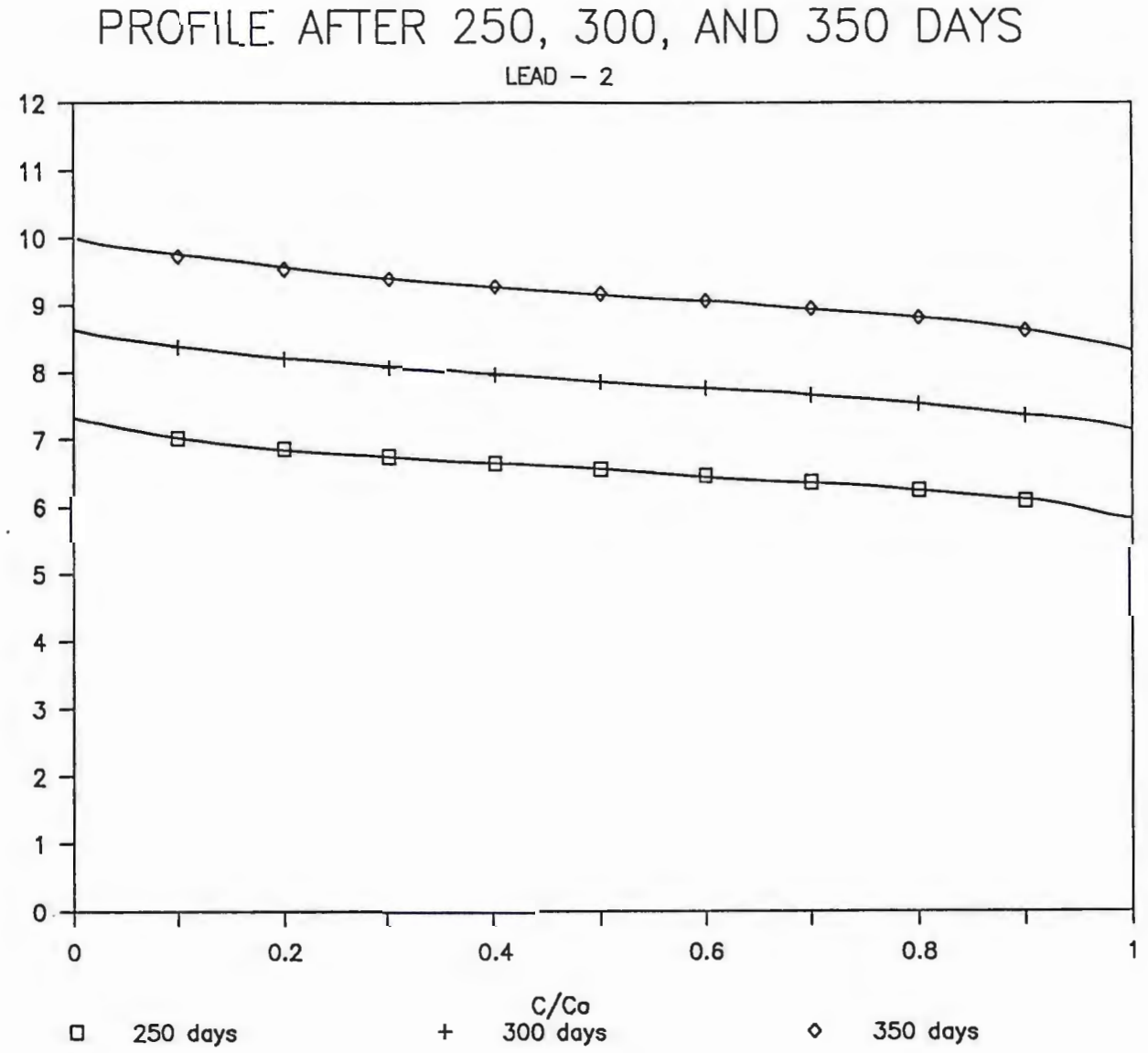
PROFILE AFTER 250, 300, AND 350 DAYS
LEAD – 2
DEPTH (M)
12
11
10
9
8
7
6
5
4
3
2
1
0
0
0.2
0.4
0.6
0.8
1
C/Co
250 days
300 days
350 days

Figure 28b

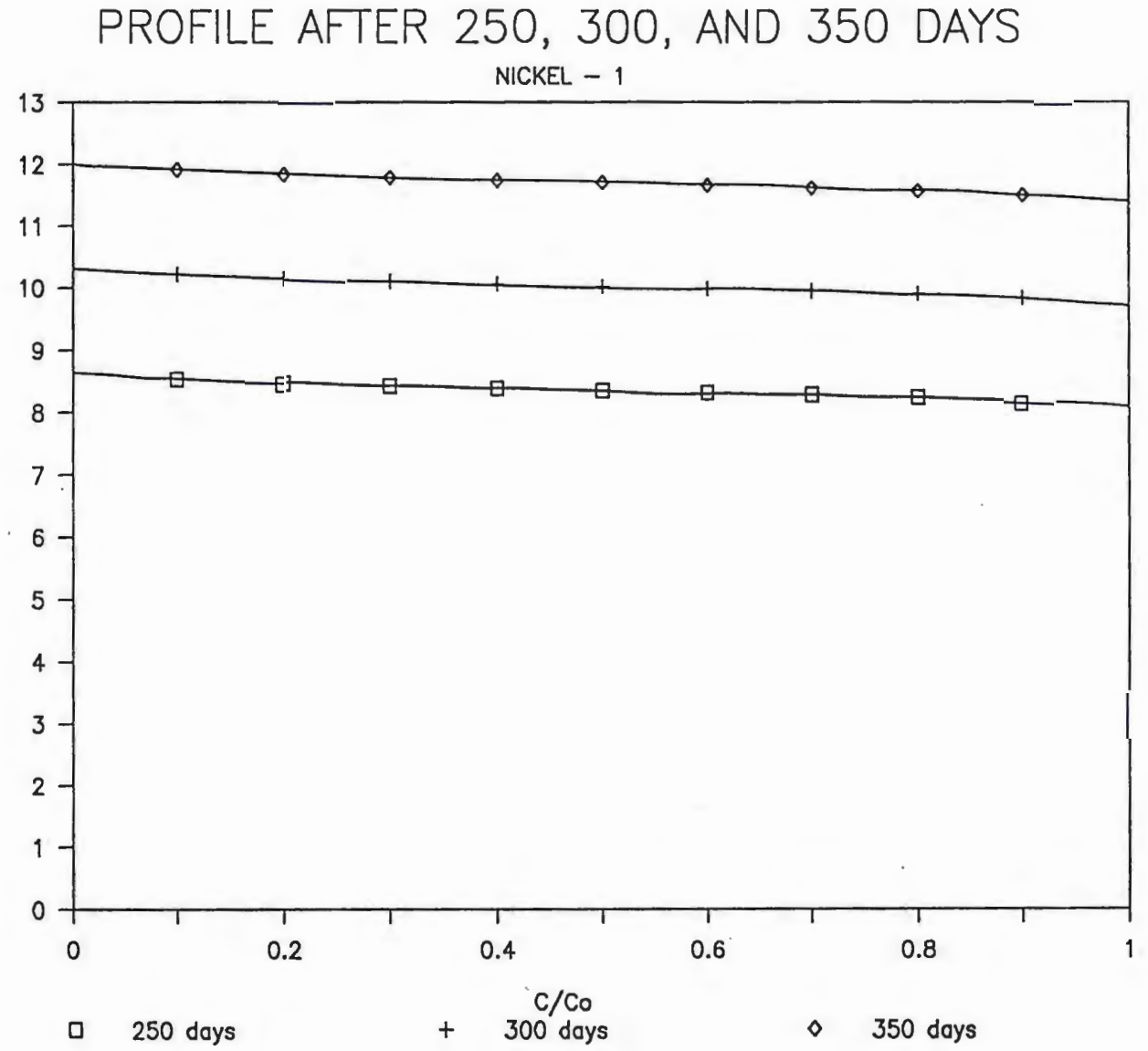
PROFILE AFTER 250, 300, AND 350 DAYS
NICKEL – 1
DEPTH (M)
13
12
11
10
9
8
7
6
5
4
3
2
1
0
0
0.2
0.4
0.6
0.8
1
C/Co
250 days
300 days
350 days

Figure 28c

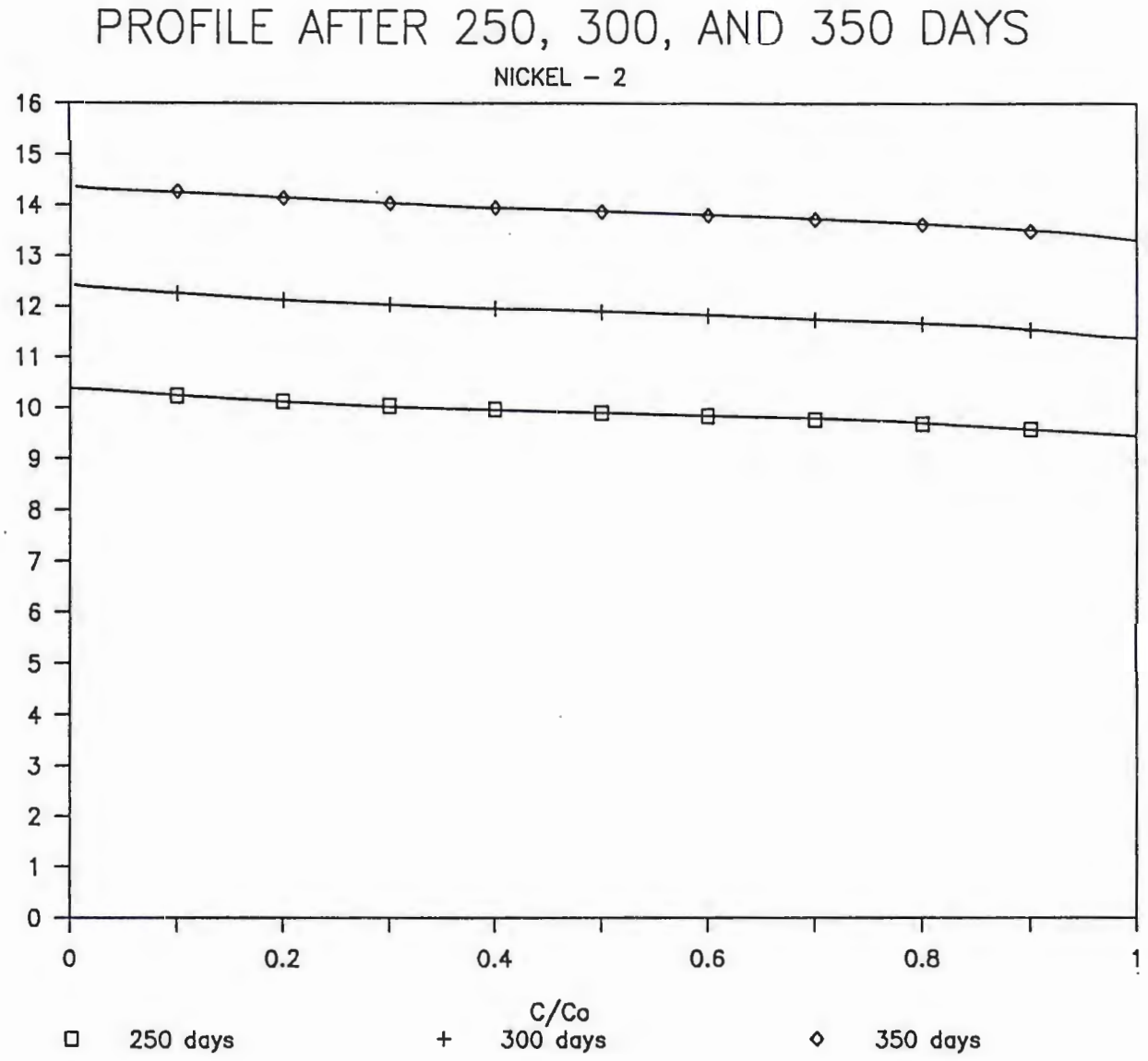
PROFILE AFTER 250, 300, AND 350 DAYS
NICKEL – 2
DEPTH (M)
16
15
14
13
12
11
10
9
8
7
6
5
4
3
2
1
0
0
0.2
0.4
0.6
0.8
1
C/Co
250 days
300 days
350 days

Figure 28d

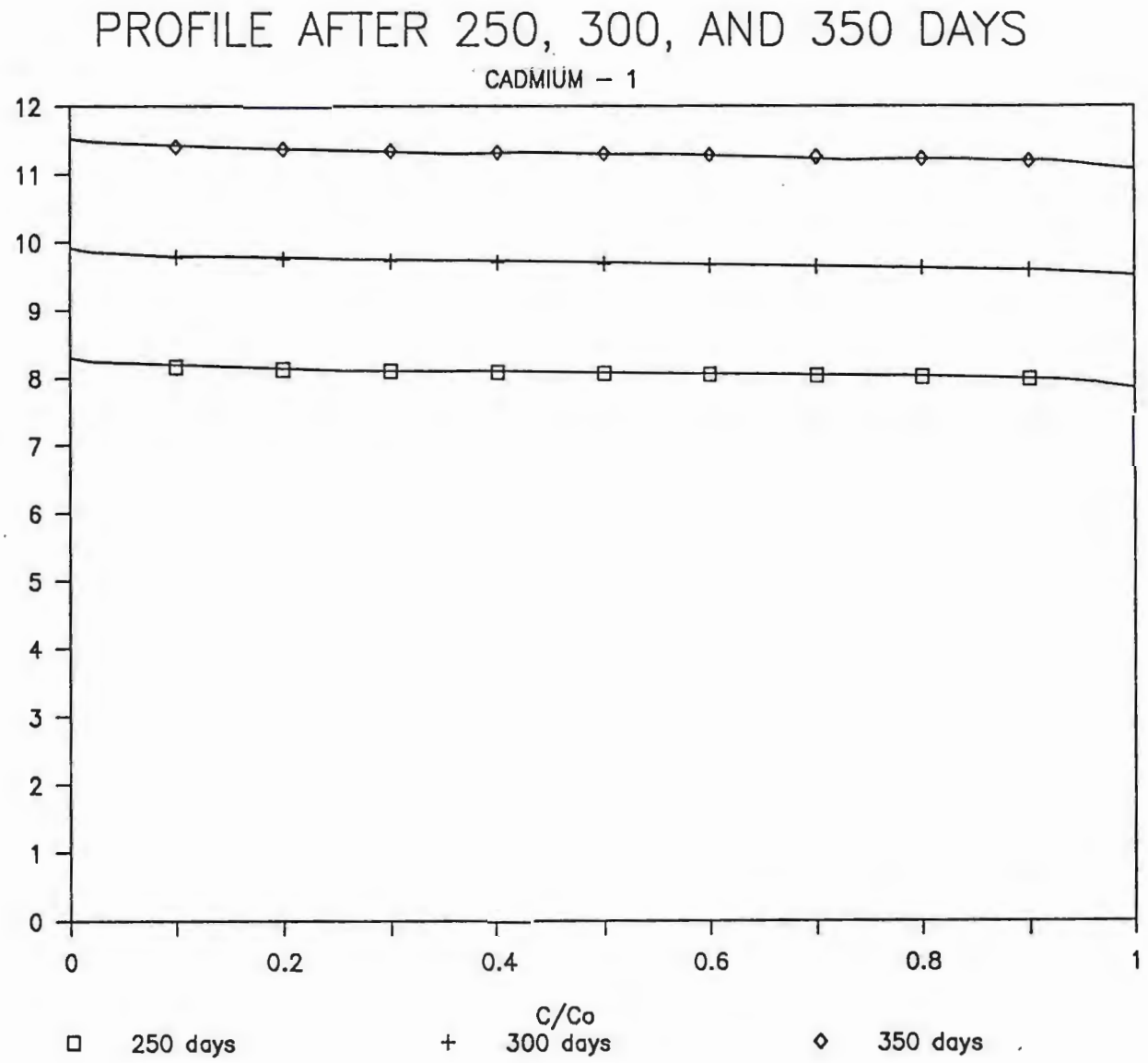
PROFILE AFTER 250, 300, AND 350 DAYS
CADMIUM – 1
DEPTH (M)
12
11
10
9
8
7
6
5
4
3
2
1
0
0
0.2
0.4
0.6
0.8
1
C/Co
250 days
300 days
350 days

Figure 28e

PROFILE AFTER 250, 300, AND 350 DAYS
CADMIUM – 2
DEPTH (M)
17
16
15
14
13
12
11
10
9
8
7
6
5
4
3
2
1
0
0
0.2
0.4
0.6
0.8
1
C/Co
250 days
300 days
350 days

Figure 28f

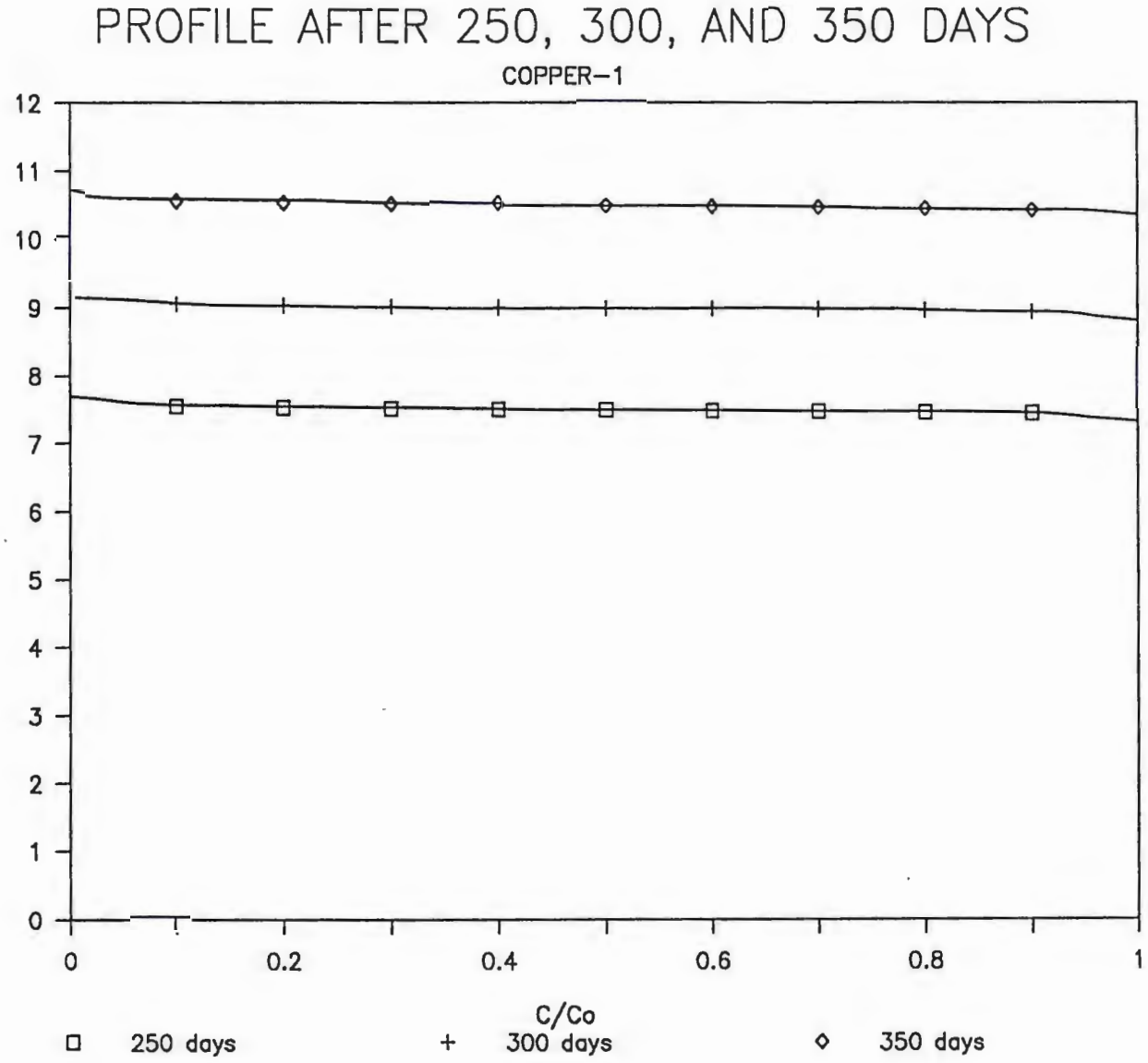
PROFILE AFTER 250, 300, AND 350 DAYS
COPPER-1
DEPTH (M)
12
11
10
9
8
7
6
5
4
3
2
1
0
0
0.2
0.4
0.6
0.8
1
C/Co
250 days
300 days
350 days

Figure 28g

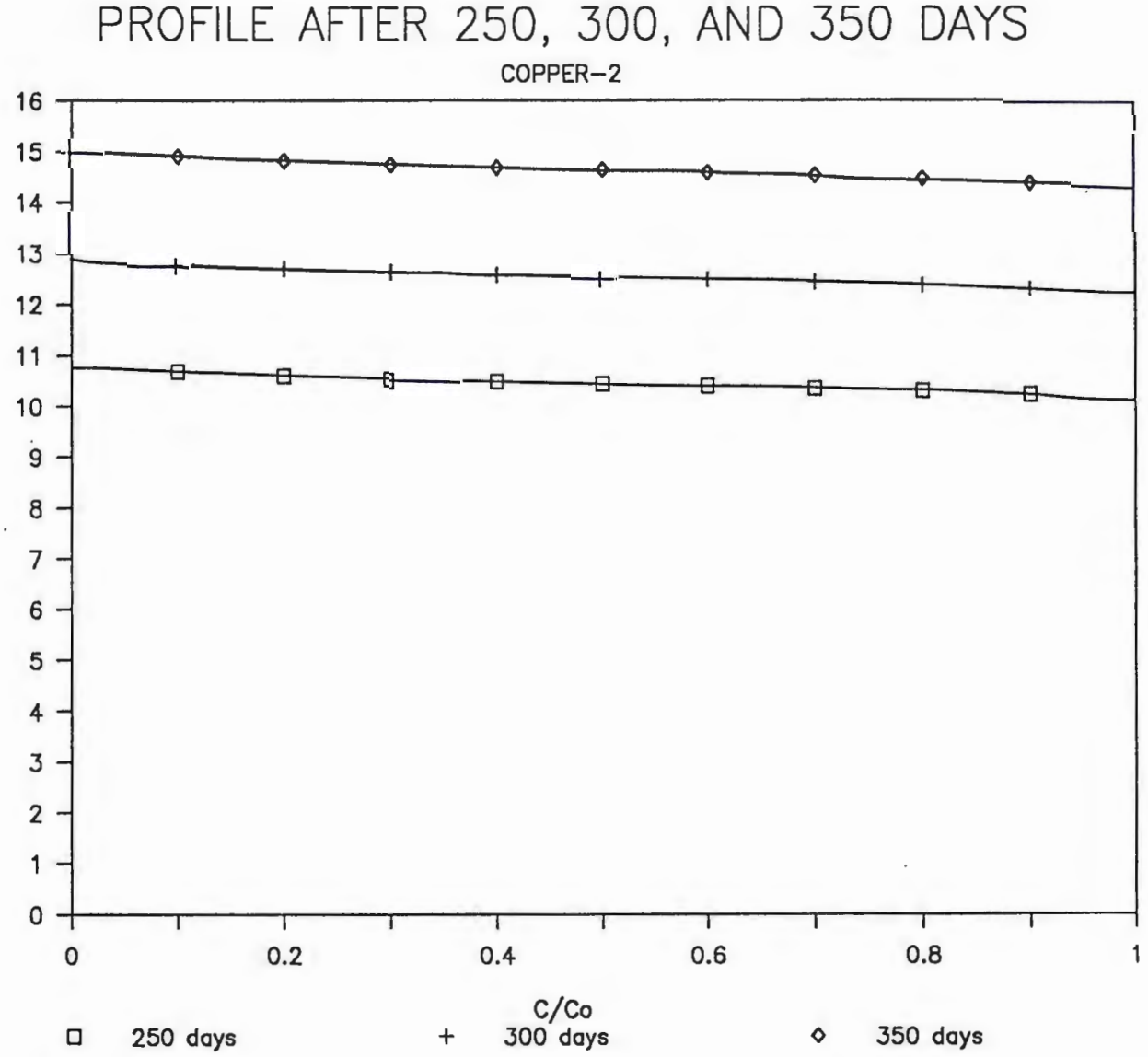
PROFILE AFTER 250, 300, AND 350 DAYS
COPPER-2
DEPTH (M)
16
15
14
13
12
11
10
9
8
7
6
5
4
3
2
1
0
0
0.2
0.4
0.6
0.8
1
C/Co
250 days
300 days
350 days

Figure 28h

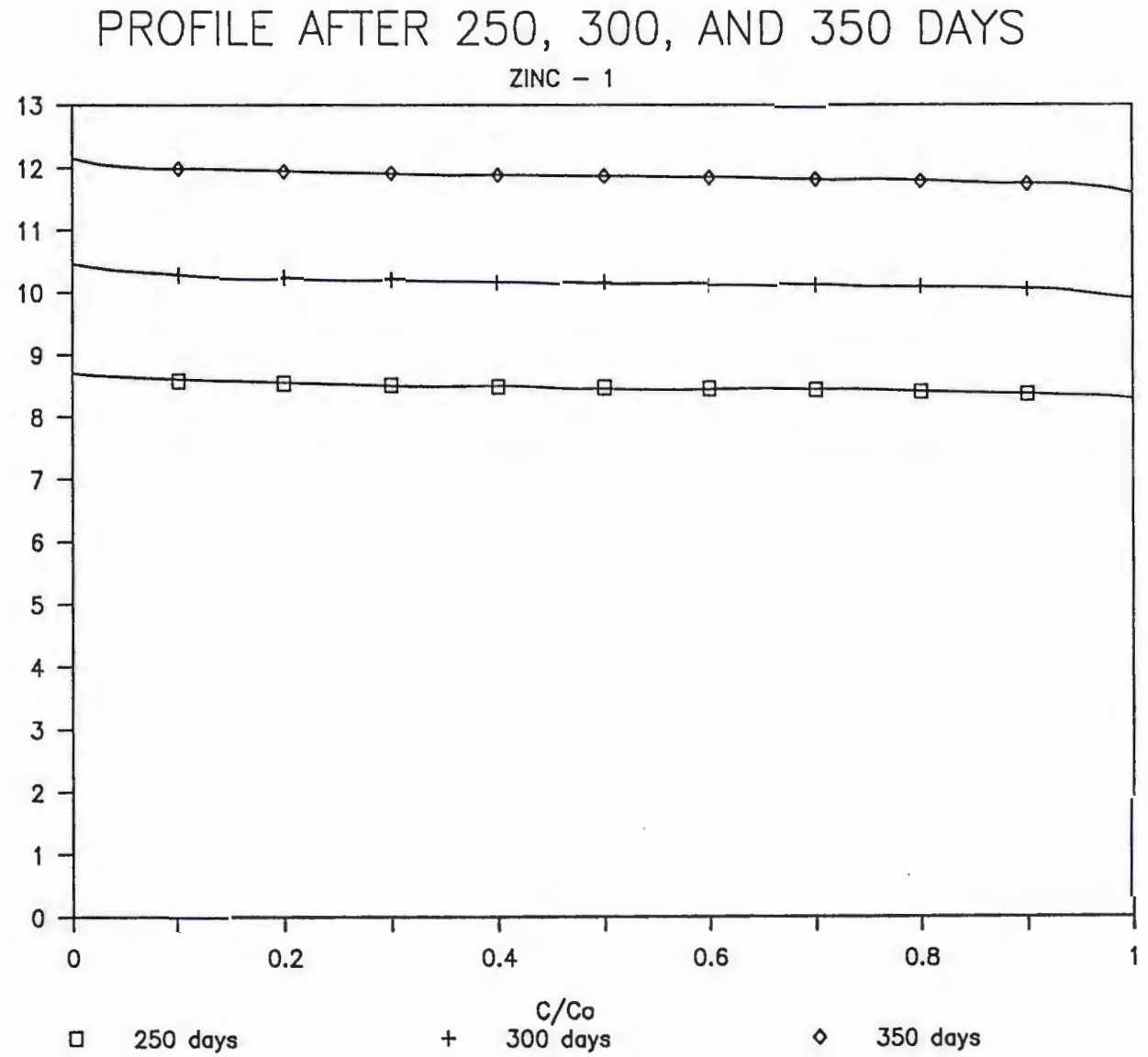
PROFILE AFTER 250, 300, AND 350 DAYS
ZINC – 1
DEPTH (M)
13
12
11
10
9
8
7
6
5
4
3
2
1
0
0
0.2
0.4
0.6
0.8
1
C/Co
250 days
300 days
350 days

Figure 28i

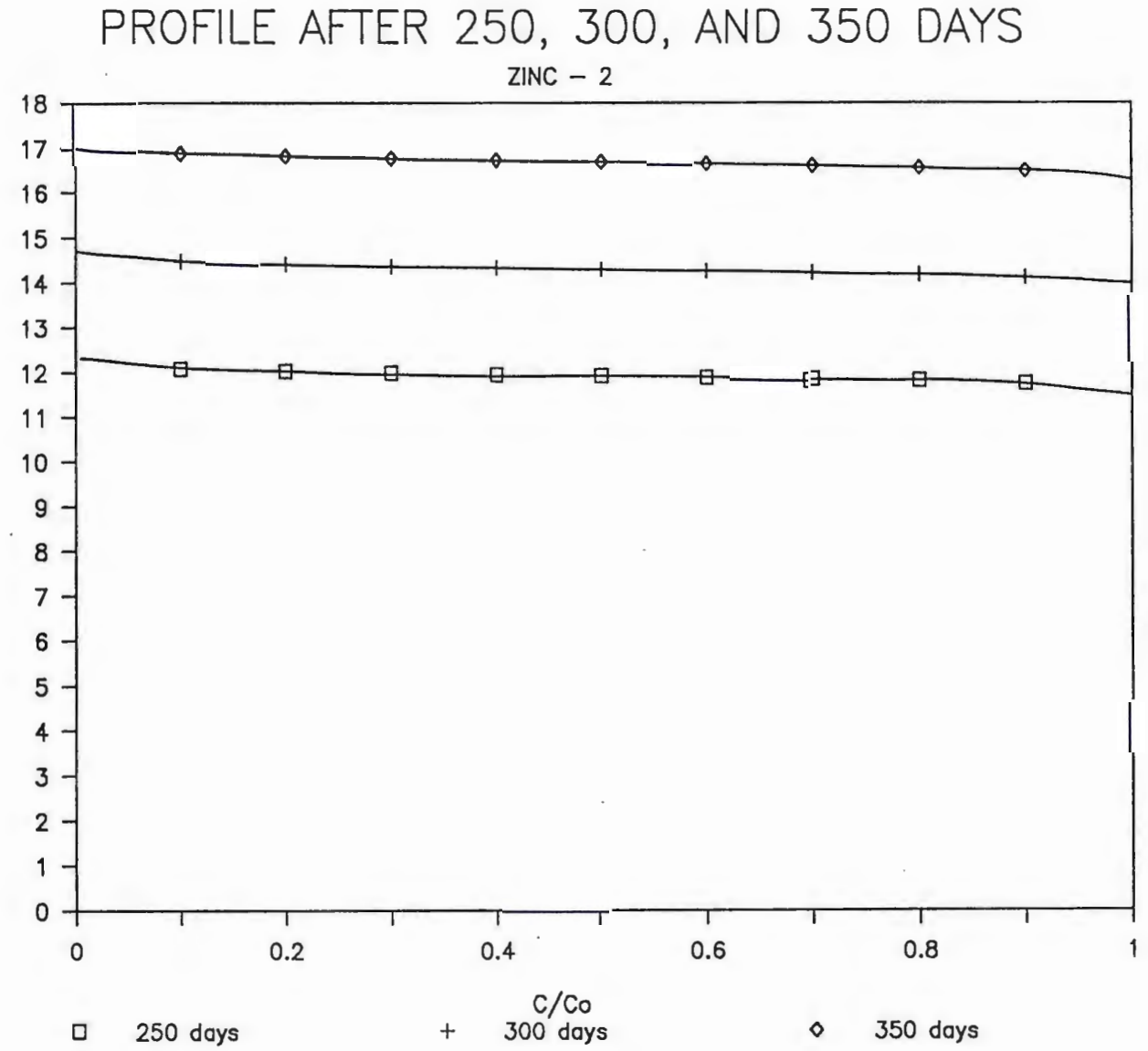
PROFILE AFTER 250, 300, AND 350 DAYS
ZINC – 2
DEPTH (M)
18
17
16
15
14
13
12
11
10
9
8
7
6
5
4
3
2
1
0
0
0.2
0.4
0.6
0.8
1
C/Co
250 days
300 days
350 days

Figure 28j

will migrate in the silt loam and sandy loam. The depth to which Cu, Cd, Ni, Pb, and Zn will migrate is significantly greater in the sandy loam than in the silt loam. Lead is projected to migrate the shortest distance in both soil types after 350 days (about .97 m in the silt loam, and about 1.86 m in the sandy loam) followed by Cu, Cd, Ni, and Zn for the silt loam, and Ni, Cu, Cd, and Zn for the sandy loam. The non-sigmoidal appearance of the solute profiles is a result of the small dispersion-diffusion coefficients (D's) used in the calculation of the profiles. Fortunately, due to the nature of Equation [5], the calculation of the solute profile is the least sensitive to variations in D compared to R or v. The insignificance of the dispersion-diffusion coefficient in calculating solute profiles has also been demonstrated by Amoozegar-Fard and others (1982; 1983).

The model presented here is for a step input of solute and can be applied to saturated and unsaturated conditions. Although the estimated parameters can be used to predict the migration rate of Pb, Ni, Cd, Cu, and Zn, the results must be considered only as a first approximation (Amoozegar-Fard and others, 1983).

Extraction and Distribution of Heavy Metals in Sediment Columns

In this study, the depth of penetration and the relative extractability of 5 adsorbed heavy metals (Pb, Ni, Cd, Cu, and Zn) are investigated. At the completion of

the leaching studies, the sediment columns were oven dried and segmented into 1 cm sections. One gram splits of each segment were digested and the extractable amounts of Pb, Cu, Cd, Ni, and Zn were determined, as described above.

Figures 29a - 29j are graphical representations of the data obtained from the metal extractions. The graphs are plotted as C/C_{max} versus depth, where C_{max} is the greatest amount of metal extracted from any segment, and C is the amount of metal extracted at other depths. The profiles were plotted using the relative concentration (C/C_{max}) versus depth, instead of the concentration of metal extracted per gram of soil versus depth, to negate the effect of the non-adsorbed heavy metals present in the pore-fluid when the core was extracted. In both sectioned columns, the top segment (1 cm) yielded the greatest extractable amounts of heavy metals. The profile curve for Pb (column 2) is discontinued at the 9 and 10 cm depths because the amount of Pb extracted was below the detection limits of the spectrophotometer.

Extraction profiles of column 1 and column 2 sediments indictate that the potential for heavy metal extraction is quite variable. The extraction curves for Cd, Cu, and Ni suggest that the metals may have reached steady or near steady-state conditions while migrating through the sediments. On the other hand, the steadily decreasing

Figure 29a - 29j: Heavy metal extraction profiles for column 1 and column 2.

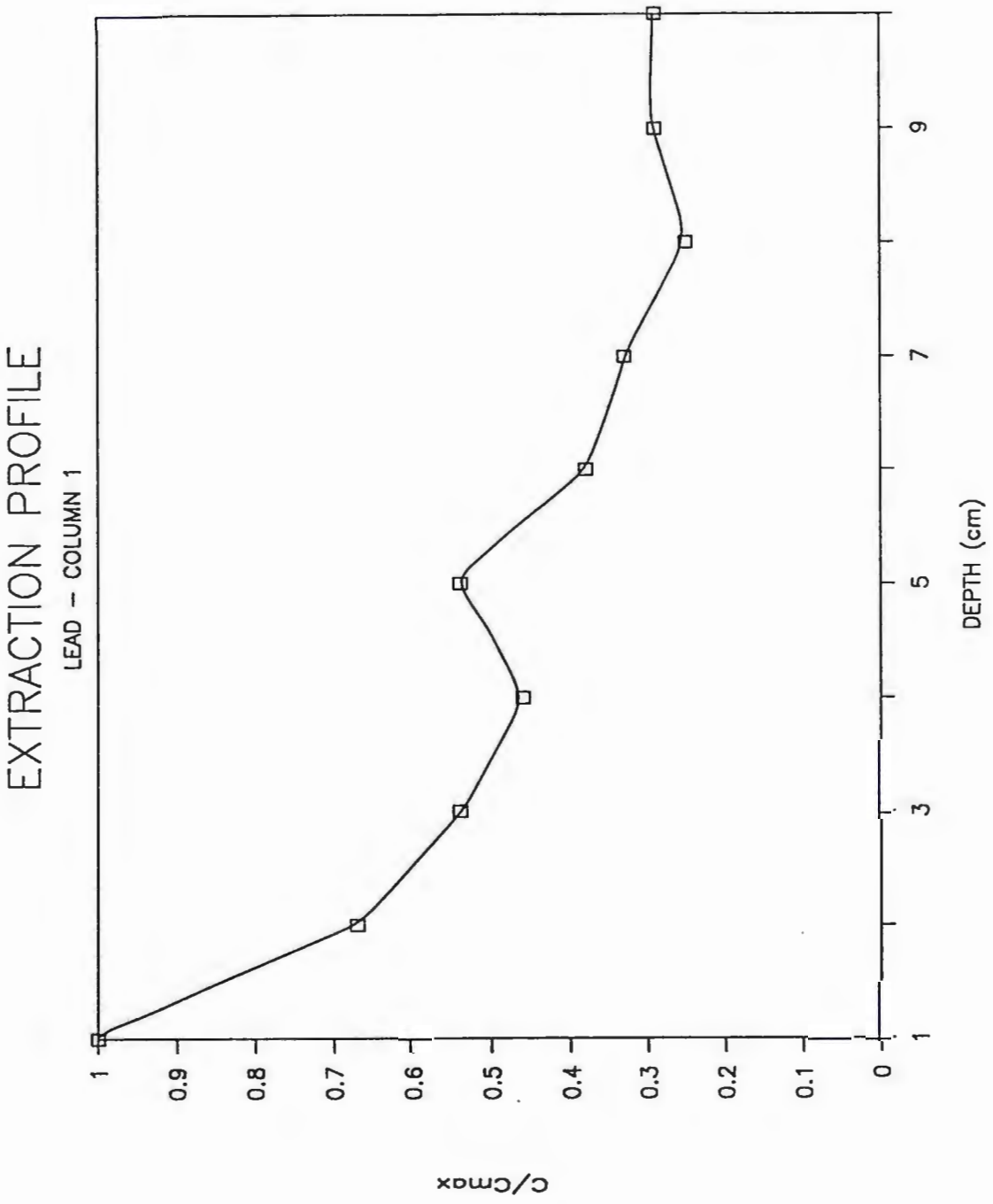
EXTRACTION PROFILE
LEAD -- COLUMN 1
C/Cmax
1
0.9
0.8
0.7
0.6
0.5
0.4
0.3
0.2
0.1
0
1
3
5
7
9
DEPTH (cm)

Figure 29a

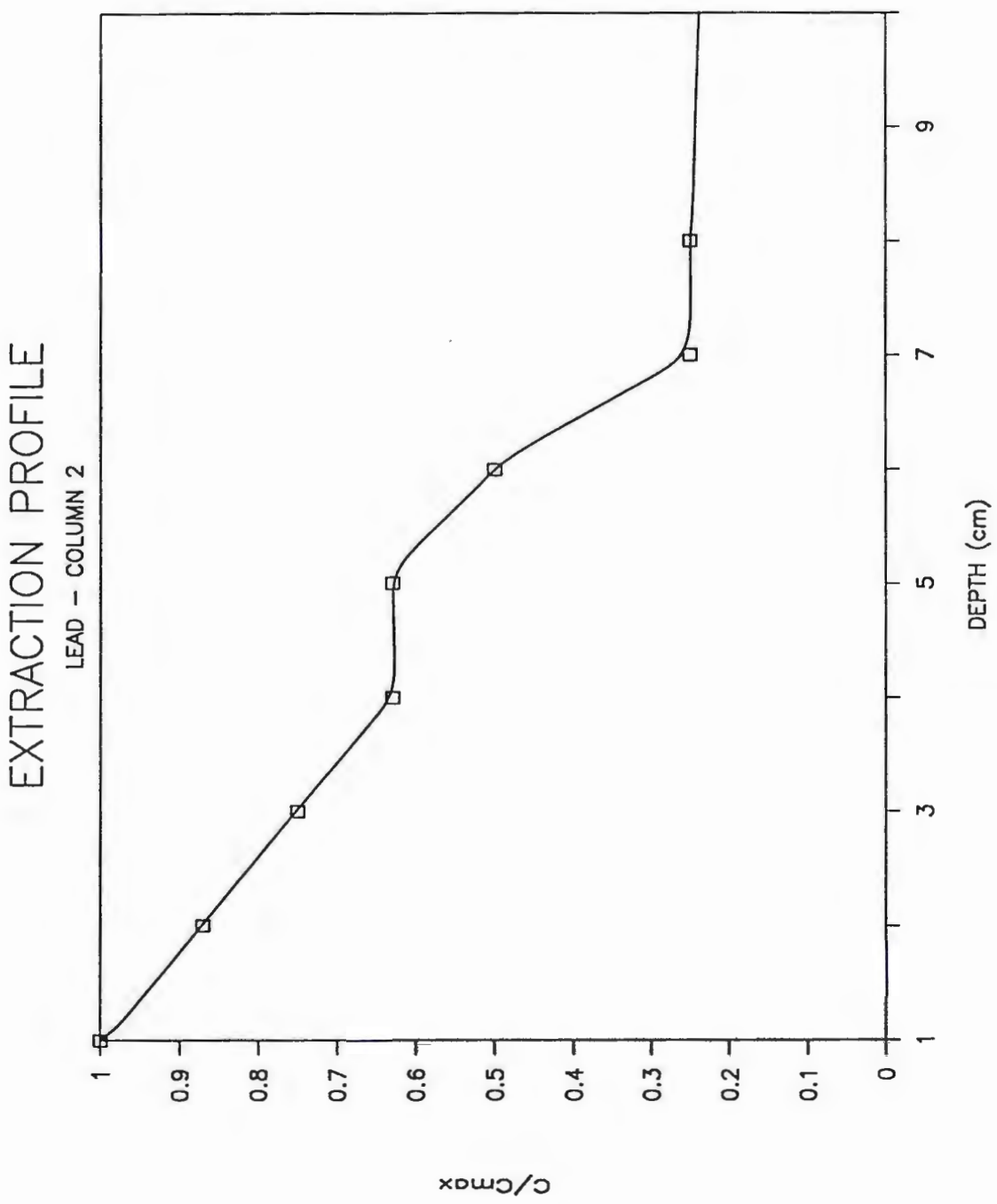
EXTRACTION PROFILE
LEAD – COLUMN 2
C/Cmax
1
0.9
0.8
0.7
0.6
0.5
0.4
0.3
0.2
0.1
0
1
3
5
7
9
DEPTH (cm)

Figure 29b

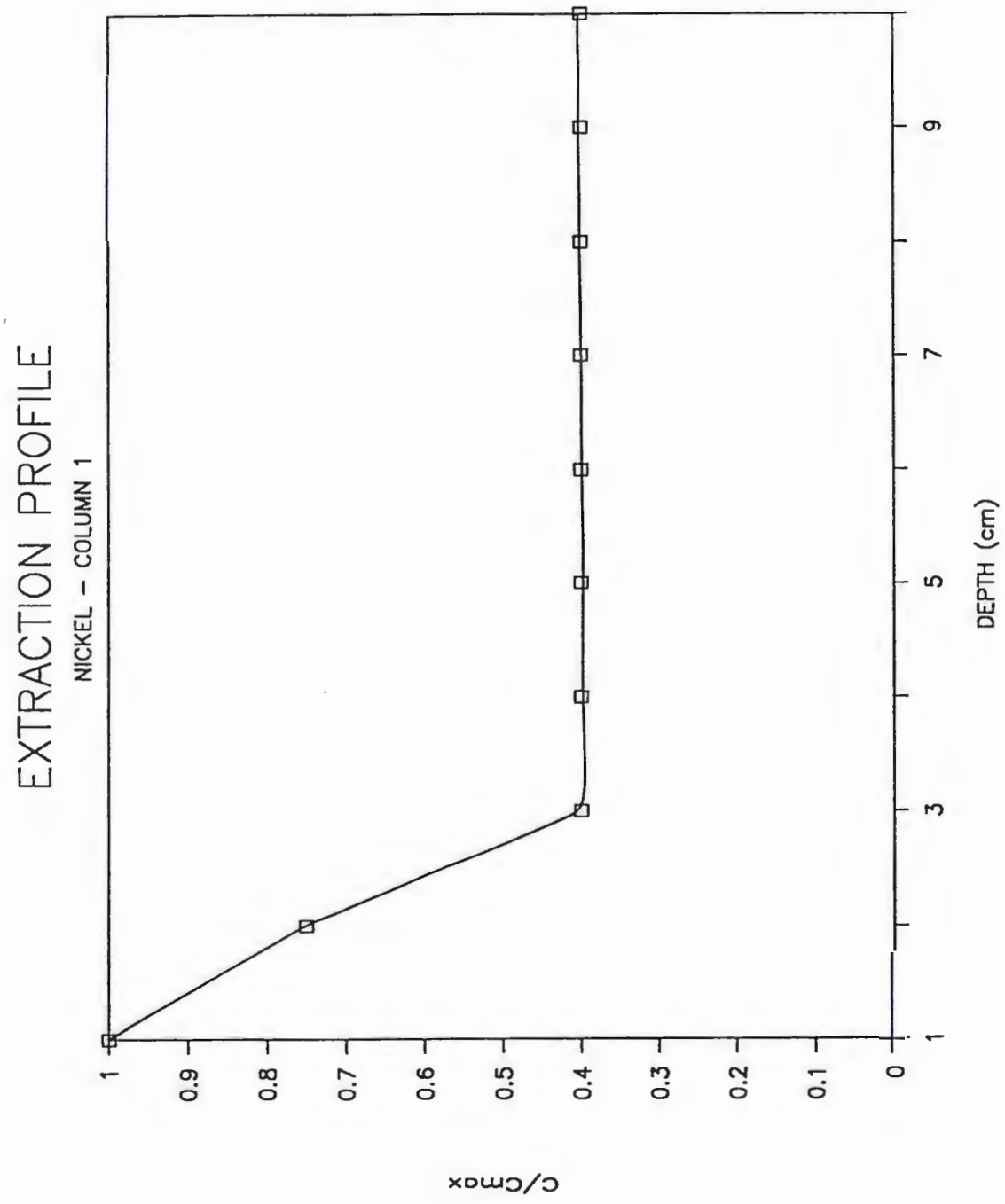
EXTRACTION PROFILE
NICKEL - COLUMN 1
C/Cmax
1
0.9
0.8
0.7
0.6
0.5
0.4
0.3
0.2
0.1
0
1
3
5
7
9
DEPTH (cm)

Figure 29c

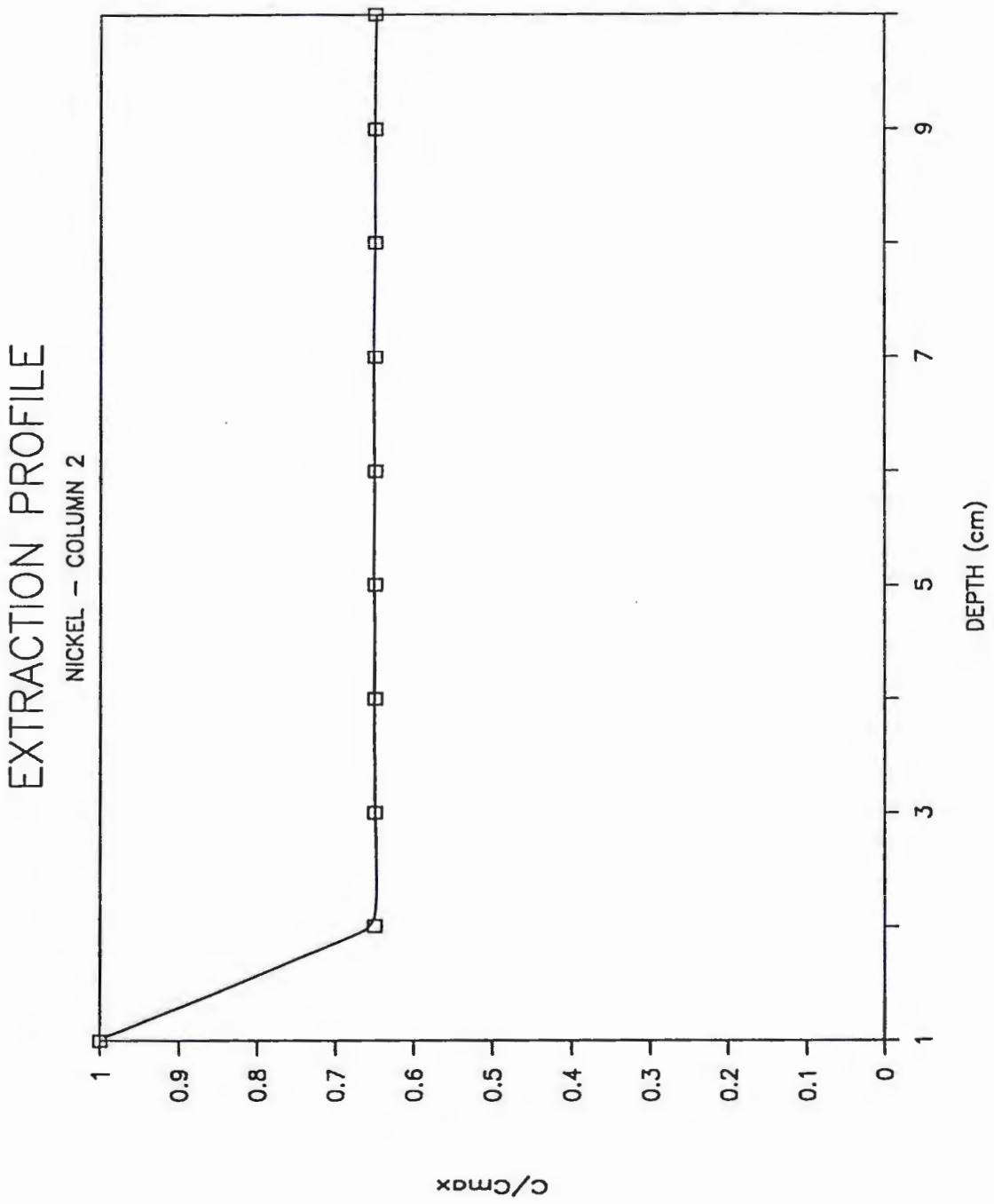
EXTRACTION PROFILE
NICKEL - COLUMN 2
C/Cmax
1
0.9
0.8
0.7
0.6
0.5
0.4
0.3
0.2
0.1
0
1
3
5
7
9
DEPTH (cm)

Figure 29d

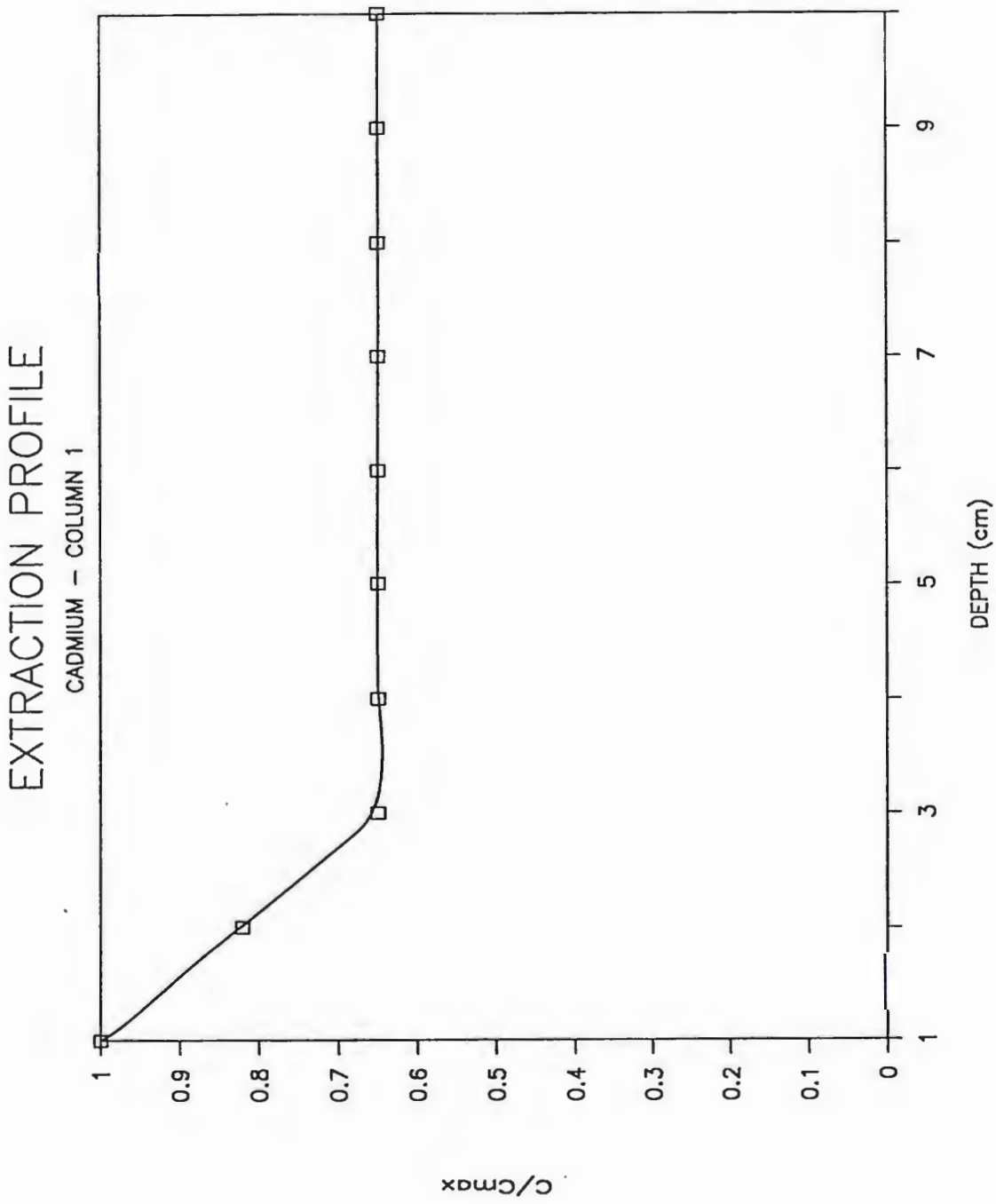
EXTRACTION PROFILE
CADMIUM - COLUMN 1
C/Cmax
1
0.9
0.8
0.7
0.6
0.5
0.4
0.3
0.2
0.1
0
1
3
5
7
9
DEPTH (cm)

Figure 29e

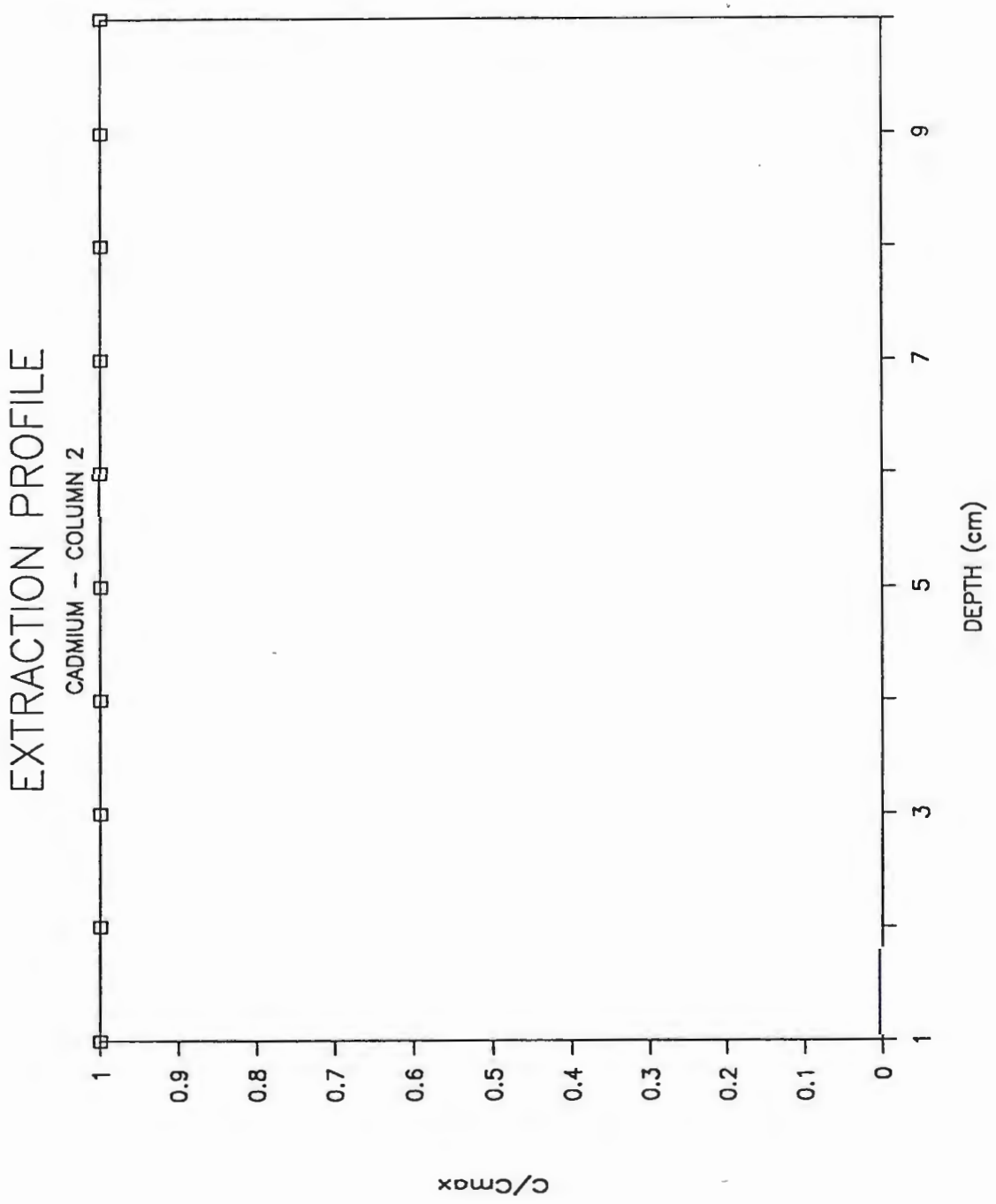
EXTRACTION PROFILE
CADMIUM - COLUMN 2
C/Cmax
1
0.9
0.8
0.7
0.6
0.5
0.4
0.3
0.2
0.1
0
1
3
5
7
9
DEPTH (cm)

Figure 29f

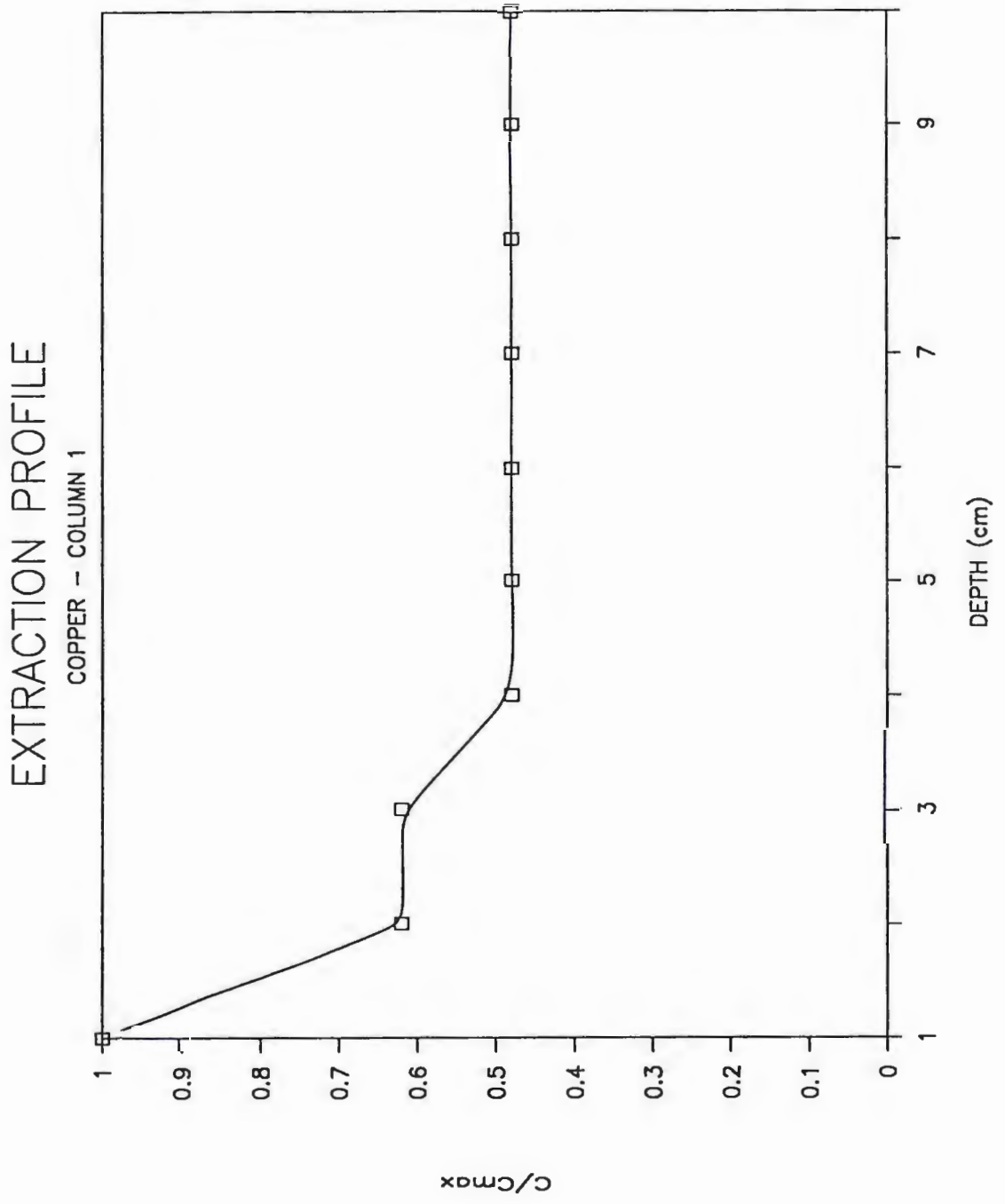
EXTRACTION PROFILE
COPPER – COLUMN 1
C/Cmax
1
0.9
0.8
0.7
0.6
0.5
0.4
0.3
0.2
0.1
0
1
3
5
7
9
DEPTH (cm)

Figure 29g

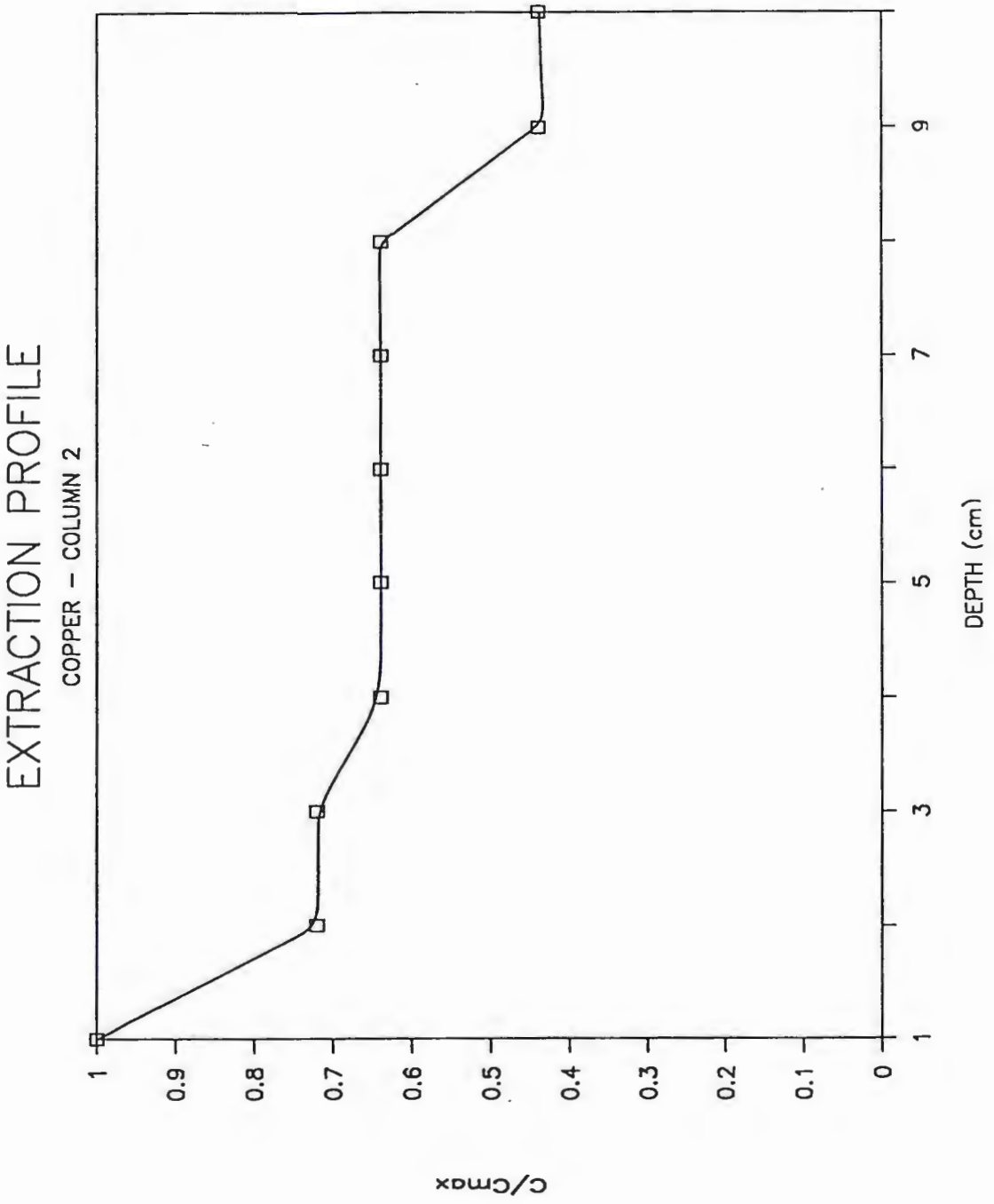
EXTRACTION PROFILE
COPPER - COLUMN 2
C/Cmax
1
0.9
0.8
0.7
0.6
0.5
0.4
0.3
0.2
0.1
0
1
3
5
7
9
DEPTH (cm)

Figure 29h

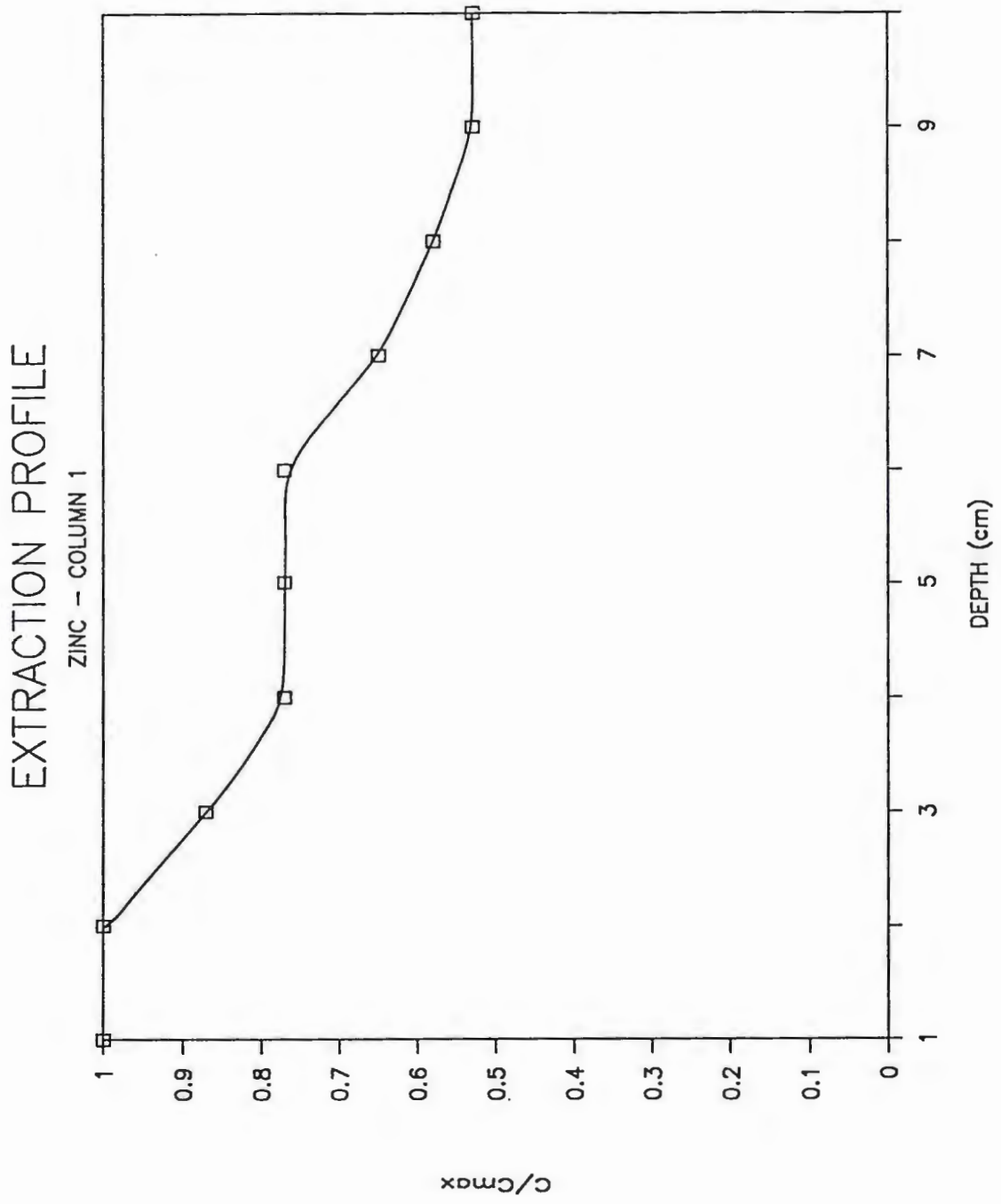
EXTRACTION PROFILE
ZINC - COLUMN 1
C/Cmax
1
0.9
0.8
0.7
0.6
0.5
0.4
0.3
0.2
0.1
0
1
3
5
7
9
DEPTH (cm)

Figure 29i

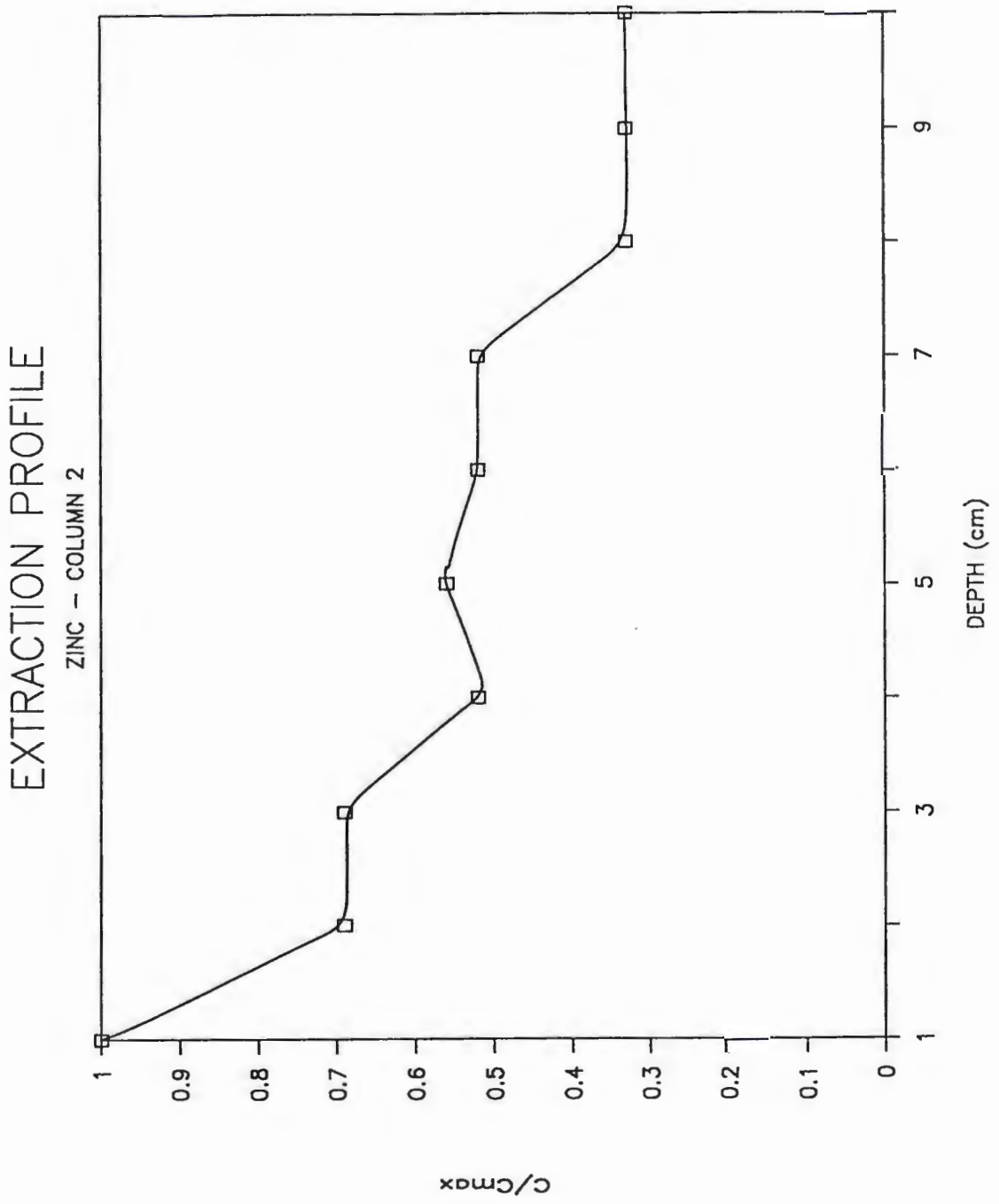
EXTRACTION PROFILE
ZINC - COLUMN 2
C/Cmax
1
0.9
0.8
0.7
0.6
0.5
0.4
0.3
0.2
0.1
0
1
3
5
7
9
DEPTH (cm)

Figure 29j

amounts of Pb and Zn extracted as a function of depth suggest that Pb and Zn had not reached steady-state conditions and were still actively involved in the ion exchange and/or adsorption reactions. It is possible that Pb dominated the filling of the available adsorption sites so much that the other competing heavy metals were subsequently flushed through the soil. The data verify the results obtained in the other studies. Pb was strongly retained by the sediment in contrast to Ni, Cd, Cu, and Zn, all of which showed moderate mobility. Soil column extraction data are contained in Appendix 6.

Summary and Conclusions

Results from column studies were incorporated into a transport model for Pb, Cu, Cd, Zn, and Ni in unconsolidated sediments. Time-dependent batch adsorption studies were conducted to characterize the adsorption of Pb, Cu, Cd, Zn, and Ni by glacially derived sediments.

The sediment showed varying degrees of affinity for the heavy metals in the batch adsorption study. Pb was the most strongly adsorbed cation: nearly 91% of the Pb in the batch 1 solution was adsorbed within the first 0.3 hr of equilibration. Cu was the next most strongly adsorbed cation followed by Cd, Zn, and Ni. The rapid adsorption of

the heavy metals suggests that the adsorption is predominantly a surface phenomenon.

The kinetics of the heavy metal adsorption was examined by fitting the Freundlich and Langmuir adsorption isotherms to the batch adsorption data. Data that fit the Freundlich isotherm indicate equilibrium (thermodynamic) adsorption, whereas data that fit the Langmuir isotherm indicate kinetic (time-dependent) adsorption. The heavy metal adsorption data conformed to the Langmuir isotherm as indicated by the relatively high correlation coefficients for C/X versus C. Some of the adsorption curves appeared to be resolvable into two linear portions, possibly indicating two adsorption sites each with different retention energies.

Elution curves generated from column studies verify the results obtained in the batch adsorption study: the sediments have a much higher affinity for Pb than for Cu, Cd, Ni, and Zn. The amount of time for the heavy metals to migrate through a silt loam was greater than for the sandy loam. This suggests that the silt loam was more effective in attenuating the heavy metals. The greater attenuation capability of the silt loam over the sandy loam appears to be related to its grain size distribution: the more fine-grained a sediment the more effective it is in attenuating heavy metals.

Elution curves produced by the step input of a heavy

metal solution in the soil column were utilized by an error function model to predict the movement of the heavy metals in the soil. The model predicts that Cu, Cd, Ni, and Zn solute fronts migrate about 2.3 m in the silt loam after 1 year, and that a Pb solute front will migrate about .97 m after 1 year. The model also predicted that the heavy metals will migrate about .7 to 1 m farther in the sandy loam.

General Conclusions/Recommendations

This study was undertaken to determine the environmental impact of ash landfilling on the groundwater environment and quality at the WLSSD landfill. During the beginning stages of this project it became apparent that two separate studies would have to be performed: (1) a hydrogeologic investigation of the study area, and (2) an investigation of the physical and chemical characteristics of heavy-metal-laden leachate and its interaction with the local substrate.

The data obtained from the hydrogeologic study gave an idea of groundwater flow velocities (needed for use in the heavy metal transport study), the water table configuration, water level fluctuations in response to precipitation events, and problems with the required gradient reversal near the southwest arm of the leachate collection system.

Since the hydrogeologic study utilized some data from previous investigations it became evident during this project that further research needs to be performed. Steps that can be taken to further describe the hydrogeologic setting of the landfill include: drilling more observation wells in the north, west and northwest portions of the study site; drilling wells in the refuse to determine the extent and size of the groundwater mound; and installing

piezometer nests to determine the vertical movement of the groundwater.

The complex nature of the sedimentary deposits at the site stresses the need for more detailed subsurface investigations, including textural analyses of the sediments interpreted in the new observation well borings. This is of importance because of the relationship between heavy metal attenuation and sediment texture.

Work that needs to be done to further describe the heavy metal interactions with the sediment should include examining the transport of chelated metals in the sediment, since heavy metals usually combine with organic compounds in a landfill environment. Unfortunately work done to date indicates that chelated heavy metals tend to migrate further than non-chelated heavy metals. Heavy metal adsorption rates with the sediment associated with pH changes should also be examined.

Research obtained in this study indicates that there will be no immediate hazard associated with the land disposal of the fly ash. This conclusion is based on three main observations: (1) that the sediment has a relatively high affinity for heavy metals, especially Pb which is leached from the the ash in the highest concentration, (2) that the groundwater flow rates observed for the area are low, therefore increasing the time for physical and chemical reactions to take place between the sediment and

the heavy metals, and (3) that the amount of heavy metals leached from the ash is very small as evidenced by the water and acetic acid leaching tests.

Although there appears to be no hazard associated with the disposal of the ash at this time, several measures should be taken during the landfilling of the ash to insure groundwater quality: the ash should be kept separate from the rest of the waste minimizing the chance of heavy metal chelation; the ash should be deposited within the landfill where the groundwater flows towards the leachate collection system; and the ash should be deposited in areas of the landfill where the underlying sediment has a high percentage of silt and clay to maximize the heavy metal adsorption potential.

Bibliography

Adamson, A. W., 1967, Physical chemistry of surfaces (second edition): New York, John Wiley and Sons, Inc.

Alesii, B. A., Fuller, W. H., and Boyle, M. V., 1980, Effect of leachate flow rate on metal migration through soil: J. Env. Quality, v. 9, no. 1, p. 119-126.

Amoozegar-Fard, A., Fuller, W. H., and Warrick, A. W., 1984, An approach to predicting the movement of selected polluting metals in soils: J. Env. Qual., v. 13, no. 2, p. 290-297.

Amoozegar-Fard, A., Warrick, A. W., and Fuller, W. H., 1983, Simplified model for solute movement through soils: Soil Sci. Soc. Am. J., v. 47, p. 1047-1049.

Amoozegar-Fard, A., Nielsen, D. R., and Warrick, A. W., 1982, Soil solute concentration distributions for spatially varying pore water velocities and apparent diffusion coefficients: Soil Sci. Am. J., v. 46, p. 3-9.

Anderson, M. A., and Rubin, A. J., 1981, Adsorption of inorganics at solid-liquid interfaces: Ann Arbor, Michigan, Ann Arbor Science Publishers, 250p.

Barr Engineering Co., 1981, Recommended operating, inspection, monitoring and maintenance plan for the leachate collection system at Rice Lake Township Sanitary Landfill, St. Louis County, Minnesota, 13p.

Bigger, J. W., and Nielson, D. R., 1960, Diffusion effects in miscible displacement occurring in saturated and unsaturated porous materials: J. Geophysical Research, v. 65, p. 2887-2895.

Bonnichsen, B., 1972, Southern Part of Duluth Complex, in Sims, P. K., and Morey, G. B., eds. Geology of Minnesota: A Centennial Volume: Minnesota Geological Survey, St. Paul, Minnesota, p. 361-387.

Craddock, C., 1972, Regional geologic setting, in Sims, P.K. and Morey, G.B., eds., Geology of Minnesota: A Centennial Volume: Minnesota Geological Survey, St. Paul, Minnesota, p. 281-291.

Christensen, T. H., 1984, Cadmium soil sorption at low concentrations: II Reversibility, effect of changes in solute composition, and effect of soil aging: Water, Air, and Soil Pollution, v. 21, p. 115-125.

Dreimanis, A., 1971, The effect of lithology upon texture of till, in Yatsu, E., and Falconer, A., eds., Research methods in Pleistocene Geomorphology, Geo Astracts Ltd., Norwich, p. 66-82.

Driscoll, F. G., 1986, Groundwater and Wells (second edition): St. Paul, MN., Johnson Division, 1089p.

Enfield, C. G., and Shew, P., 1975, Comparison of two predictive non-equilibrium one-dimensional models for phosphate sorption and movement through homogeneous soils: J. of Env. Quality, Vol. 4, p. 198-202.

Fetter, C. W., 1980, Applied Hydrogeology: Columbus, Charles E. Merril Publishing Company, 488p.

Fitter, A. H., amd Sutton, C. D., 1975, The use of the Freundlich Isotherm for soil phosphate sorption data: J. Soil Sci., v. 26, p. 241-246.

Folk, R. S., 1980, Petrology of Sedimentary Rocks: Austin, Hemphill Publishing Company, 182p.

Green, J. C., 1972, North Shore Volcanic Group, in Sims, P.K., and Morey, G.B., eds., Geology of Minnesota: A Centennial Volume: Minnesota Geological Survey, St. Paul, Minnesota, p. 294-332.

Green, J. C., 1983, Geologic and geochemical evidence for the nature and development of the Middle Proterozoic (Keweenawan) midcontinent rift of North America: Tectonophysics, v. 94, p. 413-437.

Griffin, R. A., and Shimp, N. F., 1976, Effect of pH on exchange-adsorption or precipitation of lead from landfill leachates by clay minerals: Env. Sci. and Tech., v. 10, p. 1256-1261.

Griggs, G. B., and Gilchrist, J. A., 1983, Geologic hazards, resources, and environmental planning (second edition): Belmont CA, Wadsworth Publishing Company, 502p.

Gross, L. B., 1982, The Stratigraphy and lithology of the glaciogenic sediments of the Two Harbors area, Northeastern Minnesota: unpub. M.S. thesis, University of Minnesota, 151p.

Harrison, W., and others, 1983, Geology, hydrology, and mineral resources of crystalline rock areas of the Lake Superior Region, United States: Argonne National Laboratory, p. 202-207.

Houle, M. J., and others, 1979, Industrial hazardous waste migration potential, in Proceedings, 5th Annual Res. Symp., Municipal Solid Waste: Resource Recovery: USEPA, Cincinnati, Ohio.

John, M. K., 1972, Cadmium adsorption maxima of soils as measured by the Langmuir Isotherm: Can. J. of Soil Sci., v. 52, p. 343-350.

Kanivetsky, R., 1979, Hydrogeologic map of Minnesota, quaternary hydrogeology: Minnesota Geological Survey Quaternary Hydrogeology Map S-3.

Kanivetsky, R., 1978, Hydrogeologic map of Minnesota, bedrock hydrogeology: Minnesota Geological Survey Bedrock Hydrogeology Map S-2.

Knight, S. K., Molsather, L. R., and Bonnell, M. D., 1983, Retrofitting an existing sanitary landfill with a leachate collection system, a case study: Sixth Annual Madison Conference of Applied Research and Practice of Municipal and industrial waste, p. 295-310.

Korte, N. E., and others, 1976, Trace element movement in soils: Influence of soil physical and chemical properties: Soil Sci., v. 122, no. 6, p. 350-359.

Lakehead Testing Laboratory, 1976, Report of subsurface investigation of existing landfill, Rice Lake Road, Duluth Mn.

Langmuir, I., 1918, Adsorption of gases on plane surfaces of glass, mica, and platinum: J. Am. Chem. Soc., v. 40, p. 1361-1402.

Lannon, P. M., 1986, The Quaternary stratigraphy and glacial history of the Duluth-Superior Area: unpub. M.S. thesis, University of Minnesota, 115 p.

Lapidus, L., and Amundson, N. R., 1952, Mathematics of absorption in beds. VI. The effect of longitudinal diffusion in ion exchange and chromatographic columns, J. Phys. Chem., v. 56, p. 984-988.

Minning, R. C., 1973, The electrical resistivity method, Part I: Technical Memo Number 3: Water Well J., v. 27, no. 6.

Moore, J. W., and Ramamoorthy, S., 1984, Heavy metals in natural waters: New York, Springer-Verlag, 261p.

Moss, C. M., 1977, The surficial and environmental geology of the French River Quadrangle, St. Louis County, Minnesota: unpub. M.S. thesis, University of Minnesota, 69 p.

Olcott, P. G., and others, 1978, Water resources of the Lake Superior Watershed, Northeastern Minnesota: U.S. Geological Survey, Hydrol. Inv. Atlas HA-582.

Rao, P. S., and others, 1979, Evaluation of conceptual models for describing non-equilibrium adsorption-desorption of pesticides during steady flow in soils: Soil Sci. Soc. Am. J., v. 43, p. 22-28.

RREM, Inc., 1986, Hydrologic and hydrogeologic study, pipeline spill area, 70p. Esko, MN.

RREM, Inc., 1984, Evaluation of potential sanitary landfill sites, phase 2 study, p. 46-59.

Rogers, J. E., 1962, Reconnaissance of groundwater conditions in the Duluth Municipal Airport area, Minnesota: U.S. Geol. Survey Open - File Report, 18p.

Soil Conservation Service, 1986, Soil Survey of St. Louis County.

Soil Exploration Company, 1983, Report of resistivity survey, proposed Rice Lake Landfill site, in RREM, Inc., 1984, Evaluation of potential sanitary landfill sites, phase 2 study, p. 46-59.

Udo, E. J., Bohn, H. L., and Tucker, T. C., 1970, Zinc adsorption by calcareous soils: Soil Sci. Soc. Am. - Proc., v. 34, p.405-407.

van Genuchten, M. Th., Davidson, J. M., and Wierenga, P. J., 1974, An evaluation of kinetic and equilibrium equations for the prediction of pesticide movement through porous media: New Mexico Agr. Exp. Sta. Bull. 628.

Van Schmus, W. R., 1976, Early and Middle Proterozoic history of the Great Lakes area, North America: Phill. Trans. R. Soc. Lond. V. 280, p. 605-628.

Van Schmus, W. R., Green, J.C., and Halls, H.C., 1982, Geochronology of Keeweenawen rocks of the Lake Superior Region: A summary: Geol. Soc.

Wong, K. V., and others, 1983, Heavy metal migration in soil leachate systems: Biocycle, v. 24, no. 1, p. 30-33.

Wright, H. E, Jr., 1972, Quaternary history of Minnesota, in Sims, P.K., and Morey, G.B., eds., Geology of Minnesota: A Centennial Volume: Minnesota Geological Survey, St. Paul, Minnesota, p. 294-332.

Wright, H. E. Jr., 1973, Tunnel Valleys, glacial surges, and subglacial hydrology of the Superior lobe, Minnesota: Geol. Soc. America Memoir 136, p. 251-276.

Wright. H. E., Jr., Watts, W.A., and others, 1969. Glacial and vegetational history of Northeastern Minnesota: Minnesota Geological Survey Special Publication II, 59 p. Am., Mem. 156, p. 165-171.

APPENDIX A
Soil Boring Log Data

Well No.	Land Surface Elevation (in feet)	Depth Below Land Surface (in feet)	Lithology
83-1	1421.9	0 - 8	Garbage
		8 - 15	Silty clay
		15 - 24	Silty sand with gravel and boulders
		24 - 37	Silty sand with gravel and boulders (dense)

Well No.	Land Surface Elevation (in feet)	Depth Below Land Surface (in feet)	Lithology
83-2	1420.7	0 - 9	Garbage
		9 - 14	Clayey silt
		14 - 22	Silty sand with gravel and boulders

Well No.	Land Surface Elevation (in feet)	Depth Below Land Surface (in feet)	Lithology
84-2	1428.2	0 - 13	Silty sand, brown, fine-grained, moist, very dense, with gravel and boulders
		13 - 15.5	Sand and Gravel

Well No.	Land Surface Elevation (in feet)	Depth Below Land Surface (in feet)	Lithology
P-1	1407.4	0 - 10	Silty sand with gravel and boulders

Well No.	Land Surface Elevation (in feet)	Depth Below Land Surface (in feet)	Lithology
84-4	1424.51	0 - 5	Soil cover and garbage
		5 - 9.5	Lean clay with gravel
		9.5 - 11	Silty sand with gravel, very dense
		11 - 15	Gravel
		15 - 18	Silty sand

Well No.	Land Surface Elevation (in feet)	Depth Below Land Surface (in feet)	Lithology
P-4	1415.52	0 - 1	Silty sand with some gravel
		1 - 10	Silty sand with lenses of water bearing fine sand

APPENDIX B
Grain Size Distribution Data

SAMPLE No.	PERCENTAGE SAND	SILT	CLAY
8/29/1	53	4	43
8/29/2	48	45	7
8/29/8	36	58	6
8/29/9	50	44	6
9/10/2	36	60	4
9/10/3	49	47	4
9/10/4	66	30	4
9/10/5	60	35	5
9/10/6	48	49	3
9/10/7	39	55	6
9/10/10	50	39	11
9/10/11	51	44	5
9/10/12	55	39	6
9/23/1	64	33	3
9/23/2	42	43	15
9/23/3	57	38	5
9/23/4	53	39	8
9/23/7	37	54	9
9/23/8	46	45	9
9/23/9	59	37	4
9/23/10	21	60	19
9/23/11	20	63	17
9/23/12	33	58	9
9/23/13	66	31	3
9/23/14	46	49	6

APPENDIX C
Monitor Well Water Level Data

WELL 82-1 WATER LEVEL DATA

DTW = Depth to water from top of casing (feet)
Water Level = Water level elevation (feet above MSL)
Top of casing elevation = 1407.56

Date	Julian Date	DTW	Water Level
05/31/85	151	5.19	1402.37
06/04/85	155	5.51	1402.05
06/13/85	164	5.49	1402.07
06/21/85	172	5.48	1402.08
07/01/85	182	5.58	1401.98
07/11/85	192	5.47	1402.09
07/17/85	198	5.53	1402.03
07/25/85	206	5.48	1402.08
07/31/85	212	5.46	1402.10
08/07/85	219	5.56	1402.00
08/14/85	226	5.51	1402.05
08/21/85	233	5.61	1401.95
09/04/85	247	5.31	1402.25
09/11/85	254	5.40	1401.16
09/18/85	261	5.49	1401.07
09/25/85	268	5.34	1401.17
10/09/85	282	5.45	1401.11
10/16/85	289	5.45	1402.11

WELL 82-2 WATER LEVEL DATA

DTW = Depth to water from top of casing (feet)
Water Level = Water level elevation (feet above MSL)
Top of casing elevation = 1408.42

Date	Julian Date	DTW	WaterLevel
05/31/85	151	4.37	1404.05
06/04/85	155	4.61	1403.81
06/13/85	164	5.20	1399.62
06/21/85	172	5.80	1402.62
07/01/85	182	4.86	1403.56
07/11/85	192	4.76	1403.66
07/17/85	198	5.53	1402.89
07/25/85	206	5.15	1403.27
07/31/85	212	5.43	1402.99
08/07/85	219	5.72	1402.70
08/14/85	226	5.38	1403.04
08/21/85	233	5.32	1403.10
09/04/85	247	4.24	1404.18
09/11/85	254	5.71	1402.71
09/18/85	261	5.21	1403.21
09/25/85	268	4.53	1403.89
10/09/85	282	4.60	1403.82
10/16/85	289	4.73	1403.69

WELL 82-3 WATER LEVEL DATA

DTW = Depth to water from top of casing (feet)
Water Level = Water level elevation (feet above MSL)
Top of casing elevation = 1407.11

Date	Julian Date	DTW	Water Level
05/31/85	151	5.48	1401.63
06/04/85	155	6.27	1400.84
06/13/85	164	7.49	1399.62
06/21/85	172	7.52	1399.59
07/01/85	182	7.58	1399.53
07/11/85	192	7.59	1399.52
07/17/85	198	7.60	1399.51
07/25/85	206	7.59	1399.52
07/31/85	212	7.59	1399.52
08/07/85	219	7.59	1399.52
08/14/85	226	7.37	1399.74
08/21/85	233	7.59	1399.52
09/04/85	247	7.30	1399.81
09/11/85	254	6.46	1400.65
09/18/85	261	7.48	1399.63
09/25/85	268	7.36	1399.75
10/09/85	282	7.36	1399.75
10/16/85	289	7.33	1399.78

WELL 82-4 WATER LEVEL DATA

DTW = Depth to water from top of casing (feet)
Water Level = Water level elevation (feet above MSL)
Top of casing elevation = 1407.17

Date	Julian Date	DTW	Water Level
05/31/85	151	5.33	1401.84
06/04/85	155	6.00	1401.17
06/13/85	164	6.79	1399.62
06/21/85	172	6.08	1401.09
07/01/85	182	6.85	1400.32
07/11/85	192	6.84	1400.33
07/17/85	198	7.01	1400.16
07/25/85	206	6.91	1400.26
07/31/85	212	6.97	1400.20
08/07/85	219	7.13	1400.04
08/14/85	226	6.98	1400.19
08/21/85	233	7.02	1400.15
09/04/85	247	6.45	1400.72
09/11/85	254	6.78	1400.39
09/18/85	261	6.87	1400.30
09/25/85	268	6.65	1400.52
10/09/85	282	6.73	1400.44
10/16/85	289	6.72	1400.45

WELL 82-5 WATER LEVEL DATA

DTW = Depth to water from top of casing (feet)
Water Level = Water level elevation (feet above MSL)
Top of casing elevation = 1404.37

Date	Julian Date	DTW	Water Level
05/31/85	151	4.42	1399.95
06/04/85	155	5.10	1399.27
06/13/85	164	6.30	1398.07
06/21/85	172	6.06	1398.31
07/01/85	182	5.34	1399.03
07/11/85	192	6.42	1397.95
07/17/85	198	6.51	1397.86
07/25/85	206	6.42	1397.95
07/31/85	212	6.54	1397.83
08/07/85	219	7.25	1397.12
08/14/85	226	6.62	1397.75
08/21/85	233	6.63	1397.74
09/04/85	247	5.76	1398.61
09/11/85	254	5.51	1398.86
09/18/85	261	6.48	1397.89
09/25/85	268	6.28	1398.09
10/09/85	282	6.36	1398.01
10/16/85	289	6.39	1397.98

WELL 82-6 WATER LEVEL DATA

DTW = Depth to water from top of casing (feet)
Water Level = Water level elevation (feet above MSL)
Top of casing elevation = 1403.98

Date	Julian Date	DTW	Water Level
05/31/85	151	4.48	1399.50
06/04/85	155	5.48	1398.50
06/13/85	164	5.96	1398.02
06/21/85	172	6.33	1397.65
07/01/85	182	5.79	1398.19
07/11/85	192	5.79	1398.19
07/17/85	198	6.29	1397.69
07/25/85	206	6.11	1397.87
07/31/85	212	6.33	1397.65
08/07/85	219	6.60	1397.38
08/14/85	226	6.52	1397.46
08/21/85	233	6.58	1397.40
09/04/85	247	4.77	1399.21
09/11/85	254	4.58	1399.40
09/18/85	261	6.25	1397.73
09/25/85	268	5.53	1398.45
10/09/85	282	6.48	1397.50
10/16/85	289	5.63	1398.35

WELL P-1 WATER LEVEL DATA

DTW = Depth to water from top of casing (feet)
Water Level = Water level elevation (feet above MSL)
Top of casing elevation = 1408.19

Date	Julian Date	DTW	Water Level
05/31/85	151	6.58	1401.64
06/04/85	155	6.84	1403.81
06/13/85	164	5.71	1402.48
06/21/85	172	8.71	1399.48
07/01/85	182	8.60	1399.59
07/11/85	192	8.80	1399.39
07/17/85	198	8.96	1399.23
07/25/85	206	8.78	1399.41
07/31/85	212	7.89	1400.30
08/07/85	219	6.27	1401.92
08/14/85	226	8.98	1399.21
08/21/85	233	8.95	1399.24
09/04/85	247	8.22	1399.97
09/11/85	254	8.66	1399.53
09/18/85	261	8.78	1399.41
09/25/85	268	8.51	1399.68
10/09/85	282	8.51	1399.68
10/16/85	289	8.60	1399.59

WELL P-4 WATER LEVEL DATA

DTW = Depth to water from top of casing (feet)
Water Level = Water level elevation (feet above MSL)
Top of casing elevation = 1417.52

Date	Julian Date	DTW	Water Level
06/04/85	155	7.09	1410.43
06/13/85	164	7.86	1409.66
06/21/85	172	7.44	1410.08
07/01/85	182	7.14	1410.38
07/11/85	192	7.49	1410.03
07/17/85	198	8.62	1408.90
07/25/85	206	7.08	1410.44
07/31/85	212	7.87	1409.65
08/07/85	219	8.55	1408.97
08/14/85	226	7.49	1410.03
08/21/85	233	7.67	1409.85
09/04/85	247	6.68	1410.84
09/11/85	254	7.16	1410.36
09/18/85	261	7.37	1410.15
09/25/85	268	6.88	1410.64
10/09/85	282	6.84	1410.68
10/16/85	289	6.98	1410.54

WELL W-6 WATER LEVEL DATA

DTW = Depth to water from top of casing (feet)
Water Level = Water level elevation (feet above MSL)
Top of casing elevation = 1428.88

Date	Julian Date	DTW	Water Level
06/04/85	155	14.86	1414.02
06/13/85	164	14.88	1414.00
06/21/85	172	14.87	1414.01
07/01/85	182	14.68	1414.20
07/11/85	192	14.72	1414.16
07/17/85	198	14.79	1414.09
07/25/85	206	14.87	1414.01
07/31/85	212	14.88	1414.00
08/07/85	219	14.75	1414.13
08/14/85	226	14.97	1413.91
08/21/85	233	15.08	1413.80
09/04/85	247	14.73	1414.15
09/11/85	254	14.77	1414.11
09/18/85	261	14.87	1414.01
09/25/85	268	14.75	1414.13
10/09/85	282	14.53	1414.35
10/16/85	289	14.76	1414.12

WELL C-1 WATER LEVEL DATA

DTW = Depth to water from top of casing (feet)
Water Level = Water level elevation (feet above MSL)
Top of casing elevation = 1423.63

Date	Julian Date	DTW	Water Level
06/04/85	155	5.04	1420.71
06/13/85	164	4.94	1420.81
06/21/85	172	4.81	1420.94
07/01/85	182	4.86	1420.89
07/11/85	192	4.82	1420.93
07/17/85	198	6.43	1419.32
07/25/85	206	5.24	1420.51
07/31/85	212	5.20	1420.55
08/07/85	219	5.26	1420.49
08/14/85	226	5.21	1420.54
08/21/85	233	5.23	1420.52
09/04/85	247	4.99	1420.76
09/11/85	254	4.95	1420.80
09/18/85	261	5.00	1420.75
09/25/85	268	4.96	1420.79
10/09/85	282	4.78	1420.97
10/16/85	289	4.78	1420.97

WELL C-2 WATER LEVEL DATA

DTW = Depth to water from top of casing (feet)
Water Level = Water level elevation (feet above MSL)
Top of casing elevation = 1432.58

Date	Julian Date	DTW	Water Level
06/04/85	155	5.80	1426.78
06/13/85	164	6.26	1426.32
06/21/85	172	6.23	1426.35
07/01/85	182	5.76	1426.82
07/11/85	192	5.87	1426.71
07/17/85	198	6.44	1426.14
07/25/85	206	6.51	1426.07
07/31/85	212	6.58	1426.00
08/07/85	219	7.27	1425.31
08/14/85	226	7.53	1425.05
08/21/85	233	7.53	1425.05
09/04/85	247	6.58	1426.00
09/11/85	254	6.53	1426.05
09/18/85	261	6.77	1425.81
09/25/85	268	6.58	1426.00
10/09/85	282	6.27	1426.31
10/16/85	289	6.05	1426.53

WELL W-18 WATER LEVEL DATA

DTW = Depth to water from top of casing (feet)
Water Level = Water level elevation (feet above MSL)
Top of casing elevation = 1422.75

Date	Julian Date	DTW	Water Level
06/13/85	164	5.31	1417.44
06/21/85	172	5.31	1417.44
07/01/85	182	5.28	1417.47
07/11/85	192	5.26	1417.49
07/17/85	198	5.44	1417.31
07/25/85	206	5.36	1417.39
07/31/85	212	5.49	1417.26
08/07/85	219	5.67	1417.08
08/14/85	226	5.68	1417.07
09/04/85	247	5.06	1417.69
09/11/85	254	5.23	1417.52
09/18/85	261	5.40	1417.35
09/25/85	268	5.19	1417.56
10/09/85	282	5.22	1417.53
10/16/85	289	5.18	1417.57

WELL 84-2 WATER LEVEL DATA

DTW = Depth to water from top of casing (feet)
Water Level = Water level elevation (feet above MSL)
Top of casing elevation = 1429.93

Date	Julian Date	DTW	Water Level
06/13/85	164	7.26	1422.67
06/21/85	172	6.17	1423.76
07/01/85	182	4.00	1425.93
07/11/85	192	6.09	1423.84
07/17/85	198	8.82	1421.11
07/25/85	206	5.98	1423.95
07/31/85	212	7.82	1422.11
08/07/85	219	9.98	1419.95
08/14/85	226	10.35	1419.58
08/21/85	233	6.29	1423.64
09/04/85	247	3.42	1426.51
09/11/85	254	3.68	1426.25
09/18/85	261	3.73	1426.20
09/25/85	268	3.13	1426.80
10/09/85	282	10.23	1419.70
10/16/85	289	3.17	1423.34

WELL 84-4 WATER LEVEL DATA

DTW = Depth to water from top of casing (feet)
Water Level = Water level elevation (feet above MSL)
Top of casing elevation = 1426.51

Date	Julian Date	DTW	Water Level
06/13/85	164	3.47	1423.04
06/21/85	172	3.87	1422.64
07/01/85	182	3.71	1422.80
07/11/85	192	3.53	1422.98
07/17/85	198	3.84	1422.67
07/25/85	206	3.48	1423.03
07/31/85	212	3.72	1422.79
08/07/85	219	4.26	1422.25
08/14/85	226	3.93	1422.58
08/21/85	233	4.40	1422.47
09/04/85	247	3.18	1423.33
09/11/85	254	3.50	1423.01
09/18/85	261	4.13	1422.38
09/25/85	268	3.23	1423.28
10/09/85	282	3.17	1423.34
10/16/85	289	3.28	1423.23

WELL W-10 WATER LEVEL DATA

DTW = Depth to water from top of casing (feet)
Water Level = Water level elevation (feet above MSL)
Top of casing elevation = 1423.63

Date	Julian Date	DTW	Water Level
06/21/85	172	4.02	1419.61
07/01/85	182	4.27	1419.36
07/11/85	192	4.11	1419.52
07/17/85	198	4.32	1419.31
07/25/85	206	4.16	1419.47
07/31/85	212	4.37	1419.26
08/07/85	219	4.61	1419.02
08/14/85	226	4.68	1417.07
09/04/85	247	4.12	1419.51
09/11/85	254	4.23	1419.40
09/18/85	261	4.55	1419.08
09/25/85	268	4.08	1419.55
10/09/85	282	4.02	1419.61
10/16/85	289	3.94	1419.69

APPENDIX D
1985 Precipitation Data

DAY	APR	MAY	JUN	JUL	AUG	SEP	OCT	NOV	DEC
1	0.00	0.00	T	0.16	0.00	0.00	0.13	0.12	0.14
2	0.01	0.03	0.00	0.00	0.00	2.20	0.02	0.00	T
3	0.00	T	0.00	0.26	0.00	0.49	0.00	0.00	0.06
4	0.00	0.03	0.05	1.00	2.14	0.00	T	0.00	0.02
5	T	0.01	0.00	0.00	0.04	0.00	T	0.00	0.04
6	0.00	0.17	T	T	0.00	0.04	T	0.11	0.00
7	T	0.00	0.12	T	0.00	0.00	0.63	T	T
8	0.01	T	T	T	0.01	0.05	0.06	T	0.08
9	0.00	T	0.00	0.02	0.05	0.30	0.00	T	0.01
10	0.00	0.47	0.00	0.02	0.05	0.02	0.00	0.00	T
11	0.00	0.03	0.00	0.00	0.00	0.00	T	0.01	0.00
12	0.25	0.18	T	0.00	1.44	0.00	0.52	0.04	T
13	0.01	0.00	T	0.01	0.00	0.00	0.00	T	0.00
14	0.00	0.53	0.00	0.13	T	0.00	0.00	0.01	0.02
15	0.00	0.22	0.00	0.00	0.18	0.00	0.00	0.00	0.00
16	0.01	0.35	0.77	0.00	0.16	0.02	0.00	0.52	0.00
17	0.06	T	0.04	0.71	0.09	0.01	0.00	0.00	T
18	0.02	0.00	T	1.06	0.01	T	0.00	0.56	0.00
19	0.00	0.00	0.00	0.00	T	0.39	0.00	0.03	T
20	0.12	0.00	0.02	0.05	0.05	T	0.00	0.04	T
21	0.45	0.00	0.32	T	0.00	0.04	0.00	T	0.03
22	0.74	0.00	0.05	0.00	0.83	0.33	0.01	0.34	T
23	0.46	0.00	0.00	0.00	0.18	1.12	0.14	0.02	0.19
24	0.18	T	0.00	0.70	0.22	0.00	0.00	0.00	T
25	0.00	0.54	1.07	0.00	0.00	0.00	0.00	0.22	0.07
26	T	0.06	0.48	0.00	0.00	0.00	0.00	0.08	0.11
27	T	0.00	0.24	0.00	0.00	0.00	0.00	T	T
28	0.00	T	0.02	0.00	0.26	0.02	0.00	0.05	T
29	0.00	0.43	0.00	0.00	0.08	0.42	0.25	0.04	T
30	0.03	0.72	0.00	0.02	0.00	0.57	0.00	0.14	T
31		0.67		0.00	0.12		0.00		0.01

** - Precipitation in water equivelant (inches)

APPENDIX E
Batch Adsorption Data

C = Equilibrium LEAD concentration

METAL LEAD

X = mg LEAD adsorbed per gram of soil

X2 = C/X

INITIAL SOLUTION CONC. mg\l		14.82 BATCH 1	28.96 BATCH 2	59.35 BATCH 3	91.08 BATCH 4	121.05 BATCH 5
0.3 hr shake	C (mg\l)	1.39	9.78	35.69	65.81	96.10
	% removal	90.62	66.23	39.87	27.74	20.61
	X (mg\g)	0.27	0.38	0.47	0.51	0.50
	X2	5.17	25.50	75.42	130.21	192.59
1 hr shake	C (mg\l)	1.15	10.01	37.73	73.65	100.51
	% removal	92.24	65.44	36.43	19.14	16.97
	X (mg\g)	0.27	0.38	0.43	0.35	0.41
	X2	4.21	26.41	87.26	211.27	244.67
3 hr shake	C (mg\l)	1.15	9.92	38.57	73.87	103.82
	% removal	92.24	65.75	35.01	18.90	14.23
	X (mg\g)	0.27	0.38	0.42	0.34	0.34
	X2	4.21	26.05	92.81	214.61	301.28
10 hr shake	C (mg\l)	0.91	9.54	38.50	73.65	103.82
	% removal	93.86	67.06	35.13	19.14	14.23
	X (mg\g)	0.28	0.39	0.42	0.35	0.34
	X2	3.27	24.56	92.33	211.27	301.28
30 hr shake	C (mg\l)	0.89	9.40	38.75	72.86	103.82
	% removal	93.99	67.54	34.71	20.00	14.23
	X (mg\g)	0.28	0.39	0.41	0.36	0.34
	X2	3.19	24.03	94.05	199.95	301.28

LINEAR REGRESSION EQUATION FOR LANGMUIR ADSORPTION ISOTHERM

Y = 2.886995 X + -5.83080

CORRELATION COEFFICIENT

r2 = 0.995722

LINEAR REGRESSION EQUATION FOR FREUNDLICH ADSORPTION ISOTHERM

Y = 0.050734 X + -0.51459

r2 = 0.421906

C = Equilibrium NICKEL concentration

METAL NICKEL X = mg NICKEL adsorbed per gram of soil

X2 = C/X

INITIAL SOLUTION CONC. mg\l		4.05 BATCH 1	7.16 BATCH 2	13.70 BATCH 3	16.23 BATCH 4	19.48 BATCH 5
0.3 hr shake	C (mg\l)	2.87	5.70	10.89	14.04	18.49
	% removal	29.14	20.39	20.51	13.49	5.08
	X (mg\g)	0.02	0.03	0.06	0.04	0.02
	X2	121.61	195.21	193.77	320.55	933.84
1 hr shake	C (mg\l)	3.09	6.06	11.96	15.62	19.13
	% removal	23.70	15.36	12.70	3.76	1.80
	X (mg\g)	0.02	0.02	0.03	0.01	0.01
	X2	160.94	275.45	343.68	1280.33	2732.86
3 hr shake	C (mg\l)	3.09	6.41	12.31	15.62	19.10
	% removal	23.70	10.47	10.15	3.76	1.95
	X (mg\g)	0.02	0.02	0.03	0.01	0.01
	X2	160.94	427.33	442.81	1280.33	2513.16
10 hr shake	C (mg\l)	3.20	6.52	12.39	15.63	19.37
	% removal	20.99	8.94	9.56	3.70	0.56
	X (mg\g)	0.02	0.01	0.03	0.01	0.00
	X2	188.24	509.37	472.90	1302.50	8804.55
30 hr shake	C (mg\l)	3.20	6.62	12.39	15.63	19.46
	% removal	20.99	7.54	9.56	3.70	0.10
	X (mg\g)	0.02	0.01	0.03	0.01	0.00
	X2	188.24	612.96	472.90	1302.50	48650.00

LINEAR REGRESSION EQUATION FOR LANGMUIR ADSORPTION ISOTHERM

Y = 2245.738 X + -15490.8

CORRELATION COEFFICIENT

r2 = 0.475553

LINEAR REGRESSION EQUATION FOR FREUNDLICH ADSORPTION ISOTHERM

Y = -1.19127 X + -0.95935

r2 = 0.272524

C = Equilibrium CADMIUM concentration

METAL CADMIUM — X = mg CADMIUM adsorbed per gram of soil

X2 = C/X

INITIAL SOLUTION CONC. mg\l		0.99 BATCH 1	1.97 BATCH 2	4.01 BATCH 3	6.09 BATCH 4	8.19 BATCH 5
0.3 hr shake	C (mg\l)	0.47	1.45	3.41	5.50	7.54
	% removal	52.53	26.40	14.96	9.69	7.94
	X (mg\g)	0.01	0.01	0.01	0.01	0.01
	X2	45.19	139.42	284.17	466.10	580.00
1 hr shake	C (mg\l)	0.51	1.58	3.52	5.50	7.59
	% removal	48.48	19.80	12.22	9.69	7.33
	X (mg\g)	0.01	0.01	0.01	0.01	0.01
	X2	53.12	202.56	359.18	466.10	632.50
3 hr shake	C (mg\l)	0.51	1.62	3.70	5.83	7.82
	% removal	48.48	17.77	7.73	4.27	4.52
	X (mg\g)	0.01	0.01	0.01	0.01	0.01
	X2	53.12	231.43	596.77	1121.15	1056.76
10 hr shake	C (mg\l)	0.50	1.63	3.71	5.29	7.75
	% removal	49.49	17.26	7.48	13.14	5.37
	X (mg\g)	0.01	0.01	0.01	0.02	0.01
	X2	51.02	239.71	618.33	330.63	880.68
30 hr shake	C (mg\l)	0.51	1.63	3.71	5.83	7.7
	% removal	48.48	17.26	7.48	4.27	5.98
	X (mg\g)	0.01	0.01	0.01	0.01	0.01
	X2	53.12	239.71	618.33	1121.15	785.71

LINEAR REGRESSION EQUATION FOR LANGMUIR ADSORPTION ISOTHERM

Y = 125.5761 X + 76.87334

CORRELATION COEFFICIENT

r2 = 0.754030

LINEAR REGRESSION EQUATION FOR FREUNDLICH ADSORPTION ISOTHERM

Y = -0.09032 X + -2.10128

r2 = 0.122988

C = Equilibrium COPPER concentration

METAL COPPER

X = mg COPPER adsorbed per gram of soil

X2 = C/X

INITIAL SOLUTION CONC. mg\l		1.73 BATCH 1	4.00 BATCH 2	7.98 BATCH 3	11.50 BATCH 4	15.38 BATCH 5
0.3 hr shake	C (mg\l)	0.39	2.58	6.58	10.51	15.07
	% removal	77.46	35.50	17.54	8.61	2.02
	X (mg\g)	0.03	0.03	0.03	0.02	0.01
	X2	14.55	90.85	235.00	530.81	2430.65
1 hr shake	C (mg\l)	0.43	2.83	6.79	10.91	15.09
	% removal	75.14	29.25	14.91	5.13	1.89
	X (mg\g)	0.03	0.02	0.02	0.01	0.01
	X2	16.54	120.94	285.29	924.58	2601.72
3 hr shake	C (mg\l)	0.36	2.80	7.02	11.30	15.36
	% removal	79.19	30.00	12.03	1.74	0.13
	X (mg\g)	0.03	0.02	0.02	0.00	0.00
	X2	13.14	116.67	365.62	2825.00	38400.00
10 hr shake	C (mg\l)	0.25	2.74	6.96	11.43	15.36
	% removal	85.55	31.50	12.78	0.61	0.13
	X (mg\g)	0.03	0.03	0.02	0.00	0.00
	X2	8.45	108.73	341.18	8164.29	38400.00
30 hr shake	C (mg\l)	0.20	2.63	6.74	11.43	15.36
	% removal	88.44	34.25	15.54	0.61	0.13
	X (mg\g)	0.03	0.03	0.02	0.00	0.00
	X2	6.54	95.99	271.77	8164.29	38400.00

LINEAR REGRESSION EQUATION FOR LANGMUIR ADSORPTION ISOTHERM

Y = 2225.117 X + -6793.34

CORRELATION COEFFICIENT

r2 = 0.695219

LINEAR REGRESSION EQUATION FOR FREUNDLICH ADSORPTION ISOTHERM

r2 = 0.487469

Y = -0.80651 X + -1.73608

C = Equilibrium ZINC concentration

METAL ZINC X = mg ZINC adsorbed per gram of soil

X2 = C/X

INITIAL SOLUTION CONC. mg\l		1.20 BATCH 1	2.33 BATCH 2	4.13 BATCH 3	5.83 BATCH 4	7.83 BATCH 5
0.3 hr shake	C (mg\l)	0.73	1.96	3.62	5.28	7.23
	% removal	39.17	15.88	12.35	9.43	7.66
	X (mg\g)	0.01	0.01	0.01	0.01	0.01
	X2	77.66	264.86	354.90	480.00	602.50
1 hr shake	C (mg\l)	0.69	2.06	3.75	5.41	7.39
	% removal	42.50	11.59	9.20	7.20	5.62
	X (mg\g)	0.01	0.01	0.01	0.01	0.01
	X2	67.65	381.48	493.42	644.05	839.77
3 hr shake	C (mg\l)	0.75	2.12	3.84	5.51	7.45
	% removal	37.50	9.01	7.02	5.49	4.85
	X (mg\g)	0.01	0.00	0.01	0.01	0.01
	X2	83.33	504.76	662.07	860.94	980.26
10 hr shake	C (mg\l)	0.82	2.06	3.94	5.61	7.52
	% removal	31.67	11.59	4.60	3.77	3.96
	X (mg\g)	0.01	0.01	0.00	0.00	0.01
	X2	107.89	381.48	1036.84	1275.00	1212.90
30 hr shake	C (mg\l)	0.74	2.16	4	5.69	7.74
	% removal	38.33	7.30	3.15	2.40	1.15
	X (mg\g)	0.01	0.00	0.00	0.00	0.00
	X2	80.43	635.29	1538.46	2032.14	4300.00

LINEAR REGRESSION EQUATION FOR LANGMUIR ADSORPTION ISOTHERM

Y = 568.1335 X + -592.764

CORRELATION COEFFICIENT

r2 = 0.934404

LINEAR REGRESSION EQUATION FOR FREUNDLICH ADSORPTION ISOTHERM

Y = -0.63543 X + -2.16615

r2 = 0.927855

APPENDIX F
Soil Column Elution Data

COLUMN 1

CADMIUM		COPPER	
Pore Volumes	C/C_0	Pore Volumes	C/C_0
5.1	0.03	5.7	0.00
5.3	0.08	5.9	0.04
5.5	0.14	6.1	0.15
5.7	0.23	6.3	0.25
5.9	0.36	6.5	0.39
6.1	0.47	6.7	0.55
6.3	0.59	6.9	0.74
6.5	0.71	7.1	0.93
6.7	0.89	7.3	1.00
6.9	0.98		
7.1	1.00		

NICKEL		ZINC	
Pore Volumes	C/C_0	Pore Volumes	C/C_0
5.1	0.00	4.7	0.00
5.3	0.28	4.9	0.01
5.5	0.28	5.1	0.11
5.7	0.53	5.3	0.29
5.9	0.53	5.5	0.32
6.1	0.53	5.7	0.34
6.3	0.66	5.9	0.51
6.5	0.66	6.1	0.62
6.7	0.78	6.3	0.75
6.9	1.00	6.7	0.91
		6.9	1.00

LEAD

Pore Volumes	C/C_0
11.1	0.00
11.3	0.01
11.5	0.02
11.7	0.03
11.9	0.04
12.1	0.05
12.3	0.07
12.5	0.09
12.7	0.10
12.9	0.13
13.1	0.16
13.3	0.18
13.5	0.20
13.7	0.25
13.9	0.29
14.1	0.32
14.3	0.36
14.5	0.49
14.7	0.52
14.9	0.61
15.1	0.67
15.3	0.76
15.5	0.78
15.7	0.83
15.9	0.86
16.1	0.89
16.3	0.94
16.5	0.97
16.7	0.97
16.9	1.00

COLUMN 2

CADMIUM

Pore Volumes	C/C_0
3.72	0.13
3.90	0.14
4.08	0.33
4.26	0.51
4.44	0.62
4.62	0.67
4.80	0.74
4.98	0.80
5.16	0.84
5.34	0.88
5.52	0.94
5.70	1.00

COPPER

Pore Volumes	C/C_0
3.90	0.03
4.08	0.08
4.26	0.13
4.44	0.20
4.62	0.27
4.80	0.39
4.98	0.42
5.16	0.51
5.34	0.54
5.52	0.63
5.70	0.72
5.88	0.81
6.06	0.86
6.24	0.91
6.42	0.94
6.60	0.99
6.78	1.00

NICKEL

Pore Volumes	C/C_0
3.36	0.00
3.54	0.05
3.72	0.11
3.90	0.14
4.08	0.20
4.26	0.22
4.44	0.27
4.62	0.34
4.80	0.42
4.98	0.48
5.16	0.57
5.34	0.62
5.52	0.67
5.70	0.76
5.88	0.82
6.06	1.00

ZINC

Pore Volumes	C/C_0
3.36	0.00
3.54	0.03
3.72	0.06
3.90	0.32
4.08	0.59
4.26	0.72
4.44	0.81
4.62	0.85
4.80	0.91
4.98	0.95
5.16	1.00

LEAD

Pore Volumes	C/C_0
6.48	0.00
6.66	0.02
6.84	0.03
7.02	0.05
7.20	0.07
7.38	0.09
7.56	0.09
7.74	0.12
7.92	0.14
8.10	0.19
8.28	0.21
8.46	0.27
8.64	0.29
8.82	0.36
9.00	0.40
9.18	0.51
9.36	0.56
9.54	0.60
9.72	0.66
9.90	0.69
10.08	0.73
10.26	0.78
10.44	0.81
10.62	0.88
10.80	0.96
10.98	1.00

APPENDIX G
Soil Column Metal Extraction Data

COLUMN 1

C/C_{max}

DEPTH (cm)	LEAD	CADMIUM	COPPER	NICKEL	ZINC
1	1.00	1.00	1.00	1.00	1.00
2	0.67	0.82	0.62	0.75	1.00
3	0.54	0.65	0.62	0.40	0.87
4	0.46	0.65	0.48	0.40	0.77
5	0.54	0.65	0.48	0.40	0.77
6	0.38	0.65	0.48	0.40	0.77
7	0.33	0.65	0.48	0.40	0.65
8	0.25	0.65	0.48	0.40	0.58
9	0.29	0.65	0.48	0.40	0.53
10	0.29	0.65	0.48	0.40	0.53

COLUMN 2

C/C_{max}

DEPTH (cm)	LEAD	CADMIUM	COPPER	NICKEL	ZINC
1	1.00	1.00	1.00	1.00	1.00
2	0.87	1.00	0.72	0.65	0.69
3	0.75	1.00	0.72	0.65	0.69
4	0.63	1.00	0.64	0.65	0.52
5	0.63	1.00	0.64	0.65	0.56
6	0.50	1.00	0.64	0.65	0.52
7	0.25	1.00	0.64	0.65	0.52
8	0.25	1.00	0.64	0.65	0.33
9	NA	1.00	0.44	0.65	0.33
10	NA	1.00	0.44	0.65	0.33